

**UNIVERSIDADE FEDERAL DE SANTA MARIA
CENTRO DE CIÊNCIAS NATURAIS E EXATAS
PROGRAMA DE PÓS-GRADUAÇÃO EM CIÊNCIAS BIOLÓGICAS:
BIOQUÍMICA TOXICOLÓGICA**

**AVALIAÇÃO DE NOVOS COMPOSTOS SOBRE A
ATIVIDADE DE COLINESTERASES EM MODELOS *IN
SILICO E IN VITRO***

TESE DE DOUTORADO

Thiago Henrique Lugokenski

**Santa Maria, RS, Brasil
2012**

**AVALIAÇÃO DE NOVOS COMPOSTOS SOBRE A
ATIVIDADE DE COLINESTERASES EM MODELOS *IN
SILICO* E *IN VITRO***

Thiago Henrique Lugokenski

Tese apresentada ao Programa de Pós-Graduação Ciências Biológicas: Bioquímica
Toxicológica da Universidade Federal de Santa Maria (UFSM,RS), como requisito
parcial para obtenção do grau de
Doutor em Bioquímica Toxicológica.

Orientador: Profº Dr. Félix Alexandre Antunes Soares

Co-orientadora: Profª Drª. Maria Ester Pereira

Santa Maria, RS, Brasil

2012

**Universidade Federal de Santa Maria
Centro de Ciências Naturais e Exatas
Programa de Pós-Graduação em Ciências Biológicas:**

A Comissão Examinadora, abaixo assinada, aprova a Tese de
Doutorado


**AVALIAÇÃO DE NOVOS COMPOSTOS SOBRE A ATIVIDADE DE
COLINESTERASES EM MODELOS *IN SILICO* E *IN VITRO***

Elaborada por

Thiago Henrique Lugokenski

como requisito parcial para a obtenção do grau de **Doutor em
Bioquímica Toxicológica**

COMISSÃO EXAMINADORA:



Prof. Dr. Félix Alexandre Antunes Soares (Orientador)



Prof. José Maria Monserrat (FURG)



Prof. Jeferson Luiz Franco (UNIPAMPA)



Profa. Maria Rosa Chitolina Schetinger (UFSM)



Profa. Vânia Lucia Loro (UFSM)

Santa Maria, junho de 2012.

AGRADECIMENTOS

Ao Prof^o Félix Alexandre Antunes Soares, meu orientador. Agradeço pela amizade, companheirismo e pelo enorme esforço em me proporcionar as melhores condições para que este trabalho fosse realizado.

À Prof^a Maria Ester Pereira, que me orientou no mestrado e coorientou durante o doutorado, por todo o apoio e ensinamentos.

Ao Prof^o João Batista Teixeira da Rocha, por todas as oportunidades que me proporcionou e que, ao longo de toda minha formação acadêmica, contribuiu muito com todo o seu conhecimento.

Aos meus pais, Mário e Vera, que me apoiam e incentivam em todos os momentos.

A Carol, pelo amor e companheirismo mesmo nas horas mais difíceis.

À todo o pessoal do laboratório do Prof^o Félix, pela parceria e por bons momentos passados juntos. Em especial, agradeço ao Romulo por toda a ajuda para que esta tese acontecesse.

Ao pessoal do laboratório do Prof^o João e da Prof^a Nilda, por toda a ajuda ao longo da minha vida acadêmica, e pelos bons momentos passados juntos.

À comissão examinadora desta tese pela disponibilidade e contribuições.

Aos demais professores e funcionários do PPGBTox, que contribuíram de alguma forma para minha formação.

Ao CNPq e à CAPES pelos recursos financeiros concedidos.

Enfim, agradeço à UFSM e ao PPGBTox pela possibilidade de realização deste curso.

SUMÁRIO

1 INTRODUÇÃO.....	1
1.1 AChE.....	6
1.2 Organofosforados.....	15
1.3 Oximas.....	20
1.4 Justificativas.....	24
1.5 Objetivos.....	25
1.5.1 Objetivo Geral.....	25
1.5.2 Objetivos Específicos.....	25
2 ARTIGOS CIENTÍFICOS.....	27
2.1 Artigo 1.....	28
2.2 Artigo 2.....	39
2.3 Manuscrito 1.....	49
3 DISCUSSÃO.....	80
4 CONCLUSÕES.....	85
5 REFERÊNCIAS.....	87

LISTA DE ABREVIATURAS

- ACh - Acetilcolina
- AChE - Acetilcolinesterase
- ALA-D – Delta Amino Levulinato Desidratase
- BChE - Butirilcolinesterase
- BBB – Barreira Cérebro-Sangue
- CAS – Sítio Aniônico Catalítico
- CAT - Catalase
- DCF – Diclorofluoresceína
- DCFH-DA – Diacetato Diclorofluoresceína
- DTF – Teoria do Funcional da Densidade
- GPx- Glutathiona Peroxidase
- IBTC - Isatina-3-N⁴-benziltiosemicarbazona
- LC₅₀ – Concentração letal mediana
- LD₅₀ – Dose letal mediana
- MAP - Metamidofós
- MFCC – Fracionamento Molecular com Capas Conjugadas
- MTT – Metil Tetrazólio
- NPSH – Tiol não proteico
- OMS – Organização Mundial da Saúde
- OP - Organofosforado
- OPC – Composto Organofosforado
- PAS – Sítio Aniônico Periférico
- PON - Paraoxonase
- QM/MM – Mecânica Quântica/Mecânica Molecular
- TBARS – Espécies Reativas ao Ácido Tiobarbitúrico

LISTA DE FIGURAS

INTRODUÇÃO

Figura 1 - Estrutura molecular da acetilcolina.....	7
Figura 2 - Estrutura molecular da AChE com o substrato ACh dentro do sítio ativo....	9
Figura 3 - Potencial eletrostático da AChE da <i>Torpedo californica</i>	11
Figura 4 - Mecanismo da hidrólise da ACh pela AChE.....	13
Figura 5 - Subclasses de compostos OPs.....	14
Figura 6 - Esquema da inibição da AChE por OPs.....	17
Figura 7 - Estrutura molecular do metamidofós.....	18
Figura 8 - Reativação da AChE fosforilada por oximas.....	20
Figura 9 - Estrutura molecular da pralidoxima e obidoxima.....	22

ARTIGO 1

Figura 1 - Chemical structure of IBTC.....	29
Figura 2 - Effect of IBTC treatment on Na ⁺ /K ⁺ ATPase activity on brain homogenate.....	32
Figura 3 - Effect of IBTC treatment on Delta Aminolevulinate Dehydratase.....	33
Figura 4 - Effect of IBTC on percent cytotoxicity (MTT assay).....	33
Figura 5 - Protective effect of IBTC on AChE activity from ghost erythrocytes (A) and BChE from plasma (B).....	34
Figura 6 - Reactivation effect of IBTC on AChE activity from ghost erythrocytes (A) and BChE from plasma (B).....	34
Figura 7 - Representative molecular models of IBTC binding the active site of <i>Mus musculus</i> AChE.....	35

ARTIGO 2

Figure 1 - Chemical structures of obidoxime, pralidoxime, oxime 1 and Oxime 2.....	64
Figure 2 - Kinetics of methamidophos inhibition on AChE activity.....	65
Figure 3 – Protective effect of obidoxime (A), pralidoxime (B), oxime 1 (C) and oxime 2 (D) on methamidophos (MAP)-inhibited AChE activity from rat brain homogenate.....	66

Figure 4 – Protective effect of obidoxime (A), pralidoxime (B), oxime 1 (C) and oxime 2 (D) on methamidophos (MAP)-inhibited AChE activity from human erythrocyte ghost.....	67
Figure 5 – Protective effect of obidoxime (A), pralidoxime (B), oxime 1 (C) and oxime 2 (D) on methamidophos (MAP)-inhibited BChE activity from human plasma.....	68
Figure 6 - Docking of the conformation corresponding to the oximes: oxime 1 (A), oxime 2 (B), pralidoxime (C) and obidoxime (D) inside MmAChE active site.....	69

MANUSCRITO 1

Figure 1 – Obidoxime, pralidoxime, oxime 1 and oxime 2 chemical structure.....	89
Figure 2 – The AChE dimer (A) and binding pocket of AChE (B) detaching the most important residues to the oxime binding.....	90
Figure 3 – Binding sites of obidoxime and pralidoxime.....	91
Figure 4 – Binding sites of oxime 1 and oxime 2.....	92
Figure 5 – Variation of the interaction energy as a function of the interaction radius.....	93
Figure 6 – Total AChE interaction energy of oximes for interaction radii of 4 Å, 6 Å, 8 Å, 10 Å, 12 Å and 14 Å.....	94
Figure 7 – Distances between AChE residues and obidoxime and pralidoxime.....	95
Figure 8 – Distances between AChE residues and oxime 1 and oxime 2.....	96
Figure 9 – Binding site, interaction energy and residues domain (BIRD) graphic panel showing the most relevant residues of AChE which contribute to the obidoxime binding.....	97
Figure 10 – Binding site, interaction energy and residues domain (BIRD) graphic panel showing the most relevant residues of AChE which contribute to the pralidoxime binding.....	98
Figure 11 – Binding site, interaction energy and residues domain (BIRD) graphic panel showing the most relevant residues of AChE which contribute to the oxime 1 binding.....	99
Figure 12 – Binding site, interaction energy and residues domain (BIRD) graphic panel showing the most relevant residues of AChE which contribute to the oxime 2 binding.....	100

LISTA DE TABELAS

ARTIGO 1

Tabela 1 - Effect of IBTC treatment on DCF-RS levels.....	31
Tabela 2 - Effect of IBTC treatment on TBARS levels.....	32
Tabela 3 - Effect of IBTC treatment on NPSH levels.....	33

ARTIGO 2

Tabela 1 - Percent reactivation of methamidophos-inhibited AChE by oximes.....	61
Tabela 2 - Reactivation constants.....	62
Tabela 3 - Reactivation constants.....	63

APRESENTAÇÃO

No item **INTRODUÇÃO** consta uma revisão da literatura sobre os temas trabalhados nesta tese.

A metodologia realizada e os resultados obtidos que compõem esta tese estão apresentados sob a forma de artigo e manuscritos, os quais se encontram no item **ARTIGOS CIENTÍFICOS**. Neste constam as seções: Introdução, Materiais e Métodos, Resultados, Discussão e Referências Bibliográficas.

Os itens **DISCUSSÃO E CONCLUSÕES**, encontradas no final desta tese, apresentam descrições, interpretações e comentários gerais sobre os artigos científicos incluídos neste trabalho.

As **REFERÊNCIAS BIBLIOGRÁFICAS** referem-se somente às citações que aparecem nos itens **INTRODUÇÃO, DISCUSSÃO e CONCLUSÕES** desta tese.

RESUMO

Tese de Doutorado
Programa de Pós-Graduação em Ciências Biológicas: Bioquímica Toxicológica
Universidade Federal de Santa Maria, RS, Brasil.

AVALIAÇÃO DE NOVOS COMPOSTOS SOBRE A ATIVIDADE DE COLINESTERASES EM MODELOS *IN SILICO* E *IN VITRO*

AUTOR: Thiago Henrique Lugokenski
ORIENTADOR: Prof^o Dr. Félix Alexandre Antunes Soares
CO-ORIENTADORA: Prof^a Dr^a. Maria Ester Pereira
LOCAL E DATA DA DEFESA: Santa Maria, 04 de junho de 2012.

A enzima acetilcolinesterase (EC 3.1.1.7, AChE) é responsável por terminar a ação da acetilcolina nas junções das terminações nervosas com seus órgãos efetores ou sítios pós-sinápticos. A atividade desta enzima pode ser inibida por compostos organofosforados (OP), e sua inativação resulta em um acúmulo de acetilcolina nos receptores colinérgicos, levando a crise colinérgica que pode levar a morte. No Brasil, se destaca o uso do composto OP metamidofós, que é largamente utilizado no controle de pragas em culturas agrícolas e tem sido relacionado com altas taxas de intoxicação. Atualmente, os únicos compostos capazes de reverter a inibição da AChE por OP são as oximas, tais compostos podem reativar a enzima devido a seu alto poder nucleofílico, podendo atacar e retirar o grupamento fosforil da enzima inibida. Porém, tais compostos apresentam efeitos tóxicos, e tem seu uso limitado pela alta especificidade, com cada oxima atuando na AChE inibida por apenas alguns compostos OP. Tais limitações criam a necessidade do desenvolvimento de novos fármacos com potencial reativador da AChE com menores efeitos colaterais. Neste sentido, se tem utilizado uma série de ferramentas computacionais (modelos *in silico*), com o objetivo de entender as interações que ocorrem em nível molecular e, desta forma, racionalizar o desenvolvimento de novos compostos. Sendo assim, o objetivo desta tese consiste em avaliar a atividade de três novos compostos, em comparação com duas oximas já utilizadas na clínica (obidoxima e pralidoxima), sobre a atividade da AChE inibida por metamidofós, tanto em modelos *in silico* como *in vitro*. Como resultados, observamos que os três novos compostos foram capazes de reativar a AChE de eritrócitos humanos inibida por metamidofós, contudo com menor eficiência que as oximas já utilizadas na clínica. Porém, todos os novos compostos foram capazes de reativar a enzima butirilcolinesterase (BChE), uma enzima acessória à AChE no sistema colinérgico, inibida por metamidofós, enquanto nenhuma das oximas clássicas tiveram qualquer atividade reativadora nesta enzima. Nosso trabalho também demonstrou que a pralidoxima, que obteve a melhor constante de reativação entre todos os compostos testados, ataca a ligação fosforo-oxigênio (formada entre o metamidofós e o resíduo Ser203, da tríade catalítica da AChE) via uma região conhecida como "oxyanion-hole", que compreende os resíduos Gly120, Gly121 e Ala204. Tal achado pode ajudar no desenvolvimento de novos compostos com melhor atividade reativatória na AChE inibida por OPs. Além disso, mostramos aqui pela primeira vez, a contribuição de cada resíduo de aminoácido da AChE, num raio de 14 Å do ligante, para a ligação das oximas no seu sítio ativo, usando métodos de química quântica. Tais achados mostraram a importância da presença de um nitrogênio quaternário para a estabilização das oximas no sítio ativo; assim como colheu evidências que a forma ativa das oximas seria a sua forma desprotonada, ao invés da forma protonada, o que tem sido alvo de algum debate no meio científico. Particularmente importante, foi demonstrado a contribuição fundamental de aminoácidos que se encontram distantes do ligante, para a estabilização e conformação adotada pelos compostos, e que até o momento tem sido negligenciados em estudos *in silico*. Por fim, nosso estudo também avaliou os efeitos tóxicos do composto isatina-3-N⁴-benziltiosemicarbazona (IBTC) em camundongos, o qual apresentando baixa toxicidade, com valores de dose letal mediana (LD₅₀) superiores a 500 mg/kg. Desta forma, este estudo contribuiu para o desenvolvimento de novos fármacos capazes de reativar a AChE e que apresentem menos efeitos tóxicos.

Palavras-chave: Acetilcolinesterase. Organofosforados. Metamidofós. Oximas. Modelos computacionais.

ABSTRACT

Thesis of Doctor's Degree
Graduate Course in Biological Sciences: Toxicological Biochemistry
Federal University of Santa Maria, RS, Brazil

EVALUATION OF NEW COMPOUNDS ON CHOLINESTERASES ACTIVITY IN MODELS *IN SILICO* AND *IN VITRO*

AUTHOR: Thiago Henrique Lugokenski

ADVISOR: Félix Alexandre Antunes Soares

CO-ADVISOR: Maria Estes Pereira

DATE AND PLACE OF THE DEFENSE: Santa Maria, June, 4th, 2012.

The enzyme acetylcholinesterase (EC 3.1.1.7, AChE) is responsible to terminate acetylcholine activity in the terminal nervous junctions with its effector organs or post-synaptic sites. The activity of this enzyme could be inhibited by organophosphorus (OP) compounds, and this inactivation leads to an accumulation of acetylcholine in the cholinergic receptors, leading to a cholinergic crisis that may result in death. In this way, the OP compound methamidophos has been related to its broad use in various agriculture cultures in Brazil, with high intoxication rate. Actually, the only compounds able to revert the AChE inhibition by OP, are the oxime, such compounds may reactive the enzyme activity due its high nucleophilic power, attacking the phosphoryl group of the inhibited enzyme and displacing it. However, such compounds show toxic effects, and its use is limited by the high specificity, with each oxime acting only in the reactivation of AChE induced by specific OP compounds. These limitations raise the need of development of new compounds with AChE reactivator potency, with minor side effects. In this way, have been utilized a series of computational tools (*in silico* models), with the aim of understand the interaction occurring at a molecular level and, so, rationalize the new compounds development. Thus, the aim of this thesis is to evaluate the activity of three new compounds in reactivate the AChE inhibited by methamidophos, in comparison with two others oximes used in clinical (obidoxime and pralidoxime), both in *in silico* and *in vitro* models. Our work demonstrate that the newly synthesized compounds are able to reactivate human erythrocyte AChE, however less efficiently than pralidoxime and obidoxime, and reactivate human plasma butyrylcholinesterase (BChE), where the classical oximes failed. We also show that pralidoxime, which obtained the best reactivation constant among all tested compounds, attack the phosphorus-oxygen moiety (formed between the methamidophos and the AChE catalytic triad residue Ser203) via a region known as "oxyanion-hole", composed by the residues Gly120, Gly121 and Ala204. Such found may help in the development of new compounds with better reactivatory activity on AChE inhibited by OP compounds. Furthermore, we show for the first time the individual contribution of each amino acid of AChE, in a radii of 14 Å from the ligand, to the oxime bonding to its active site, using quantum chemistry methods. Here, we demonstrate the important of a quaternary nitrogen to the stabilization of the oximes into the active site; as well as, we obtained evidences that the active form of oximes should be the unprotonated one, instead the protonated, which has been target of debate in the scientific society. Particularly important, we show the critical contribution of amino acids that lies distant from the ligand to the adopted conformation and stabilization of the compounds into the active site of AChE, which has been neglected until far. Finally, our study also evaluates the toxic effects of the compound isatin-3-N4-benzilthiosemicarbazone (IBTC) in mice, which presented low toxicity, with median lethal dose superior at 500 mg/kg. Concluding, this study contributes significantly to the development of new drugs able to restore the AChE activity with minor toxic effects.

Keywords: Acetylcholinesterase. Organophosphorus. Methamidophos. Oximes. Computational models.

1 INTRODUÇÃO

A enzima acetilcolinesterase (EC 3.1.1.7, AChE) é responsável por terminar a ação da acetilcolina nas junções das terminações nervosas com seus órgãos efetores ou sítios pós-sinápticos. A atividade desta enzima pode ser inibida por compostos organofosforados (OP), que são utilizados como pesticida no controle de pragas e como aditivo para lubrificantes, além de terem sido largamente desenvolvidos com a finalidade de ser utilizado como armas de guerra (WHO, 1993). A inativação da AChE resulta em um acúmulo de acetilcolina nos receptores colinérgicos, levando a crise colinérgica que pode levar a morte (Marrs, 1993). Logo, o principal mecanismo de toxicidade de compostos OP em mamíferos é a progressiva inibição da acetilcolinesterase (AChE) levando a uma espécie enzimática inativa (Zayed e cols, 1984, Worek e cols, 2004).

Além disso, compostos OP também podem inibir a enzima butirilcolinesterase (BChE), e dados da literatura mostram uma importante função desta enzima na atividade de neurônios cardíacos intrínsecos (Darvesh e cols., 2004), sendo assim, uma possível reativação desta enzima pode ajudar a reverter os efeitos da crise colinérgica no coração. Em adição, a inibição da BChE também aumenta os níveis de acetilcolina (Giacobini, 2000; Greig e cols., 2000), sugerindo uma função co-regulatória da butirilcolina na ação da acetilcolina (Darvesh e cols., 2003). Sua inibição leva à um aumento dose-dependente nos níveis de acetilcolina (ACh) no cérebro (Darvesh e Hopkins, 2003).

Uma depleção de 30-50% da atividade da AChE é acompanhada por sintomas muscarínicos (miose, sudorese, aumento das secreções brônquicas, salivação, lacrimejamento, vômitos, náuseas e diarreia, bradicardia e dores abdominais) de

intoxicação. A subsequente inibição de 50-70% da atividade enzimática original é caracterizada por sintomas muscarínicos, nicotínicos (tremores e câimbras, hipertensão arterial, fasciculação muscular e flacidez, eventualmente morte por parada respiratória ou edema pulmonar) e também no sistema nervoso central. Se a reativação da enzima for considerada, um aumento na atividade enzimática maior que 10% pode salvar a vida de um organismo intoxicado e reduzir os sintomas tóxicos (Karasova e cols., 2009).

O metamidofós é um dos organofosforados mais usados em culturas agrícolas no Brasil, sendo um problema com relação à intoxicação, seja pela ingestão de alimentos contaminados (Caldas e cols., 2006) seja por exposição ocupacional (Recena e cols., 2006a). Estudo recente de Recena e cols. (2006b) demonstrou que mais de 90% de pequenos agricultores utilizam metamidofós com regularidade e, destes, aproximadamente 60% exibem sintomas típicos de intoxicação por organofosforados. Trabalhos *in vitro* demonstraram que o metamidofós apresenta atividade anti-colinesterase em humanos (Worek e cols., 2004 e 2007). Além disso, Tomlin (1994) mostrou que este composto tem alta toxicidade em organismos aquáticos, configurando também um problema ambiental.

Atualmente, o tratamento contra o envenenamento por OP consiste na estabilização do paciente, redução da absorção e o uso de altas doses de atropina e a administração de oximas para reativar a AChE inativada pelo OP, e dessa maneira reduzir a duração de paralisia dos músculos respiratórios (Howland e Aaron, 1999; Paris e Rios, 2001). A pralidoxima vem sendo largamente utilizada contra o envenenamento por OP, e é comercializada sob o nome de Contrathion (N-metil-alfa-piridilaldoxima). A ação das oximas é atribuída a sua habilidade de retirar o grupamento fosforil da enzima inibida por OP, isso ocorre em virtude da alta afinidade da oxima pela enzima e seu alto poder nucleofílico (Jokanović e Stojiljković, 2006). Além de reativar AChE, as

oximas também podem apresentar efeitos farmacológicos diretos como inibição da liberação de acetilcolina (Van Helden e cols., 1998) e da síntese de neurotransmissores (Clement, 1979), além de poderem hidrolisar diretamente acetilcolina (Zhang e cols., 2007) e butirilcolina (Petroianu e cols., 2004), reduzindo os níveis desses neurotransmissores na fenda sináptica, contornando os efeitos causados por compostos OP.

A experiência clínica com o uso de pralidoxima no tratamento de vítimas do ataque com gás sarin em Tóquio foi extremamente favorável (Stolijjkovic e Jokanovic, 2005). Porém, essa oxima não mostrou efeito satisfatório em envenenamento por tabun e soman (Kassa, 2005). Da mesma maneira, a obidoxima se mostrou um eficiente protetor contra envenenamento por tabun, sarin (Inns e Leadbeater, 1983; Maksimovic e cols., 1989) e VX (Maksimovic e cols., 1989) em modelos experimentais. Porém, se mostrou ineficiente em envenenamento por soman (Maksimovic e cols., 1980; Hamilton e Lundy, 1989). Além disso, a obidoxima pode apresentar alto potencial hepatotóxico (Marrs, 1991). Com relação ao metamidofós, Pohanka e cols. (2008) demonstraram que obidoxima e pralidoxima reativaram a AChE inibida por metamidofós em aproximadamente 80% à 100 μ M, contudo o protocolo experimental utilizado foi otimizado para propósitos analíticos, em condições não fisiológicas. Além disso, Wan e cols. (2007) mostraram efeitos positivos da administração de pralidoxima em indivíduos envenenados com metamidofós, e Satar e cols. (2004) demonstraram efeito hepatoprotetor da pralidoxima contra metamidofós (30 mg/kg). A necrose do diafragma induzido por metamidofós também é atenuado por pralidoxima em modelos *in vivo* (Santos e cols., 2002).

Tendo em vista que o metamidofós pode ser um problema de saúde e ambiental, e considerando a escassez de dados a respeito das únicas oximas disponíveis no

mercado (pralidoxima e obidoxima) frente à intoxicação induzida por metamidofós, cria-se a necessidade de novos estudos com essas oximas na intoxicação por metamidofós. Além disso, o desenvolvimento de novas oximas capazes de reativar colinesterases inibidas por organofosforados com melhores resultados experimentais também é uma necessidade atual.

Neste sentido, uma série de novas metodologias baseadas em estudos computacionais tem surgido com o objetivo de racionalizar a busca por novos compostos com atividade biológica e explicar fenômenos ocorridos a âmbito molecular, e que possam favorecer também o desenvolvimento de novos fármacos. Uma dessas metodologias é o atracamento molecular (“docking”) que pretende explicar as interações entre ligantes e proteínas e também servem como função escore entre diferentes possíveis fármacos. Vários programas tem apresentado algum sucesso em obter o modo de ligação correto de um ligante no sítio ativo de enzimas (Taylor e cols., 2002). Contudo, o cálculo da energia livre de ligação tem se mostrado desafiador (Warren e cols., 2006), uma vez que há uma complexa inter-relação entre o ligante e a proteína que interferem nesta energia. Então, apesar destes programas conseguirem uma boa predição da conformação mais provável de um ligante em uma proteína, as funções escore são comprometidas, principalmente devido aos cálculos utilizados por estes programas serem simplistas e/ou baseados em potências estatísticos.

Devido às limitações impostas pelo método de atracamento molecular, métodos baseados em cálculos quânticos, como o QM/MM, estão começando a serem empregados para computar as afinidades de ligantes e proteínas. Alguns pesquisadores, como Khandelwal e cols. (2005) têm usado uma abordagem que envolve o uso de várias ferramentas computacionais para resolver problemas envolvendo a ligação de ligantes

em proteínas, como o uso de atracamento molecular, otimização QM/MM, dinâmica molecular e cálculo da energia de interação usando QM/MM.

Por outro lado, níveis mais altos da teoria quântica, como a Teoria do Funcional da Densidade (DFT, do inglês “Density Functional Theory”) têm sido usados para calcular funções de onda de macromoléculas. Gao e cols. (2004) descreveram a aplicação de um esquema de matriz de densidade baseado no método de Fracionamento Molecular com Capas Conjugadas (MFCC, do inglês “Molecular Fractionation with Conjugated Caps”), onde a matriz de densidade é calculada para fragmentos “encapsulados” em altos níveis da teoria quântica e a energia total é considerada a soma dos fragmentos da matriz de densidade. Recentemente, da Costa e cols. (2012) aplicaram com sucesso um esquema baseado no método MFCC para calcular a contribuição individual de cada resíduo de aminoácido e a energia livre de ligação de diferentes estatinas no sítio ativo da enzima HMG-CoA redutase, usando cálculos baseados na teoria DFT.

Especificamente no caso de oximas, o mecanismo molecular pelo qual estes fármacos reativam a AChE inibida por compostos OP tem sido alvo de um grande número de estudos baseados no atracamento molecular. De modo geral, estes estudos apontam para uma importante participação dos resíduos aromáticos Tyr124, Trp286, Tyr337 e Tyr341 na estabilização de compostos bisquaternários mono-oxima no sítio ativo da AChE, principalmente pela ocorrência de interações do tipo π - π e cátion- π (Musilek e cols., 2011). Além disso, Ekstrom e cols (2009) aplicaram simulação por dinâmica molecular na reativação da AChE inibida por sarin pela oxima HI6, encontrando que um dos anéis aromáticos desta oxima se encontra “prensado” pelos resíduos Tyr124 e Trp286. Por outro lado, o anel piridina onde se encontra o grupo oxima se mostra desordenado e poderia chegar ao resíduo de serina (Ser203)

modificado pelo OP através de uma rede de interações de hidrogênio. Apesar destes dados serem muito interessantes, todas as técnicas empregadas são muito limitadas em quantificar a contribuição de cada resíduo para a ligação de oximas no complexo AChE-OP. O conhecimento de tais contribuições é essencial para o entendimento da ação do ligante no sítio ativo da enzima, e o subsequente processo de reativação enzimática, e deve ser muito útil para o desenvolvimento de novos fármacos.

Neste sentido, nosso grupo tem proposto o estudo de algumas novas oximas na tentativa de melhorar a reverter à inibição por OP, tais como a butano-2,3-dionatiosemicarbazona oxima e a 3-(fenilhidrazona)butan-2-one oxima, duas novas oximas sintetizadas pelo nosso grupo de pesquisa, e que já mostraram satisfatório potencial de reativação na AChE inibida pelos OPs clorpirifós, diazinon e malation (Costa e cols., 2011). Além de terem sido relacionadas com sua atividade antioxidante, sem sinais de toxicidade após uso *in vivo* e *ex vivo* (Puntel e cols., 2008 e 2009), com valores de LD50 similares aos obtidos com pralidoxima e obidoxima (Arena, 1979). Além destes compostos, nosso grupo tem testado as possíveis atividades biológicas de um derivado da tiosemicarbazona, a isatina-3-N⁴-benziltiosemicarbazona (IBTC). Os derivados de tiosemicarbazona apresentam ampla utilidade farmacológica (Beraldo e Gambino, 2004), e têm sido relacionados à sua atividade quelante de radicais livres (Wada e cols., 1994). Neste sentido, nosso grupo demonstrou recentemente que a IBTC apresenta atividade antioxidante e antiarterogênica (Barcelos e cols., 2011).

1.1 AChE

A enzima acetilcolinesterase (AChE, EC 3.1.1.7) é membro da família das hidrolases (Frobert e cols., 1997) e exerce uma função vital no sistema colinérgico por

hidrolisar o neurotransmissor ACh (Figura 1) em colina e acetato, e portanto terminando o impulso elétrico. A ACh foi o primeiro agente químico conhecido por estabelecer uma comunicação entre duas células distintas em mamíferos, e age por propagar um estímulo elétrico através da junção sináptica. Neste contexto, a ação da AChE pode ser resumida de seguinte forma: a ACh é liberada pelo neurônio pré-sináptico em resposta a um potencial de ação e difunde através da sinapse e se ligando a receptores de ACh (os quais controlam a entrada de íons K^+ para o neurônio pós-sináptico ou célula muscular, entre outras funções). Após esta ligação, ocorrem vários eventos que resultam no começo do potencial de ação na célula pós-sináptica. Neste momento, a AChE rapidamente hidrolisa a ACh, terminando a entrada de íons, mediada pela ACh, através do receptor e interrompendo a transmissão do impulso nervoso (Quinn, 1987). A transmissão do impulso químico leva ao redor de 1 ms e demanda uma integração precisa entre os componentes estruturais e funcionais na sinapse (Aldunate e cols., 2004). Conseqüentemente, a AChE é uma das enzimas mais eficientes conhecidas, hidrolisando a ACh à uma taxa próxima da taxa de difusão de ACh na fenda sináptica (Bazelyansky e cols., 1986). Os valores de *turnover* da AChE é aproximadamente de $7,4 \times 10^5$ a 3×10^7 moléculas de ACh por minuto por molécula de enzima (Rothenberg e Nachamnsohn, 1947; Wilson e Harrison, 1961), esta alta taxa catalítica é a base da resposta rápida e repetitiva que ocorre na neurotransmissão colinérgica.

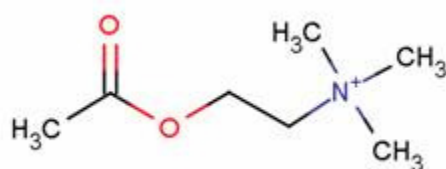


Figura 1 – Estrutura molecular da acetilcolina.

A neuro-transmissão mediada pela ACh é um processo vital para sobrevivência, sendo que sua interrupção é letal e sua redução gradual é associada a deterioração

progressiva das funções cognitivas e neuromusculares, como no caso da doença de Alzheimer. Contudo, a AChE parece estar envolvida em outros processos biológicos, tais como neurogenese, adesão e diferenciação celular, dentre outros (Shen, 2008). Da mesma maneira, a ACh também tem outras funções além do correto funcionamento do sistema nervoso central e periférico, estudos recentes indicam que este neurotransmissor pode ter parte na regulação de vários outros processos como, crescimento celular, locomoção e apoptose (Shen, 2008).

A AChE de vertebrados tem sido classificada baseado em vários critérios, a nomenclatura, segundo Bon e cols. (1979), é baseada na estrutura quaternária e no número de subunidades catalíticas de atividade similar. Neste caso, formas globulares são nomeadas como G1, G2 e G4 que contém uma, duas ou quatro subunidades catalíticas, respectivamente, enquanto as formas assimétricas são nomeadas como A4, A8 e A12 e são caracterizadas pela presença de uma “cauda” associada com um, dois ou três tetrâmeros (Bon e cols., 1979; Aldunate e cols., 2004). Além disso, as formas globulares da AChE podem ser distinguidos em anfifílicas ou não-anfifílicas, devido a presença, ou não, de um domínio hidrofóbico responsável por ancorar a enzima em membranas (Aldunate e cols., 2004). Em vertebrados, as diferentes AChE serem codificadas por um único gene, sendo que as várias formas moleculares existentes são geradas por *splicing* alternativo e modificações pós-translacionais (Frobert e cols., 1997). As modificações geradas por *splicing* formam regiões C-terminal distintas e são caracterizadas como domínios R (“read-through”), H (hidrofóbico), T (caudado) e S (solúvel).

A estrutura molecular da AChE (Figura 2) é bastante similar a das lipases e serina hidrolases, e pertence a família das α/β hidrolases, onde uma estrutura em folhas- β e rodeada por α -hélices. Ela possui uma plataforma de folhas β que comporta a

maquinaria catalítica e, nas suas características gerais, é bastante similar em todos os membros da família. De fato, os três membros da tríade catalítica, Ser200, Glu327 e His440 (para a AChE da espécie de arraia *Torpedo californica*, em AChE de humanos a sequência é Ser203, Glu334 e His447; as explicações abaixo se referem a AChE proveniente da *T. californica*, devido a grande similaridade estrutural e funcional entre as AChEs das duas espécies, e ao maior número de estudos envolvendo a AChE de *T. californica*) aparecem na mesma ordem ao longo da cadeia polipeptídica em todas as enzimas da família α/β hidrolases. As α -hélices e os “loops” tem suas funções atribuídas a manipulação de elementos específicos, como os substratos dos diferentes membros da família que são muito variados. A característica mais interessante da AChE é a presença de uma “fenda” estreita e profunda, de aproximadamente 20 Å e que penetra praticamente até o meio da enzima, que possui um diâmetro aproximado de 40 Å. Isto pode resultar numa dificuldade de entrada do substrato, e a explicação mais aceita para a importância de um sítio tão profundo foi provida por Harel e cols., (1996), onde ele sugere que se o sítio ativo é muito profundo, o substrato vai estar rodeado em quase 360° pela proteína, permitindo múltiplas interações enzima/substrato que, por sua vez, pode gerar um estado de transição mais efetivo.

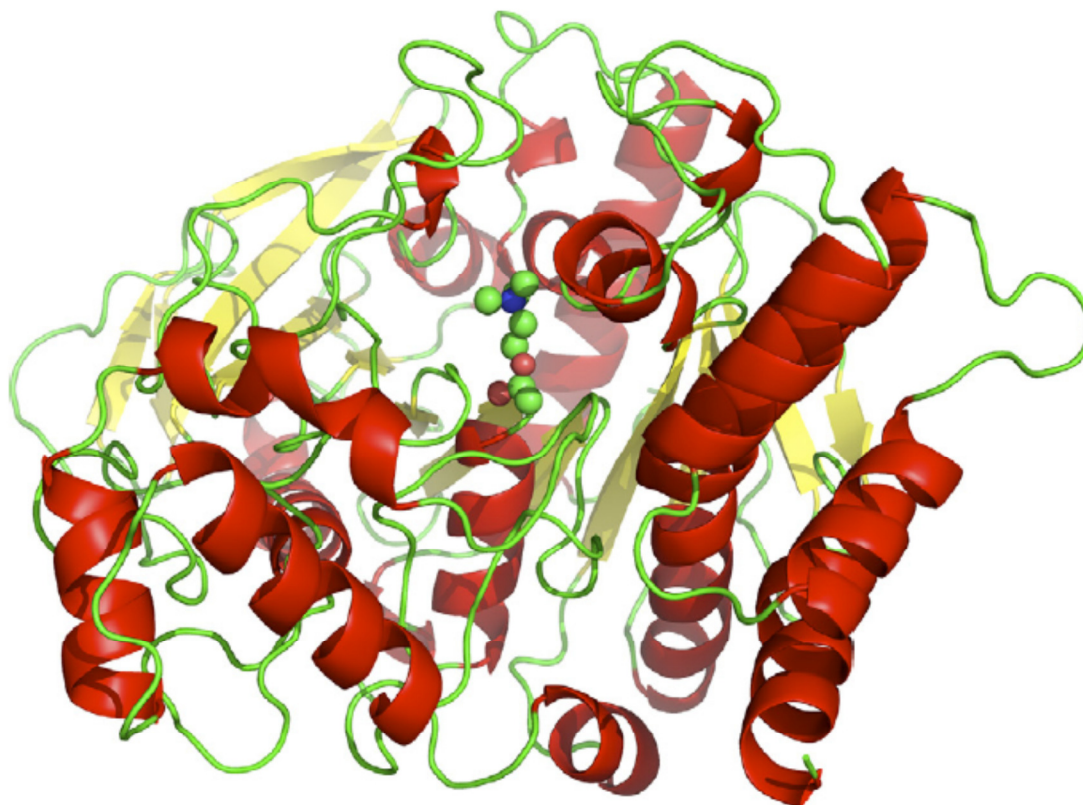


Figura 2 – Estrutura molecular da AChE com o substrato ACh dentro do sítio ativo. Figura retirada de Siman e Joel (2008).

O sítio no qual se encontra a tríade catalítica é delineado por 14 resíduos aromáticos e dois resíduos ácidos, Asp285 e Glu273 que se encontram no topo e um, Glu199, na base. Os resíduos aromáticos representam os elementos mais importantes do sítio aniônico da AChE, sendo que dois deles, Trp84 e Phe300 contribuem para o sítio catalítico aniônico (CAS) e, os resíduos Tyr70, Tyr121 e Trp279 para o sítio aniônico periférico (PAS), localizado no lado oposto a entrada do sítio (Barak e cols., 1994). A superfície aromática da fenda pode servir como uma coluna de afinidade através da qual o substrato pode “pular” e “deslizar” pelo sítio ativo por sucessivas interações do tipo cátion- π , ou π - π no caso de ligantes artificiais com anéis aromáticos. A AChE possui um amplo momento dipolo, orientado ao longo do sítio ativo (Figura 3), e que pode servir para atrair o substrato positivamente carregado para dentro do sítio ativo. Também foi demonstrada a presença de um gradiente potencial ao longo de todo

comprimento do sítio ativo, o qual “empurra” o substrato para o centro do sítio, uma vez que a tríade catalítica está “enterrada” praticamente no centro da enzima (Felder e cols., 1997). Este potencial pode afetar também ligantes não carregados, e parece ser formado primariamente pelo resíduo Asp72 presente no meio da fenda, e pelos resíduos Glu199 e Glu443 próximos a base. A fraca hidratação da ACh favorece as interações cátion- π com os resíduos aromáticos, inicialmente no topo do sítio e subsequentemente interações através da fenda até a tríade catalítica. A ACh interage, inicialmente, com os resíduos do PAS, aumentando a probabilidade de interação com os resíduos do CAS, sugerindo um efeito alostérico da ligação do substrato ao PAS (Johnson e cols., 2005).

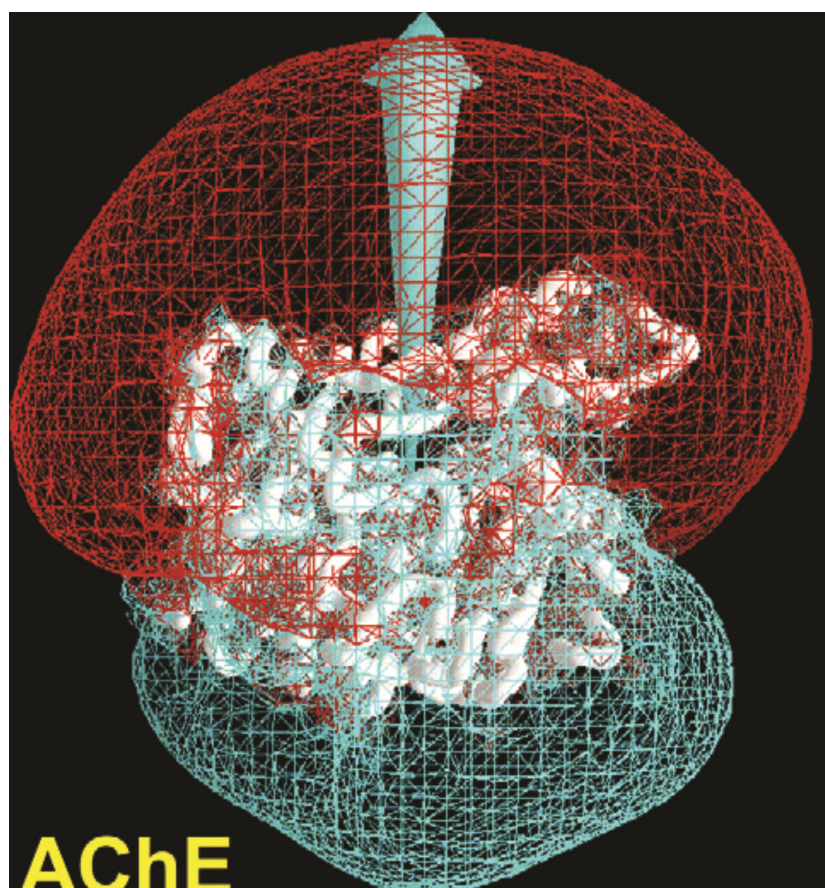


Figura 3 – Potencial eletrostático da AChE de *Torpedo californica*, onde a superfície vermelha representa o contorno iso-potencial negativo e a superfície azul, o positivo. A flecha indica a direção do dipolo. Figura retirada de Ripoll e cols., (1993).

Outras regiões importantes para o processo catalítico também estão presentes na AChE. Os resíduos Trp84, Glu199 e Phe330 são os principais componentes do subsítio aniônico (também conhecido como sitio de ligação da colina), e são responsáveis pela ligação da colina ao sítio ativo via, principalmente, interações cátion- π . Há uma forte interação entre o grupo amônia quaternário da ACh (Fuxreiter e Warshel, 1998; Ordentlich e cols., 2004) e os anéis aromáticos dos resíduos Phe330 e, principalmente, o resíduo Trp84, o qual se encontra a apenas 3,7 Å de distância do grupo amônia (Ma e Dougherty, 1997). Além destes, os resíduos Phe288 e Phe290 (os quais correspondem aos resíduos Phe295 e Phe297 na AChE humana) são importantes na delimitação do espaço onde o grupamento acil da ACh se acomoda, sendo designado como “acyl pocket”. Tais resíduos são responsáveis pela alta especificidade da AChE quando comparada com a BChE, pois o grande volume da cadeia lateral destes resíduos limitam o espaço disponível no “acyl pocket”, impedindo que substratos maiores, como a butirilcolina, acessem o fundo do sítio ativo (Vellon e cols., 1993; Hosea e cols., 1995). Outros dois resíduos completam esta região, Trp233 e Phe331, os quais estão envolvidos na manutenção da correta orientação do resíduo His440 para que o processo catalítico ocorra (Barak e cols., 2002; Kaplan e cols., 2004).

Uma vez que o substrato, ACh, consiga chegar ao fundo do sítio ativo, onde se encontra a tríade catalítica, ocorre a catalise em si. Este processo de conversão da ACh em colina e acetato ocorre em dois estágios, o estágio de alquilação e o de desalquilação, onde ocorrem dois ataques nucleofílicos e duas transferências de prótons. Estes processos estão esquematizados na figura 4. No caso da AChE de *T. californica*, os resíduos Ser200 e His440 estão envolvidos na reação com o substrato ACh durante a catalise, e o resíduo Glu327 age como um estabilizador da carga da His440. A reação procede após a transferência de um próton da Ser200 para o anel imidazol da His400 e a

subsequente adição nucleofílica do átomo de oxigênio da Ser200 (na forma Ser-O⁻) ao substrato ACh e formação de um estado de transição tetraédrico. A His440 protonada é estabilizada pela carga negativa da Glu327. A estabilização das cargas existentes no estado de transição resulta no excepcional poder catalítico da AChE (Sant'anna e cols., 2006; Nemukhin e cols., 2008). Vale ressaltar que o resíduo His440 apresenta alta mobilidade durante o processo catalítico (Millard e cols., 1999a), e seu correto posicionamento é fundamental para obter uma atividade catalítica ótima. Este posicionamento é obtido pelo impedimento estérico pela Phe288 e pelas interações π com a Phe332 (Barak e cols., 2002; Kaplan e cols., 2004). O processo de alquilação é rapidamente seguido pela desalquilação, onde a acil-enzima formada é hidrolisada de volta a sua forma original, com a duração da acil-enzima formada sendo de aproximadamente 10 μ s.

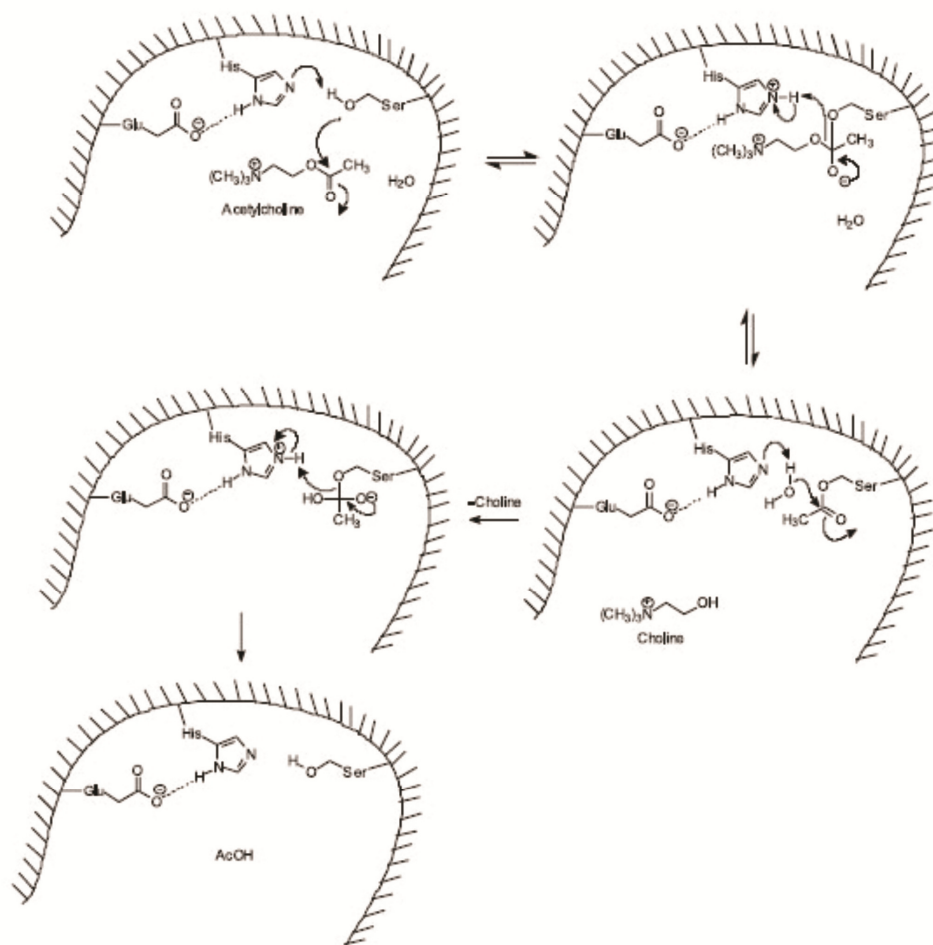


Figura 4 – Mecanismo da hidrólise da ACh pela AChE. Figura retirada de Delfino e cols., (2009).

Durante o processo catalítico, um intermediário acil-enzima é formado onde ocorre a presença de um grupamento carbonil (na forma C-O⁻) com carga negativa que precisa ser estabilizada. A presença de doadores de interações de hidrogênio ocorre em uma região contígua a tríade catalítica, chamada de “oxyanion hole” e contém os resíduos Gly118, Gly119 e Ala201, os quais formam interações de hidrogênio com o grupo carbonil (Harel e cols., 1996; Ordentlich e cols., 2004). Desta forma, estes resíduos contribuem para a estabilização do intermediário sem a necessidade de grandes modificações conformacionais, aumentando a eficiência catalítica da enzima.

1.2 Organofosforados

Os compostos organofosforados (OP) são compostos orgânicos, derivados principalmente de ésteres de fosfato, os quais apresentam uma ligação fosforil (P=O) ou tiosfosforil (P=S) (Gupta, 2006). A classificação de OPs é bastante complexa, pois apresenta grande variedade de cadeias laterais que podem ser ligadas ao átomo de fósforo, não havendo sistema de nomenclatura largamente aceito. O modo de classificação de OPs mais comum é baseado nos átomos e radicais ligados ao átomo central de fósforo e, de acordo com Gupta (2006), podem ser divididos em 13 diferentes subclasses, de acordo com a figura 5.

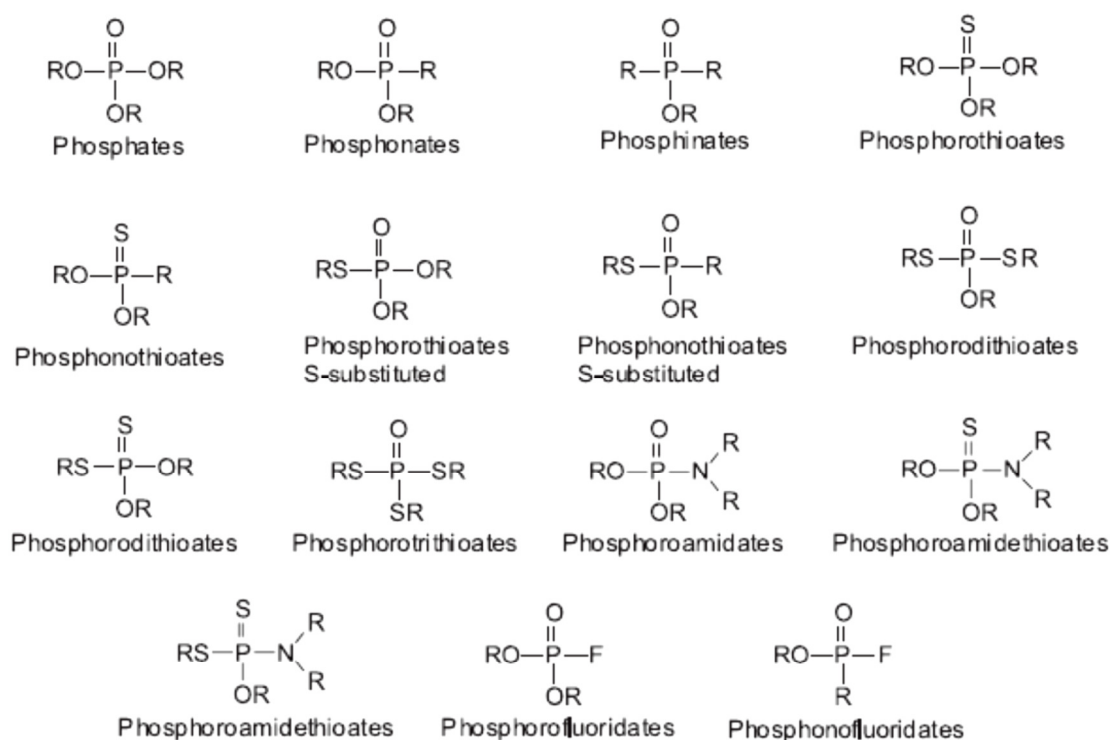


Figura 5 – Subclasses de compostos OPs, de acordo com Gupta (2006).

A descoberta dos efeitos tóxicos de OPs em insetos é do ano de 1937, cinco anos após o primeiro relato de toxicidade destes compostos em humanos. Em 1940, foi comprovado que a enzima AChE é o alvo principal de OPs em humanos, sendo posteriormente confirmado o mesmo mecanismo em insetos (Casida e Quistad, 2005).

Já na década de 1940, foi iniciado o uso de OPs como inseticidas, com uma grande expansão entre os anos de 1960 e 1980, quando gradualmente foram substituindo os inseticidas organoclorados (mais nocivos ao meio ambiente) (Santos e cols., 2007). Outros usos foram dados para tal classe de compostos, na segunda guerra mundial a Alemanha nazista desenvolveu uma série de compostos OPs para fins bélicos (Ecobichon, 1996). Alguns destes compostos inclusive chegaram a ser utilizados para tal fim, como no ataque aos Curdos no Iraque, em 1988 e no atentado terrorista a um metro em Tóquio no ano de 1995, nos quais foram utilizados o gás sarin (Ferrer e Cabral, 1995).

O mecanismo de ação dos compostos OPs envolve primariamente a inibição da AChE, reduzindo a hidrólise do neurotransmissor ACh. A acumulação de ACh nos receptores colinérgicos, resultante desta inibição enzimática, leva a super-estimulação de neurônios pós-sinápticos ou fibras musculares, que resulta em uma série de sintomas que podem ser divididos de acordo com o grau de envenenamento: em intoxicações leves a moderadas miose, sudorese, aumento das secreções brônquicas, salivação, lacrimejamento, vômitos, náuseas e diarreia, bradicardia e dores abdominais; no caso de intoxicações severas os principais sintomas são tremores e câimbras, hipertensão arterial, fasciculação e flacidez muscular que pode, eventualmente, resultar no óbito da vítima por parada respiratória ou edema pulmonar (Karasova e cols., 2009).

O tratamento médico dado a vítimas de envenenamento por OPs são praticamente os mesmo aplicados na intoxicação por outras substâncias tóxicas. Procura-se, inicialmente, terminar a exposição ao agente tóxico, seguido pela estabilização do paciente e administração dos antídotos adequados. No caso de contaminação por OPs, as drogas mais utilizadas são: a atropina, um agente anticolinérgico que antagoniza os efeitos da acumulação da ACh nos receptores

colinérgicos muscarínicos, porém sem atividade antagonista em receptores colinérgicos nicotínicos; o diazepam, depressor do sistema nervoso central que age como anticonvulsivante e reduz espasmos musculares frequentes em intoxicações com OPs; e uma oxima, como um reativador da enzima AChE (Jokanovic e Stojiljkovic, 2006).

Em nível molecular, a inibição da AChE por OPs envolve o ataque nucleofílico do resíduo de serina da tríade catalítica (Ser200 em *T. californica*, Ser203 na maioria dos mamíferos) ao átomo de fosforo do OP. Após a ligação do OP à Ser200, forma-se a enzima fosforilada que, ao contrário da AChE acetilada que rapidamente se converte em ácido acético, esta espécie enzima é bastante estável. A falta de atividade enzimática ocorre devido a serina da tríade catalítica se encontrar impedida de hidrolisar a ACh (Worek e cols., 2004; Majundar e cols., 2006). A figura 6 mostra um esquema geral da inibição da AChE por compostos OPs, que envolve inicialmente a formação de um complexo enzima-OP, seguida pela fosforilação e inativação da enzima, com a substituição de um dos grupos R do OP, chamado de grupo de saída, pelo oxigênio da serina da tríade catalítica. Tal complexo é estável, porém pode sofrer dois processos diferentes. Uma das possibilidades é a reativação espontânea devido ao potencial nucleofílico da água, com eliminação do OP. Tal tipo de reativação é lenta e pouco significativa em quadros clínicos de intoxicação aguda por OP, mas pode ser acelerado com o uso de outros nucleófilos tais como as oximas (Worek e cols., 2005). Outra possibilidade é que ocorra um processo chamado “aging” (figura 6), onde ocorre a quebra de uma ligação PO-C da enzima fosforilada, com a perda de um grupo alquila (Marrs, 2007). Após tal fenômeno a inibição se torna virtualmente irreversível, pois tal complexo passa a possuir uma carga negativa no sítio ativo, impedindo o ataque de nucleófilos à ligação O-P. Além disso, forças não-covalentes passam a estabilizar mais fortemente o complexo OP-AChE (Shafferman e cols., 1996; Millard e cols., 1999b).

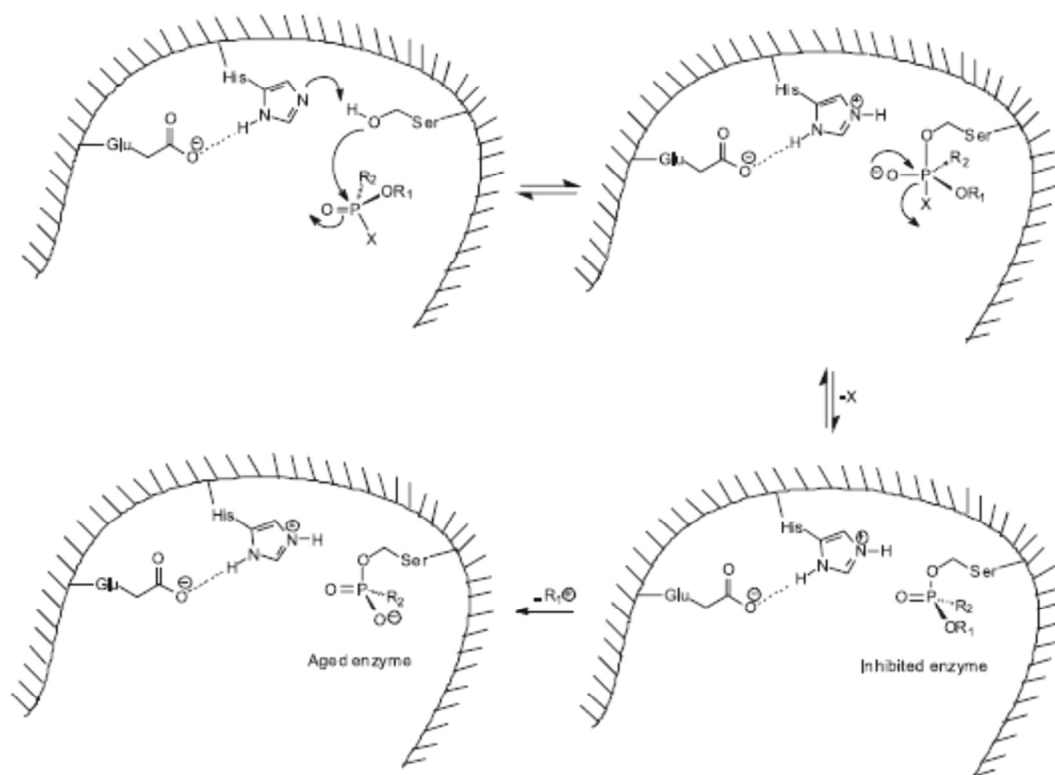


Figura 6 – Esquema da inibição da AChE por OPs. Figura retirada de Delfino e cols., (2009).

Dados mais recentes demonstram que o uso de OPs já representam cerca de 40% do mercado mundial de pesticidas (Santos e cols., 2007), sendo que a exposição acidental ou tentativas de suicídio usando OPs representam um sério problema de saúde pública, principalmente nos países de terceiro mundo. Relatório da Organização Mundial da Saúde (OMS) (Carlton e cols., 1998) estimou em aproximadamente 3 milhões de casos de intoxicação por ano com mais de 220.000 casos óbitos em decorrência da exposição a compostos OPs. Dentre estes compostos, destaca-se o uso indiscriminado do pesticida Tamaron (Moreira, 1995), cujo princípio ativo é o OP metamidofós, o qual tem sido relacionado com alta taxa de intoxicação em humanos (Recena e cols., 2006a e 2006b).

O metamidofós (O,S-dimetilfosforamidotioato; C₂H₈NO₂PS) (figura 7), é um pesticida de largo espectro de ação, e é obtido como subproduto do acefato. Este pesticida tem ampla aplicação no controle de pragas, sendo utilizado em culturas agrícolas muitas variadas, tais como: algodão, batata, feijão, tomate, tabaco, pimentão, milho, brócolis, couve-flor, repolho, morango, pêsego e soja (Hassal, 1990; ILSE, 1995). Tal composto é altamente tóxico, tanto na exposição por via oral e respiratória como por via cutânea. A dose letal mediana (LD₅₀) pela via oral é de 21 mg/kg em ratos e de 10-30 mg/kg em coelhos, gatos e cachorros. A LD₅₀ para a via inalatória é de 9 mg/kg em ratos e 19 mg/kg em camundongos. Outros animais da fauna, não considerados pragas, também são muito suscetíveis a intoxicação, tais como espécies de abelhas e pássaros (Gary e Lorenzen, 1989). A concentração letal mediana (LC₅₀) é de aproximadamente 35 mg/L em trutas, 46 mg/L em peixes do tipo *guppies* e 100 mg/L para carpas. Os crustáceos, em especial, apresentam alta suscetibilidade a intoxicação por metamidofós, sendo que concentrações de aproximadamente 2,2 x 10⁻⁷ mg/L são letais a larvas destas espécies (Chan e cols., 1996).

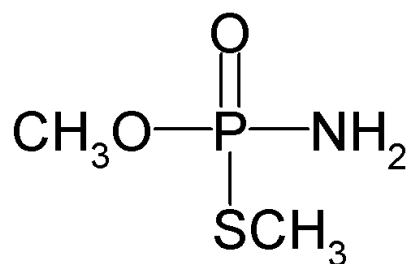


Figura 7 – Estrutura molecular do metamidofós.

Com relação à exposição humana ao metamidofós, vários dados na literatura indicam que ele talvez seja o OP mais utilizado pela comunidade rural. Araújo e cols. (2007) demonstraram que 90% dos agricultores da comunidade rural de Córrego de São Lourenço – RJ, utilizam tal composto, e alguns relataram sinais claros de envenenamento por OPs. No município de Paty do Alferes – RJ, o metamidofós é

utilizado em 53% das lavouras (Delgado e Paumgarten, 2004), e a maioria dos agricultores admitiram não usar qualquer tipo de proteção. Em longo estudo de Soares e cols. (2003), que durou de 1991 até 2000, foi verificado que o metamidofós foi o agrotóxico mais utilizado, correspondendo a 39,61% dos trabalhadores rurais. Também foi feita a dosagem de colinesterases, que revelou que cerca de 50% destas pessoas se mostravam intoxicadas.

1.3 Oximas

A terminação oxima foi definida no século XIX, e provem dos termos oxigênio e imida (oxigênio+imida = oxima). Tais compostos são caracterizados pela presença de um grupo $C=N-OH$, e tem por fórmula geral R_1R_2CNOH , podendo ser classificadas como aldoximas ou cetoximas, de acordo com os grupos R presentes na molécula. As aldoximas provêm da condensação de um aldeído com uma porção hidroxilamida (NH_2OH) e são caracterizadas pela presença de uma cadeia lateral orgânica e outra com a presença de somente um hidrogênio. As cetoximas, por sua vez, derivam da condensação de uma porção hidroxilamida com uma cetona, e apresentam as duas cadeias laterais orgânicas ligadas ao carbono do grupo oxima (Arena, 1979).

As oximas são compostos utilizados farmacologicamente no tratamento de intoxicação por pesticidas OPs. Sua ação antídoto se deve primariamente a sua habilidade de reativar a AChE fosforilada (Wilson, 1992). De maneira geral, o processo de reativação consiste de dois passos: primeiro, ocorre à formação de um complexo OP-AChE-oxima, seguido da retirada da ligação oxima-fosfato deste complexo (figura 8). O oxigênio do grupo oxima é capaz de atacar a ligação do átomo de fosfato ao oxigênio Ser200, devido ao seu alto poder nucleófilo, sendo este ataque pode ser facilitado pela

polarização da ligação fosforil, que se encontra aumentada pela influência dos resíduos Gly120, Gly121 e Ala204 (na AChE humana) que constituem a região chamada de “oxyanion hole” (Wong e cols., 2000).

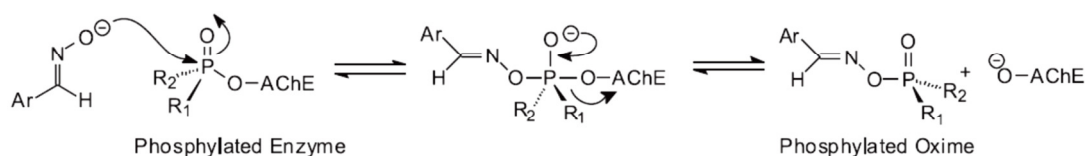


Figura 8 – Reativação da AChE fosforilada por oximas. Figura retirada de Delfino e cols., (2009).

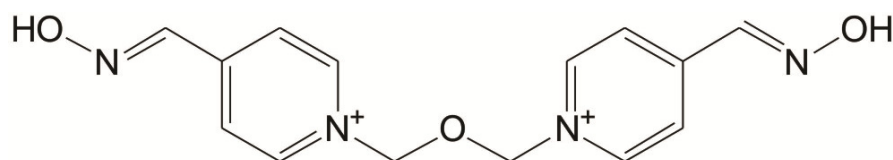
Usualmente, é considerado que a oxima reage na sua forma desprotonada (oximato) no processo de reativação. Porém, Castro e Figueroa-Villar (2002) demonstraram que, ao menos para a pralidoxima, a forma protonada apresenta maior densidade eletrônica ao redor do oxigênio do grupo oxima, levantando, então, a hipótese que as formas protonadas destes compostos podem ser as formas mais vantajosas no processo de reativação.

O processo de reativação só ocorre se um dos substituintes ligados ao átomo de fósforo não foram hidrolisados, ou seja, se não ocorreu o processo de “aging”. A taxa de reativação das diferentes oximas depende de vários fatores, sendo os principais: da concentração e da estrutura molecular da oxima, da estrutura da ligação fosforil ligado a enzima, e da taxa de desalquilação (“aging”). Outro fator que pode afetar o processo de reativação é a excessiva formação de fosforil-oximas estáveis, as quais são produzidas como produto do processo de reativação e, muitas vezes, tem atividade anticolinesterásica superior ao próprio inibidor inicial (Harvey e cols., 1986). Contudo, em situações fisiológicas, fosforil-oximas são usualmente instáveis, dependendo de qual oxima e OP está envolvido no processo de inibição e reativação da AChE. Além disso,

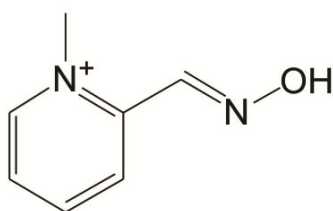
tais produtos da reativação podem ser hidrolisados por enzimas hidrolases, principalmente a paraoxonase (PON) (Luo e cols., 1999).

Duas das principais oximas disponíveis na clínica atualmente são, a pralidoxima e a obidoxima (figura 9). A pralidoxima foi primeiramente sintetizada nos Estados Unidos em 1955 (Wilson e Gisnburg, 1955), e foi demonstrada ser eficiente na reativação da AChE inibida pelos OPs sarin e VX (O-ethyl S-[2-(diisopropylamine)ethyl]-methyl-phosphonothioate), dois dos principais OPs desenvolvidos com propósitos homicidas (Harris e Stitche, 1983, Mesic e cols., 1991; Masuda e cols., 1995; Nozaki e cols., 1995), porém se mostrou inefetivo na reativação da enzima inibida pelos OPs tabun e soman (Inns e Leadbeater, 1983; Boskovic e cols., 1984). Uma das principais limitações desta oxima, como um sal de piridina quaternário, é não penetrar a barreira cérebro-sangue (BBB) e, portanto, não atuar diretamente no sistema nervoso central. Para reverter tal situação, foi tentado sintetizar a pralidoxima numa forma de pró-droga, que atravessaria a barreira cérebro-sangue e seria metabolizada, e ativada, diretamente no cérebro. Surpreendentemente, tal composto se mostrou menos efetivo em combater o envenenamento com paraoxon do que a própria pralidoxima (Boskovic e cols., 1980). Evidências apontam que a pralidoxima poderia, ao menos em parte, passar a BBB quando aplicada com atropina (Stojilkovic e cols., 2001) e o próprio processo de envenenamento pode causar danos a BBB, diminuindo sua seletividade e, desta maneira, aumento o acesso de oximas ao sistema nervoso central (Shrot e cols., 2009). Por fim, a experiência clínica com o uso da pralidoxima, no tratamento das vítimas do ataque de Tóquio com gás sarin, se mostrou extremamente favorável (Stojilkovic e Jokanovic, 2005), sendo uma das drogas indicadas no caso de envenenamento por OPs, mesmo não apresentando amplo espectro de ação contra diferentes OPs.

A obidoxima, também conhecida pelo nome LüH-6 em homenagem a Lüttringhaus e Hagedorn que pela primeira vez sintetizaram tal composto (Lüttringhaus e Hagedorn, 1964), apresenta um significativo efeito protetor em experimentos com animais contra a intoxicação induzida pelos OPs tabun (Inns e Leadbeater, 1983; Maksimovic e cols., 1989), sarin (Inns e Leadbeater, 1983) e VX (Maksimovic e cols., 1989). Porém, tal como a pralidoxima, não apresentou efeito antídoto contra a intoxicação com soman em camundongos (Heilbronn e Tolagen, 1965), porcos da Índia (Inns e Leadbeater, 1983) e primatas (Hamilton e Lundy, 1989).



Obidoxime



Pralidoxime

Figura 9 – Estrutura molecular da pralidoxima e obidoxima.

Recentemente, nosso grupo de pesquisa tem estudado os efeitos biológicos de novas oximas. Dentre as moléculas estudadas até o momento, se destaca a atividade dos compostos butano-2,3-dionatiosemicarbazona oxima e a 3-(fenilhidrazona)butan-2-one oxima, em reativar a AChE inibida pelos OPs clorpirifós, diazinon e malation (Costa e cols., 2011). Além de terem sido relacionadas com sua atividade antioxidante, e não apresentarem sinais de toxicidade após uso *in vivo* e *ex vivo* (Puntel e cols., 2008 e

2009), com valores de LD50 similares aos obtidos com pralidoxima e obidoxima (Arena, 1979).

1.4 Justificativas

Há uma forte correlação entre a inibição da AChE e os efeitos tóxicos de compostos OPs, sendo as oximas os únicos reativadores da AChE disponíveis na clínica. Neste sentido, o metamidofós tem sido relatado como o OP mais utilizado em cultivos agrícolas no Brasil, com alta taxa de intoxicação tanto por via ocupacional como alimentar. As oximas usadas atualmente no combate ao envenenamento do OPs apresentam a desvantagem de não apresentarem amplo espectro de ação, sendo efetivas com apenas alguns OPs, e apresentarem efeitos tóxicos significantes. Desta maneira, faz-se vital a procura por novos compostos com potencial reativador sobre a atividade da AChE e com baixa toxicidade. Para tal, tem-se empregado uma série de modelos computacionais que visam prever e quantificar a conformação e as energias de interação entre um ligante e uma enzima. Tais métodos tem a vantagem de poderem triar grande quantidade de compostos em tempo, e com custo, muito menores que os tradicionais testes experimentais, além de detalharem relações estruturais que ocorrem no processo de ligação do ligante à enzima, informações que podem ser usadas para a racionalização da síntese de novas moléculas. Desta forma, este trabalho visa a aplicação de ferramentas computacionais e experimentos *in vitro* para determinar a efetividade de novos compostos - butano-2,3-dionatiosemicarbazona oxima, 3-(fenilhidrazona)butan-2-one oxima e isatina-3-N⁴-benziltiosemicarbazona - em reativar a AChE e relacionar a estrutura molecular destes compostos a sua atividade reativadora, buscando novos parâmetros para o desenho de novas moléculas com atividade sobre a AChE. Além

disso, este trabalho também objetiva testar os efeitos tóxicos de um novo composto, que apresentou potencial farmacológico, em camundongos.

1.5 Objetivos

1.5.1 Objetivo Geral

O objetivo geral desta tese consiste em avaliar a atividade dos novos compostos sobre a atividade da AChE inibida por metamidofós, tanto em modelos *in vitro* como *in silico*. Bem como avaliar parâmetros toxicológicos da isatina-3-N⁴-benziltiosemicarbazona composto com potencial farmacológico.

1.5.2 Objetivos Específicos

Análises *in vitro*

- Avaliar a capacidade dos compostos butano-2,3-dionatiosemicarbazona oxima, 3-(fenilhidrazona)butan-2-one oxima e isatina-3-N⁴-benziltiosemicarbazona em reativar a AChE inibida por metamidofós, em comparação com a obidoxima e a pralidoxima.
- Avaliar os efeitos reativadores dos novos compostos na enzima BChE inibida por metamidofós, em comparação com a obidoxima e a pralidoxima.

Análises *in silico*

- Analisar a conformação mais provável adotada pelos compostos no sítio ativo da AChE inibida por metamidofós.
- Avaliar as contribuições específicas de cada resíduo de aminoácido da AChE para a ligação das oximas no sítio ativo da enzima inibida por metamidofós.

Análises *ex vivo*

- Analisar parâmetros bioquímicos de toxicidade do novo composto isatina-3-N⁴-benziltiosemicarbazona (IBTC).

2 ARTIGOS CIENTÍFICOS

Os resultados que fazem parte desta tese estão apresentados sob a forma de artigos científicos (2) e manuscritos (1). Os itens Materiais e Métodos, Resultados, Discussão e Referências Bibliográficas, encontram-se nos próprios artigos e manuscritos. Um dos **artigos** está disposto na forma com que foi publicado na revista Toxicology in Vitro, enquanto o segundo trabalho encontra-se na forma como foi submetido à revista Basic and Clinical Pharmacology and Toxicology. O **manuscrito** está disposto na forma em que normalmente se submete para publicação.

2.1 Artigo 1: “Isatina-3-N⁴-benzilthiosemicarbazona, um derivato não-tóxico da tiosemicarbazona, protege e reativa colinesterases de ratos e humanos inibidas por metamidofós *in vitro* e *in silico*.”

Toxicology in Vitro
Doi: 10.1016/j.tiv.2012.04.008

Isatin-3-N⁴-benzilthiosemicarbazone, a non-toxic thiosemicarbazone derivative, protects and reactivates rat and human cholinesterases inhibited by methamidophos in vitro and in silico

Rômulo Pillon Barcelos, Rafael de Lima Portella, Thiago Henrique Lugokenski,
Edovando José Flores da Rosa, Guilherme Pires Amaral, Luiz Filipe Machado Garcia,
Leandro Bresolin, Vanessa Carratu, Félix Alexandre Antunes Soares, Nilda Berenice de

Vargas Barbosa



Contents lists available at SciVerse ScienceDirect

Toxicology in Vitro

journal homepage: www.elsevier.com/locate/toxinvit

Isatin-3-N⁴-benzylthiosemicarbazone, a non-toxic thiosemicarbazone derivative, protects and reactivates rat and human cholinesterases inhibited by methamidophos in vitro and in silico

Rômulo Pillon Barcelos^a, Rafael de Lima Portella^a, Thiago Henrique Lugokenski^a, Edovando José Flores da Rosa^a, Guilherme Pires Amaral^a, Luiz Filipe Machado Garcia^a, Leandro Bresolin^b, Vanessa Carratu^b, Félix Alexandre Antunes Soares^{a,*}, Nilda Berenice de Vargas Barbosa^a

^a Departamento de Química, Centro de Ciências Naturais e Exatas, Universidade Federal de Santa Maria, Campus UFSM, 97105-900 Santa Maria, RS, Brazil

^b Departamento de Química, Fundação Universidade de Rio Grande, Campus Carreiros, Rio Grande, RS, Brazil

ARTICLE INFO

Article history:

Received 8 February 2012
Accepted 10 April 2012
Available online xxxx

Keywords:

Antioxidant
Cholinesterases
Molecular docking
Thiosemicarbazones
Methamidophos

ABSTRACT

Organophosphates (OPs), which are widely used as pesticides, are acetylcholinesterase (AChE) and butyrylcholinesterase (BChE) inhibitors. The inactivation of AChE results in the accumulation of acetylcholine at cholinergic receptor sites, causing a cholinergic crisis that can lead to death. The classical treatment for OP poisoning is administration of oximes, but these compounds are ineffective in some cases. Here we determined whether the new compound isatin-3-N⁴-benzylthiosemicarbazone (IBTC), which in our previous study proved to be an antioxidant and antiatherogenic molecule, could protect and reactivate AChE and BChE. Toxicity of IBTC after subcutaneous injection in mice was measured using assays for oxidized dichlorofluorescein (DCF), thiobarbituric acid reactive substances (TBARS), non-protein thiol (NPSH) levels, and catalase (CAT), sodium potassium (Na⁺/K⁺) ATPase, delta-aminolevulinic acid dehydratase (ALA-D), and glutathione peroxidases (GPx) enzyme activities. The cytotoxicity was evaluated and the enzymatic activity of cholinesterase was measured in human blood samples. Molecular docking was used to predict the mechanism of IBTC interactions with the AChE active site. We found that IBTC did not increase the amount of DCF-RS or TBARS, did not reduce NPSH levels, and did not increase CAT, (Na⁺/K⁺) ATPase, ALA-D, or GPx activities. IBTC protected and reactivated both AChE and BChE activities. Molecular docking predicted that IBTC is positioned at the peripheral anionic site and in the acyl binding pocket of AChE and can interact with methamidophos, releasing the enzyme's active site. Our results suggest that IBTC, besides being an antioxidant and a promising antiatherogenic agent, is a non-toxic molecule for methamidophos poisoning treatment.

© 2012 Elsevier Ltd. All rights reserved.

1. Introduction

Organophosphates (OPs), which inhibit cholinesterase, have been widely used as pesticides and additives for lubricants and have been developed as warfare nerve agents (WHO, 1993). The toxic action of OPs is related to the binding of these compounds to the active site of the acetylcholinesterase enzyme (AChE; EC 3.1.1.7), thus inhibiting hydrolysis of the acetylcholine neurotransmitter (ACh) at central and peripheral synapses (Holmstedt, 1959; Taylor et al., 1995). The inactivation of AChE results in an accumulation of acetylcholine at cholinergic receptor sites and a cholinergic crisis that can lead to death, usually via respiratory failure due to paralysis of the diaphragm and intercostal muscles, as well as

cerebral respiratory center depression and excessive bronchial secretion (Marrs, 1993).

The enzymes associated with antioxidant defense mechanisms are altered under the influence of pesticides, leading to an imbalance between generation of oxidant molecules and intracellular antioxidant systems (Banerjee et al., 1999), which may induce oxidative stress in rats (Gultekin et al., 2000; Gupta et al., 2001), mice (da Silva et al., 2006, 2008), and humans (Banerjee et al., 1999). Moreover, OPs cause lipid peroxidation in rat brains (Verma and Srivastava, 2001) and human erythrocytes (Gultekin et al., 2000). However, the exact mechanism by which OPs induce oxidative damage is not fully understood (Abdollahi et al., 2004).

Methamidophos (MAP) is an OP and a potent AChE inhibitor used to control insects that plague a variety of crops such as brassaica, cotton, tobacco, sugar beet, lettuce, potatoes, and tree fruits (WHO, 1993). MAP is highly toxic to aquatic organisms (Tomlin, 1994) and mice (Zayed et al., 1984). It also has anticholinesterase

* Corresponding author. Tel.: +55 55 3220 9522.

E-mail addresses: felix_antunes_soares@yahoo.com.br, felix@ufsm.br (F.A.A. Soares).

activity in humans (Worek et al., 2007, 2004). Acetylcholinesterase (AChE) inhibition by OPs can generally be reversed by treatment with oximes (Worek et al., 2004). However, there is a need for more efficient compounds with broader reactivation activity after exposure to different OPs and that are less toxic to humans.

The crystal structure of AChE (Bourne et al., 1995; Ekström et al., 2006; Kryger et al., 1998; Sussman et al., 1991) allows for detailed structural studies on ligand access to the enzyme's active center gorge and the steric constraints within the active center gorge that govern selectivity during reactivation (Ashani et al., 1995; Grosfeld et al., 1996; Kovarik et al., 2004; Wong et al., 2000). The orientation of the compound within the narrow confines of the gorge when the active serine is phosphorylated is an important determinant of the reactivation mechanism (Musilek et al., 2011). There are several *in silico* studies that illustrate the ability of this structural model to reliably predict molecular interactions.

There is considerable interest in thiosemicarbazones due to their wide pharmacological utility (Beraldo and Gambino, 2004) and versatility as ligands. They have recently been investigated as radical scavengers (Wada et al., 1994) and our previous study (Barcelos et al., 2011) revealed that a thiosemicarbazone derivative, isatin-3-*N*⁴-benzilthiosemicarbazone (IBTC), is also effective as an antioxidant and antiatherogenic molecule. Although the use of thiosemicarbazone as an antiatherogenic molecule has been suggested previously (Barcelos et al., 2011), *in vitro* and *in vivo* toxicological screening is still needed.

Therefore, the aim of this study was to test the toxicological effects of IBTC, a thiosemicarbazone derivative, and to identify the effective concentration of IBTC for protecting and reactivating cholinesterases after exposure to MAP. In addition, any possible inhibitory effects of IBTC on the thiol-containing enzymes from the blood/liver and brain, namely delta-aminolevulinic acid dehydratase (ALA-D) and Na⁺/K⁺-ATPase, respectively, were also evaluated. Docking studies were carried out *in silico* to evaluate the minimal energy IBTC conformations in the active site of human AChE when the active site serine is phosphorylated by MAP.

2. Materials and methods

2.1. Synthesis of isatin-3-*N*⁴-benzilthiosemicarbazone

The synthesis of isatin-3-*N*⁴-benzilthiosemicarbazone (IBTC) was performed as described previously (Fonseca et al., 2010) and the chemical structure of IBTC is depicted in Fig. 1.

2.2. Chemical reagents

The reagents thiobarbituric acid (TBA), dichlorofluorescein diacetate (DCFH-DA), methyltetrazolium (MTT), ethylene glycol tetraacetic acid (EGTA), Ellman's reagent (5,5'-dithiobis-(2-nitrobenzoic acid) or DTNB), *N,N,N,N*-tetramethylbenzidine and ouabaine were supplied by Sigma-Aldrich Chemical Co. (St. Louis, MO); acetylthiocholine iodide supplied by Merck. The other used reagents were obtained from local suppliers.

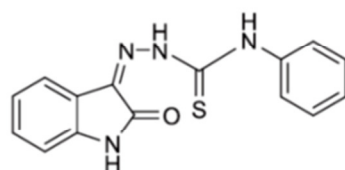


Fig. 1. Chemical structure of IBTC.

2.3. Separation of human red blood cells

Human red blood cells (RBC) were separated from heparinized blood that was drawn from a healthy donor. The blood was centrifuged at 2000 rpm for 10 min to separate the RBCs from plasma, then the RBCs were washed three times with phosphate-buffered saline (PBS) at pH 7.4.

2.4. Isolation of lymphocytes from human blood

Lymphocytes were isolated from human blood collected from a healthy donor with EDTA and separated on Ficoll-Histopaque density gradients as described previously (Böyum, 1968).

2.5. Cell culture

Cell culture Murine J774 macrophage-like cells were obtained from the American Type Culture Collection (ATCC, Rockville, MD, USA). These cells were maintained with Dulbecco's Modified Eagle Medium (DMEM) supplemented with 2 mM glutamine, 10 mM HEPES, 100 U/mL penicillin, 100 µg/mL streptomycin and 10% fetal bovine serum (FBS) in a 5% CO₂ humidified atmosphere at 37 °C.

2.6. Experimental animals

Untreated adult male swiss albino mice (25–30 g) were obtained from our own breeding colony. The animals were maintained in an air conditioned room (20–25 °C) under a 12 h light/dark cycle, and with water and food *ad libitum*. All the experimental procedures performed were conducted according to the guidelines of the Committee of Ethics in Research of the Federal University of Santa Maria, Brazil.

2.7. Animal treatment

Adult male swiss albino mice received a single subcutaneous injection of the IBTC dissolved in DMSO in different doses (1, 10, 50, 100, 250 or 500 mg/kg) (*n* = 4 animals/dose). Control animals received DMSO at 5 mL/kg. To determine the potential lethality of the IBTC, animals were observed for up to 24 h after compound administration. LD₅₀ was calculated using "GraphPad Software" (GraphPad Software, San Diego, CA). After this period, animals were euthanized by cervical dislocation. The liver, kidney, heart and brain were quickly removed, placed on ice, and homogenized within 10 min, in 10 volumes of cold Tris 10 mM (pH 7.4). The homogenates were centrifuged at 4000g at 4 °C for 10 min to yield a low-speed supernatant fraction (S1) for each tissue that was used for *ex vivo* analysis.

2.8. Whole blood and blood components

Mice were euthanized and the whole blood was collected (cardiac puncture) in previously heparinized tubes and kept under refrigeration. Whole blood samples were precipitated with TCA 40% (1:1) and centrifuged (4000g at 4 °C for 10 min) in order to obtain the supernatant fraction that was used for non protein thiol measurement determination. Other heparinized blood samples were used for Delta Aminolevulinic Dehydratase (δ-ALA-D) activity measurement and other were centrifuged at 1000g at 4 °C for 10 min in order to obtain cellular blood fractions which were used for oxidized dichlorofluorescein and Delta Aminolevulinic Dehydratase (δ-ALA-D) activity measurement (Puntel et al., 2011).

2.9. Oxidized dichlorofluoresceine (DCF-RS) levels

DCF-RS levels were determined as an index of the peroxide production by the cellular components (Myhre et al., 2003). Aliquots cellular blood fraction (10 μ L) or liver, kidney, heart and brain S1 (50 μ L) were added to a medium containing Tris–HCl buffer (0.01 mM; pH 7.4) and DCFH-DA (7 μ M). After DCFH-DA addition, the medium was incubated in the dark for 1 h until fluorescence measurement procedure (excitation at 488 nm and emission at 525 nm and both slit widths used were at 5 nm). DCF-RS levels were determined using a standard curve of DCF and the results were corrected by the protein content (Pérez-Severiano et al., 2004).

2.10. Thiobarbituric acid reactive substances (TBARS) levels

Analyses were performed in liver, kidney, heart and brain S1 samples according to the method described previously (Pérez-Severiano et al., 2004). Aliquots of 200 μ L of liver, kidney, heart and brain S1 were added to color reaction. TBARS levels were measured at 532 nm using a standard curve of MDA and corrected by the protein content (Ohkawa et al., 1979).

2.11. Catalase (CAT)

The CAT enzyme activity was determined in liver, kidney and heart S1 according to the method proposed by Aebi H (Aebi, 1984). Briefly, S1 aliquot (50 μ L) was added to a medium containing potassium phosphate buffer (50 mM; pH 7.4) and H₂O₂ (1 mM). The kinetic analysis of CAT was started after H₂O₂ addition and the color reaction was measured at 240 nm. One unit of the enzyme is considered as the amount which decomposes 1 μ mol H₂O₂/min at pH 7.

2.12. Sodium potassium (Na⁺/K⁺) ATPase

The cerebral Na⁺/K⁺ATPase enzyme activity was determined in brain S1 samples according to the method proposed by Muszbek et al. (1977), with some modifications. Briefly, the aliquots of skeletal muscle S1 (20 μ L) were added to a reaction medium containing NaCl (115 mM), MgCl₂ (2.5 mM), KCl (18 mM) and Tris–HCl buffer (45 mM and pH 7.4), with or without the Na⁺/K⁺ ATPase enzyme inhibitor ouabaine (5 μ M). The method for ATPase activity measurement was based on the determination of the inorganic phosphate (Pi) released to the reaction medium by the hydrolysis of the ATP according to the method proposed by Atkinson A (Atkinson et al., 1973). The reaction was initiated with the addition of the substrate ATP (1.5 mM) to the reaction medium and was finished by the addition of the color reagent (1 mL) containing ammonium molybdate (2%), Triton-X 100 (5%) and H₂SO₄ 1.8 M (10%) after 15 min of incubation at 37 °C. The formed molybdate–Pi complexes were measured spectrophotometrically at 405 nm. Values were calculated in relation to a standard curve constructed with Pi at known concentrations and corrected by the protein content.

2.13. Delta Aminolevulinatase (δ -ALA-D) activity assay

The enzyme was assayed as described previously (Sassa, 1982) by measuring the rate of product porphobilinogen (PBG) formation. After 10 min of pre-incubation with homogenized liver or total blood from treated mice at 37 °C, in a medium containing 100 mM potassium phosphate buffer, pH 6.8, the enzymatic reaction was initiated by adding the substrate aminolevulinic acid (ALA) to a final concentration of 2.5 mM. The incubation was carried out for 1 h, at 37 °C, and was stopped by adding 10% TCA containing 10 mM HgCl₂. The reaction product was determined using a

modified Ehrlich's reagent at 555 nm, with a molar absorption coefficient of 6.1×10^4 for the Ehrlich porphobilinogen salt. The enzyme activity was expressed in percent of the control.

2.14. Glutathione peroxidases (GPx) assay.

GPx was determined as described previously (Paglia and Valentine, 1967). Tissue supernatants (200–400 μ g protein) were added to the assay mixture consisting of 1 mM sodium azide, 1 mM GSH, 50 mM potassium phosphate (pH 7.0), and 0.1 unit of glutathione reductase. Reaction was started by the addition of hydrogen peroxide (H₂O₂) to give a final concentration of 0.4 mM. Conversion of NADPH to nicotinamide adenine dinucleotide phosphate (NADP⁺) was monitored continuously at 340 nm for 2 min. GPx activity was expressed as nmol of NADPH oxidized per minute per milligram of protein, using an extinction coefficient 6.22×10^6 M⁻¹ cm⁻¹ for NADPH.

2.15. Non protein thiol measurement (NPSH)

To estimate GSH content we determined NPSH as follows: 500 μ L of 10% TCA was added to 500 μ L of either the S1 homogenates of liver, or kidney, or heart or brain. After centrifugation (4000g at 4 °C for 10 min), the protein pellet was discarded and free –SH were determined in the clear supernatant (which was previously neutralized with 0.1 M NaOH) according to Ellman (1959).

2.16. Cytotoxicity assays

2.16.1. Percent of hemolysis in human red blood cells

The 5% suspension RBCs in PBS (pH 7.4) was incubated under air atmosphere at 37 °C for 240 min, into IBTC concentrations from 10 to 200 μ M were added to the medium. The reaction mixture was shaken gently while being incubated at 37 °C. The extent of hemolysis was determined spectrophotometrically as described previously (Kuang et al., 1994). Briefly, aliquots of the reaction mixture were taken out at appropriate time intervals, diluted with NaCl (0.15 M), and centrifuged at 2000 rpm for 10 min to separate the RBCs. The percentage hemolysis was determined by measuring the absorbance of the supernatant at 540 nm and compared with that of complete hemolysis by treating the same RBC suspension with distilled water.

2.16.2. MTT assay

Percent cytotoxicity of IBTC was assessed using the 3-(4,5-dimethylthiazol-2-yl)-2, 5-diphenyl tetrazolium bromide (MTT) assay as described previously (Mosmann, 1983). Briefly, Murine J774 macrophage-like cells (1×10^4) were allowed to adhere for 24 h under high humid environment in 5% CO₂ at 37 °C in 96 well culture plates. Also human lymphocytes were freshly isolated as described previously (Böyum, 1968) and plated in 96-well flat bottom tissue culture plate at a concentration of 1×10^5 cells/well containing 200 μ L of RPMI-1640 supplemented with 10% FCS tissue culture medium. Then, for the both type of cells, IBTC concentrations from 10 to 200 μ M were added to the medium and incubated for 24 h. After the respective exposure, MTT (5 mg/ml of stock in PBS) was added (10 μ L/well in 100 μ L of cell suspension), and plates were incubated for 4 h. At the end of incubation period, 200 μ L of DMSO was added to each well. The plates were kept on shaker for 5 min at room temperature and then read at 550 nm using FisherBiotech Microkinetics Reader BT 2000. Untreated sets were also run under identical conditions and served as basal control.

2.17. Cholinesterase's activity

2.17.1. Preparation of erythrocyte ghosts and plasma

Hemoglobin-free erythrocyte ghosts were prepared as previously described (Worek et al., 2002) with minor modifications. Briefly, blood of non-fasted healthy voluntary donors was collected. Heparinised human blood was centrifuged (3000g, 10 min) and the plasma removed and kept to test butyrylcholinesterase activity. Erythrocytes were washed three times with two volumes of sodium/potassium phosphate buffer (0.1 M, pH 7.4). Then, the packed erythrocytes were diluted in 20 volumes of hypotonic sodium/potassium phosphate buffer (6.7 mM, pH 7.4) to facilitate the hemolysis, followed by centrifugation at 30,000g (30 min, 4 °C). The supernatant was removed and the pellet resuspended in hypotonic phosphate buffer. After two additional washing cycles, the pellet was resuspended in sodium/potassium phosphate buffer (0.1 M, pH 7.4), passed through one more centrifugation at 30,000g (30 min, 4 °C) and were kindly removed. Next, the AChE activity was adjusted to the original activity by appropriate dilution with phosphate buffer (0.1 M, pH 7.4). Aliquots of the erythrocyte ghosts were stored at –20 °C until use.

Hemoglobin content present in ghost membranes was measured at 540 nm as the cyano-met-Hb form, but no hemoglobin was detected.

2.17.2. Measure of cholinesterases activity

Ghost erythrocyte acetylcholinesterase and human plasma butyrylcholinesterase activities were estimated by Ellman method (Ellman et al., 1961), using acetylthiocholine iodide as substrate. The rate of hydrolysis of acetylthiocholine iodide is measured at 412 nm through the release of the thiol compound that, when reacted with DTNB, produces the color-forming compound TNB. Whole blood AChE was measured by Ellman method (Ellman et al., 1961) with modifications (Worek et al., 1999a,b). For butyrylcholinesterase activity, the same protocol was used, but butyrylthiocholine iodide was used as the substrate.

2.17.3. Reactivation/protection of OP-inhibited cholinesterase

Ghost erythrocyte acetylcholinesterase and human plasma butyrylcholinesterase were exposed to IBTC in two different assay conditions in order to identify a possible protective or a reactivation capacity of IBTC:

- Protection: the enzyme was exposed to methamidophos (MAP) 25 µM and IBTC (10–100 µM) at the same time into a total incubation period of 60 min.
- Reactivation: the enzyme was firstly exposed to MAP 25 µM by 10 min (estimated time before aging). After this, the IBTC (10–100 µM) tested was added into the medium and the incubation followed by 50 min (to perform an equal total incubation time period of 60 min). Enzyme activities were referred to control activity.

The different protocols aim to test the prophylactic and therapeutic effect of IBTC on MAP-induced AChE inhibition.

2.18. Protein determination

The protein content was determined as described previously (Lowry et al., 1951) using bovine serum albumin (BSA) as standard.

2.19. Molecular docking

Docking simulations of the oximes with *Mus musculus* AChE were carried out using AutoDock Vina 1.1.1 (Trott and Olson,

2010), followed by redocking with Autodock 4.0.1. The non-aged MAP-inhibited *Mus musculus* AChE obtained from the RCSB Protein Data Bank (<http://www.rcsb.org/pdb/>) was used as macromolecule (PDB code 2jge). IBTC was constructed using the program Avogadro 0.9 and their geometry were optimized with the MMFF 94 force field. Both ligand and macromolecule are previously prepared using AutoDock Tools (Morris et al., 2009) and Chimera 1.5 (Pettersen et al., 2004). All rotatable bonds within the ligands were allowed to rotate freely, and the receptor was considered rigid. The grid was centered on the active site of from AChE and the dimensions of the grid box were consisted of 30 Å × 22 Å × 30 Å points, with spacing of 1 Å. The exhaustiveness was set to 50. All other parameters were used as defaults. For the ligand docked, the conformation from the lowest binding free energy with inferred inhibitory reactivity was accepted as the best affinity model. The redocking calculation were carried out using Autodock 4.0.1, following method of Musilek et al. (2011). Briefly, a Lamarckian genetic algorithm (Amber force field) was used, and a population of 150 individuals and 2500,000 function evaluations were applied. The structure optimization was performed for 27,000 generations. Docking calculations were set to 100 runs. At the end of calculation, Autodock performed cluster analysis. The 3D affinity grid box was designed to include the full active and peripheral site of AChE. The number of grid points in the x-, y- and z-axes was 60, 60 and 60 with grid points separated by 0.253 Å. The conformations and interactions were analyzed using the programs Accelrys Discovery Studio Visualizer 2.5 and PyMOL (Seeliger and de Groot, 2010).

2.20. Statistical analysis

Data are expressed as means ± SEM. Statistical analysis was performed using one-way analysis of variance (ANOVA), followed by Student–Newman–Keuls test when appropriate. In addition, linear regression was performed to identify a possible dose dependent effect. Values of $p < 0.05$ were considered significant.

3. Results

3.1. Ex vivo toxicology screening

Table 1 shows that IBTC did not significantly affect DCF-RS levels in tissue homogenates. In addition, lipid peroxidation, indicated by TBARS levels (Table 2), did not change significantly in liver, kidney, or brain homogenates after treatment with any concentration of IBTC. However, there was a significant reduction in TBARS level in heart homogenates after treatment with most of the concentrations of IBTC. NPSH levels did not change in liver, kidney,

Table 1
Effect of IBTC treatment on DCF-RS levels on liver, kidney, heart and brain homogenates.

	DCF-RS levels (Mean ± SEM)			
	Liver	Kidney	Heart	Brain
Control	100.00 ± 0.95	100.00 ± 1.13	100.00 ± 2.26	100.00 ± 1.08
1 mg/kg	115.73 ± 5.63	109.41 ± 0.72	88.4 ± 5.02	95.26 ± 6.21
10 mg/kg	114.10 ± 4.98	104.91 ± 2.13	93.52 ± 6.15	92.04 ± 1.94
50 mg/kg	107.24 ± 3.69	102.86 ± 1.32	110.08 ± 1.25	103.39 ± 2.54
100 mg/kg	115.16 ± 5.68	101.41 ± 1.54	89.03 ± 4.51	80.10 ± 6.20
250 mg/kg	121.09 ± 7.64	103.71 ± 3.37	99.82 ± 4.26	81.74 ± 5.76
500 mg/kg	112.03 ± 4.97	100.14 ± 3.43	102.26 ± 5.49	91.20 ± 1.49

Data are expressed as percentage of the control. The values are expressed as mean ± SEM of four independent experiments in duplicate. Data were analyzed by analysis of variance (ANOVA), followed by Student–Newman–Keuls post hoc test. Values of $p < 0.05$ were considered significant.

Table 2
Effect of IBTC treatment on TBARS levels on liver, kidney, heart and brain homogenates.

	TBARS levels (Mean ± SEM)			
	Liver	Kidney	Heart	Brain
Control	100.00 ± 4.35	100.00 ± 1.18	100.00 ± 1.74	100.00 ± 4.86
1 mg/kg	99.75 ± 17.49	95.66 ± 7.52	67.96 ± 8.93*	111.17 ± 10.3
10 mg/kg	84.10 ± 6.54	75.98 ± 6.95	58.41 ± 9.10*	114.54 ± 5.90
50 mg/kg	106.45 ± 12.08	69.07 ± 11.57	69.55 ± 10.25*	80.48 ± 7.82
100 mg/kg	120.95 ± 11.09	96.60 ± 12.91	61.24 ± 2.67*	86.30 ± 7.83
250 mg/kg	115.83 ± 7.76	94.09 ± 10.21	65.99 ± 9.99*	76.64 ± 10.53
500 mg/kg	118.91 ± 1.27	89.91 ± 3.29	81.65 ± 8.06	92.44 ± 5.93

Data are expressed as percentage of the control. The values are expressed as mean ± SEM of four independent experiments in duplicate. Data were analyzed by analysis of variance (ANOVA), followed by Student–Newman–Keuls post hoc test. Values of $p < 0.05$ were considered significant.

* Indicates statistical difference from control group ($p < 0.05$).

Table 3
Effect of IBTC treatment on NPSH levels on liver, kidney, heart, brain homogenates.

	NPSH levels (Mean ± SEM)			
	Liver	Kidney	Heart	Brain
Control	100.00 ± 0.61	100.00 ± 4.44	100.00 ± 2.92	100.00 ± 1.55
1 mg/kg	91.09 ± 5.22	133.30 ± 15.22	90.44 ± 5.67	125.79 ± 1.01
10 mg/kg	91.90 ± 15.14	111.93 ± 12.46	86.15 ± 7.00	104.61 ± 1.45
50 mg/kg	95.78 ± 2.25	154.59 ± 14.39	100.35 ± 11.38	108.69 ± 7.67
100 mg/kg	83.00 ± 8.33	131.21 ± 6.53	97.49 ± 13.59	159.13 ± 14.13*
250 mg/kg	96.67 ± 13.73	133.16 ± 9.94	96.81 ± 10.75	186.15 ± 28.37*
500 mg/kg	98.75 ± 2.27	135.65 ± 16.61	113.22 ± 8.56	176.34 ± 12.24*

Data are expressed as percentage of the control. The values are expressed as mean ± SEM of four independent experiments in duplicate. Data were analyzed by analysis of variance (ANOVA), followed by Student–Newman–Keuls post hoc test. Values of $p < 0.05$ were considered significant.

* Indicates statistical difference from control group ($p < 0.05$).

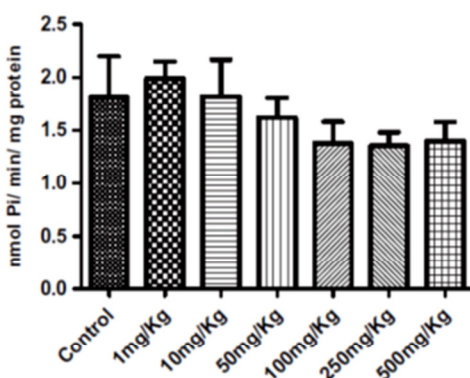


Fig. 2. Effect of IBTC treatment on Na⁺/K⁺ ATPase activity on brain homogenate. Na⁺/K⁺ ATPase activity is expressed as nmol Pi/min/mg protein. The values are expressed as mean ± SEM of four independent experiments in duplicate. Data were analyzed by analysis of variance (ANOVA), followed by Student–Newman–Keuls post hoc test. Values of $p < 0.05$ were considered significant.

or heart homogenates, but increased significantly in brain homogenates after treatment with IBTC (Table 3). Catalase and GPx activities did not change significantly (data not shown). In addition, Na⁺/K⁺ ATPase activity in the brain (Fig. 2) and ALA-D activity in liver and blood (Fig. 3A and B) did not change significantly. In addition, LD₅₀ was considered higher than 500 mg/kg.

3.2. Cell viability

3.2.1. Percent of hemolysis

The percent of hemolysis in RBCs in the presence of various concentrations (10–200 μM) of IBTC did not change significantly compared to controls (data not shown).

3.2.2. MTT assay

Murine J774 macrophage-like cells and isolated human lymphocytes were used to test the cytotoxicity of IBTC. Fig. 4 shows the MTT levels in these cell types. Concentrations of 50 μM of IBTC and above significantly reduced MTT levels compared to controls in J774 macrophage-like cells (Fig. 4A). The MTT levels did not change significantly compared to controls in isolated human lymphocytes (Fig. 4B).

3.3. Cholinesterase activity

MAP exposure at a concentration of 25 μM inhibited AChE and BChE activity in all samples. None of the IBTC concentrations tested had a significant effect on AChE or BChE activity (data not shown). No direct hydrolytic effect of IBTC on acetylthiocholine or butyrylthiocholine was observed (data not shown).

IBTC protected against MAP-inhibition of AChE and BChE in human erythrocyte ghosts (Fig. 5A and B). Treatment with MAP plus IBTC (at 10, 25, 50, and 100 μM) resulted in significantly increased cholinesterase activity compared to MAP alone (Fig. 5A and B). IBTC also significantly ($p < 0.05$) reactivated the AChE and BChE enzyme activities at concentrations of 10, 25, 50, and 100 μM (Fig. 6A and B) compared to MAP alone.

3.4. Molecular docking results

Since different enantiomers of methamidophos can bind to Ser203, Sp and Rp we performed docking studies with both Sp (SGX) and Rp (SGR) enantiomers of MAP-inhibited AChE from *Mus musculus* (PDB code: 2jge) (Fig. 7). In the Rp conformation of methamidophos, IBTC was located in the active site between the peripheral anionic site (PAS) (Tyr124) and the internal anionic site (Tyr341). The binding energy was −9.2 kcal/mol for the Rp enantiomer. The thiocarbonyl group was 7.707 angstroms from the

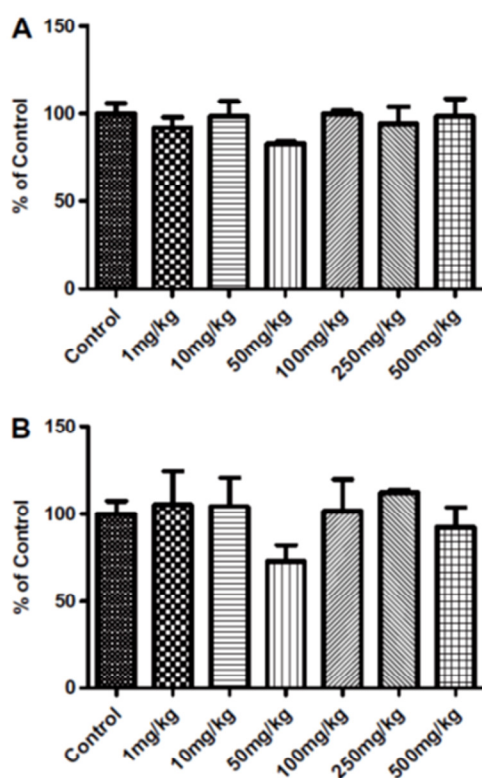


Fig. 3. Effect of IBTC treatment on Delta Aminolevulinate Dehydratase (δ -ALA-D) activity on liver (A) homogenate and on total blood (B). Data are expressed as percentage of the control. The values are expressed as mean \pm SEM of four independent experiments in duplicate. Data were analyzed by analysis of variance (ANOVA), followed by Student–Newman–Keuls post hoc test. Values of $p < 0.05$ were considered significant.

phosphate of SGR203, and the hydrazinic nitrogen of the thiosemicarbazone function was 2.873 Å from the carboxylic oxygen of residue Asp74 and 3.305 Å from the oxygen of residue Tyr341. The terminal thioamidic nitrogen hydrogen bonded with residue Tyr124 of the peripheral anionic site. The other fragment of the molecule was located close to the internal anionic site and stabilized by hydrogen bonds with residues Thr83 (nitrogen of the indole group) and Tyr337 (hydrogen bond with the amidic oxygen and the iminic nitrogen present on the thiosemicarbazone function). Only one cation– π interaction occurred between IBTC and the enzyme active site, which was between the aromatic ring from the terminal thioamidic function and phosphate of the SER203.

In the Sp conformation of methamidophos, similar to the Rp enantiomer of the serine modified by MAP, IBTC was stabilized in the active site between the peripheral anionic site (PAS) (Tyr124) and the internal anionic site (Tyr341). The binding energy was -8.95 kcal/mol. The thiocarbonyl group was 6.311 Å from the phosphate of SGX203 and the hydrazinic nitrogen of the thiosemicarbazone function was 2.818 Å from the carboxylic oxygen of residue Asp74 and 3.271 Å from the oxygen of residue Tyr341. In this conformation (SGX), the sulfur group was closer to the phosphate of the modified serine than in the SGR conformation. The aromatic ring from the terminal thioamidic function was stabilized in a hydrophobic region between the PAS (Tyr337 and Tyr341) and the acyl binding pocket (Phe338). The amidic oxygen formed a hydrogen bond with residue Tyr337 as well as with the iminic nitrogen. There was also a hydrogen bond between residue Thr87

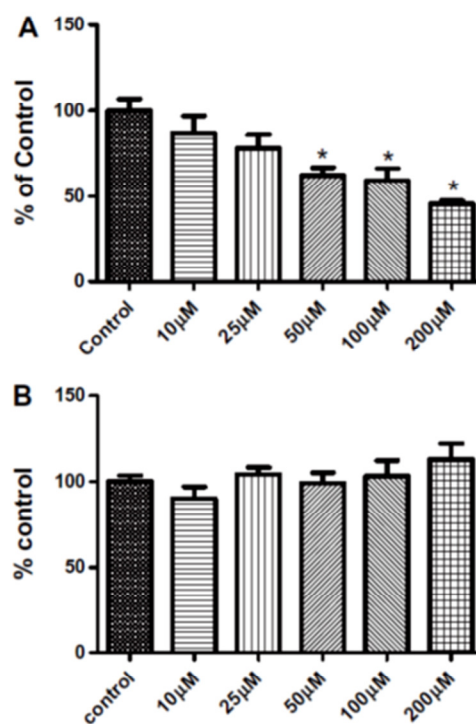


Fig. 4. Effect of IBTC on percent cytotoxicity (MTT assay) in Murine J774 macrophage-like cells (A) and in human isolated lymphocytes (B). Both types of cells were exposed to various concentrations of IBTC for 24 h prior to the addition of MTT for 4 h. The values are expressed as mean \pm SEM of three independent experiments in triplicate. Data were analyzed by analysis of variance (ANOVA), followed by Student–Newman–Keuls post hoc test. Values of $p < 0.05$ were considered significant. * indicates statistical difference from control group ($p < 0.05$).

and the iminic nitrogen. π interactions did not directly occur with the molecule.

4. Discussion

One purpose of our study was to investigate the potential toxic properties of IBTC, a compound that has been investigated in many biological models of oxidative stress. In our previous study (Barcelos et al., 2011) we demonstrated that this compound has high antiatherogenic potential. However, its toxicity to organisms as well as its possible action on cholinesterases had not been yet elucidated. In the present study we showed that subcutaneous injection of IBTC did not increase oxidative stress, had no impact on enzymes usually affected by pesticide compounds (Banerjee et al., 1999; Gultekin et al., 2000; Gupta et al., 2001), and did not induce alterations in several antioxidant enzymes (Tables 1–3; Figs. 2 and 3). In addition, our study clearly demonstrates that IBTC can protect and reactivate AChE and BChE inhibited by MAP (Figs. 5 and 6).

We investigated IBTC *in vivo* in order to determine whether it had any toxic effects in mice. We found that IBTC has low toxicity when administered by subcutaneous (s.c.) injection, with an LD₅₀ of higher than 500 mg/kg, and had no effect on body weight (data not shown). No cytotoxicity was detected in isolated human lymphocytes and only concentrations of 50 μ M and higher lowered MTT levels in murine J774 macrophage-like cells. Moreover, the presence of IBTC did not change the percent of hemolysis in RBCs

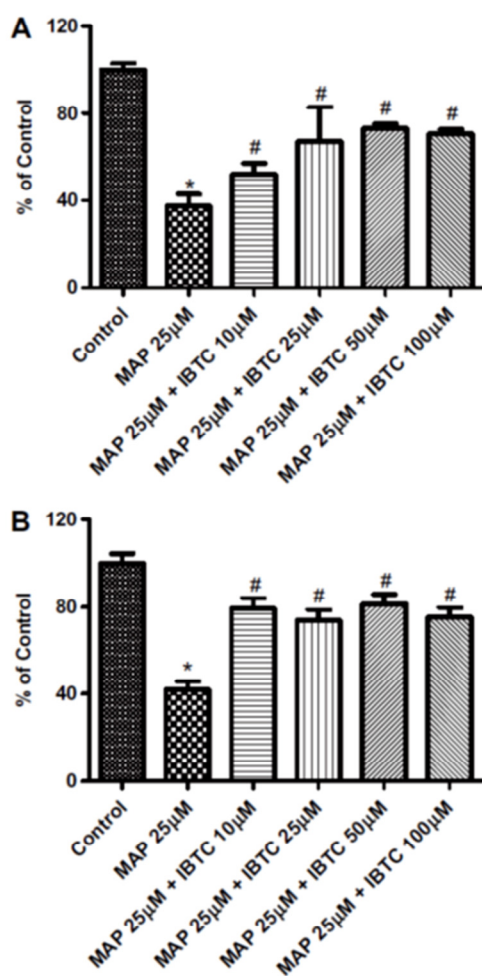


Fig. 5. Protective effect of IBTC on AChE activity from ghost erythrocytes (A) and BChE from plasma (B) on methamidophos (MAP) inhibition. IBTC was added to the reaction medium at the same time of methamidophos. The data are expressed as percentage from control group (100%) of five independent experiments in duplicate. Data were analyzed by analysis of variance (ANOVA), followed by Student–Newman–Keuls post hoc test. Values of $p < 0.05$ were considered significant. * indicates statistical difference from control group ($p < 0.05$) # indicates statistical difference from methamidophos 25 µM group ($p < 0.05$).

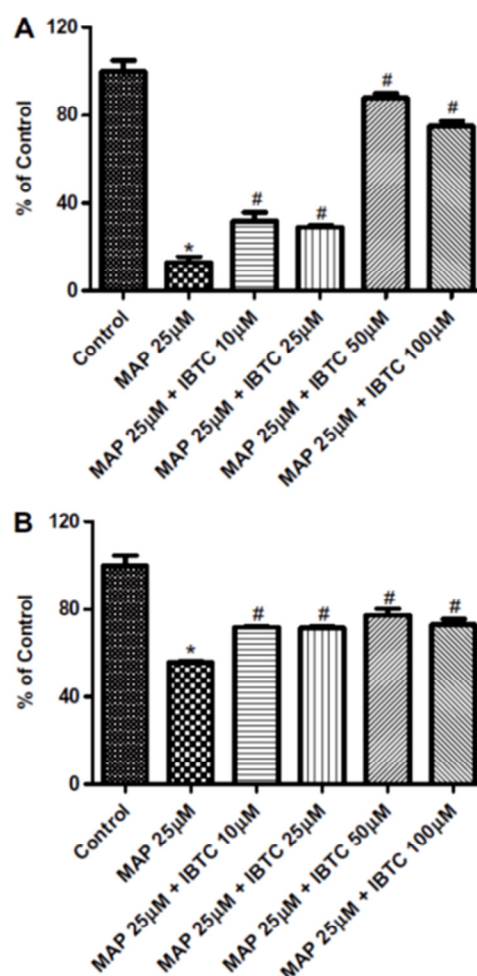


Fig. 6. Reactivation effect of IBTC on AChE activity from ghost erythrocytes (A) and BChE from plasma (B) on methamidophos (MAP) inhibition. IBTC was added 10 min after methamidophos in the reaction medium. The data are expressed as percentage from control group (100%) of five independent experiments in duplicate. Data were analyzed by analysis of variance (ANOVA), followed by Student–Newman–Keuls post hoc test. Values of $p < 0.05$ were considered significant. * indicates statistical difference from control group ($p < 0.05$) # indicates statistical difference from methamidophos 25 µM group ($p < 0.05$).

compared to controls. These results corroborate those of Puntel et al. (2009) who found that thiosemicarbazone-derived compounds have low toxicity.

Although we did not specifically measure RS formation, it is well known that excessive RS could not only induce DCF-RS formation but also contribute to the initiation of a complex cascade of reactions that culminates with lipid peroxidation (increase in TBARS levels). We demonstrated that IBTC did not change DFC-RS levels and did not increase lipid peroxidation, indicating that IBTC does not produce excessive RS itself or disrupt the cellular environment such that RS production increases. In addition, we found that there was no depletion in NPSH levels and no changes in catalase and GPx activities, indicating that there was no depletion or alteration of these antioxidant systems.

δ -ALA-D is an enzyme that catalyzes the condensation of two δ -aminolevulinic acid (ALA) molecules into porphobilinogen. Consequently, δ -ALA-D inhibition may impair heme biosynthesis (Jaffe,

1995) and can result in the accumulation of δ -ALA, which may affect aerobic metabolism and have some prooxidant activity (Bec-hara et al., 1993). Moreover, δ -ALA-D activity is a good marker of oxidative stress (Maciel et al., 2000) and can be inhibited by thiol oxidized radicals (Farina et al., 2001; Folmer et al., 2003). Here we demonstrated that there were no significant effects on δ -ALA-D activity, indicating that IBTC does not affect the essential -SH groups on the active site of the enzyme or increase oxidative stress.

Na^+/K^+ -ATPase, a sulfhydryl-containing enzyme, is embedded in the cell membrane and is responsible for the active transport of sodium and potassium ions in the nervous system. Since Na^+/K^+ -ATPase is crucial for maintaining ionic gradients in neurons (Xiong and Stringer, 2000), a reduction in the activity of this enzyme may affect neural activity and memory storage (Balk et al., 2010). Our study demonstrated that the Na^+/K^+ -ATPase activity was not modified by IBTC at any of the concentrations tested, indicating that IBTC has no toxic properties to neurons. Previous reports have

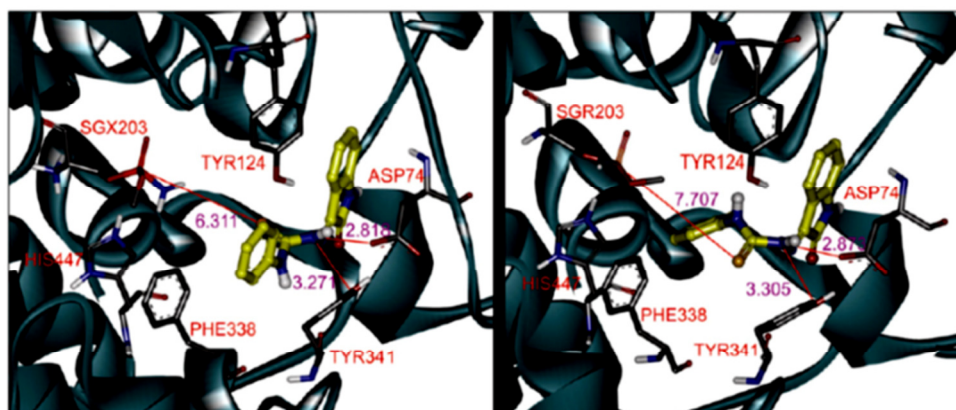


Fig. 7. Representative molecular models of IBTC binding the active site of *Mus musculus* AChE in the two different enantiomers for the methamidophos-modified Ser203: SGX (left panel) and SGR (right panel). Ligand is shown in ball-and-stick drawing, the carbons of the ligand is shown in yellow. (For interpretation of the references to colour in this figure legend, the reader is referred to the web version of this article.)

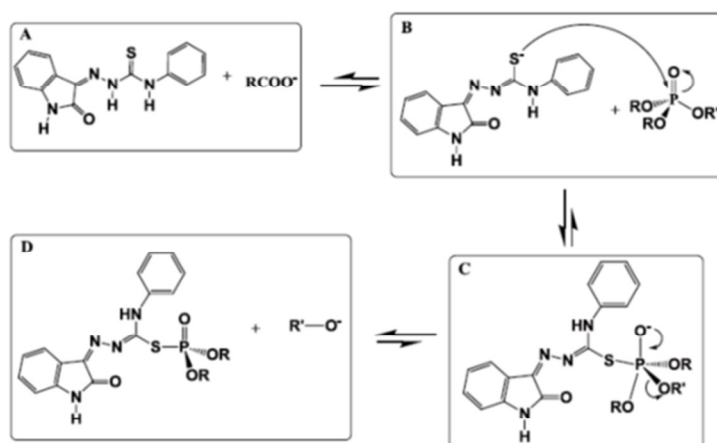
demonstrated the importance of thiol groups for Na^+/K^+ -ATPase catalysis and $-\text{SH}$ groups of this enzyme are highly susceptible to oxidizing agents (Bavaresco et al., 2003; de Assis et al., 2003). The unchanged NPSH levels found here are in agreement with the unchanged activities of ALA-D and Na^+/K^+ -ATPase.

We also demonstrate that IBTC did not alter the activity of AChE and BChE, enzymes related to dysfunctions in the cholinergic neurotransmission (Mukherjee et al., 2007) and to systemic inflammatory conditions, such as diabetes mellitus, hypertension, insulin resistance, and hyperlipidemia (Das, 2007).

AChE and BChE are strongly related to the intoxications caused by pesticides and the implications of pesticides residues on human health have yet to be comprehensively documented. Pesticides may induce oxidative stress, leading to generation of free radicals and alterations in antioxidants, oxygen free radicals, scavenging enzyme systems, and lipid peroxidation. This way, after verifying that IBTC does not alter antioxidant systems and has no toxic effects, we tested the capacity of IBTC to protect and reactivate the activity of AChE and BChE after inhibition with MAP. In human erythrocyte ghost and in human plasma BChE, IBTC was able to protect and reactivate both enzymes from MAP inhibition at all concentrations tested (Figs. 5 and 6). The protective activity for AChE and BChE against MAP inhibition works via competitive inhibition.

Molecular docking results indicate that IBTC can enter the active site of AChE by binding to the peripheral anionic site (Trp134 and Tyr124) and internal anionic site (Thr83 and Tyr337), thus preventing MAP from accessing the catalytic residue Ser203 and protecting AChE and BChE from inhibition, and proving that IBTC cannot itself inhibit AChE or BChE, since in vitro tests demonstrate that the presence of IBTC on these sites do not affect AChE and BChE activities.

Our most interesting result is that IBTC can reactivate AChE and BChE after inhibition by MAP. As far as we know, there are few compounds that are not oximes that can reactivate AChE and BChE inhibited by OPs and there is no literature concerning the use of thiosemicarbazones against OP intoxication. In that way, our study demonstrates for the first time that a thiosemicarbazone derivative can protect and reactivate AChE and BChE from OP inhibition. The use of many different oximes, the classical therapy for OPs poisoning, is controversial since metabolic degradation of oximes can have deleterious effects, such as formation of toxic products such as hydrogen cyanide, and numerous side effects, including nausea, vomiting, dizziness, loss of consciousness, visual alterations, confusion, headache, tachycardia, neuromuscular blockage, and muscular weakness (Bardin et al., 1994; Carlton et al., 1998; Hardman et al., 1996). New and more effective drugs with fewer toxicological effects are necessary for cholinesterases reactivation.



Scheme 1. Possible mechanism of IBTC reactivation on methamidophos-inhibited AChE.

In addition, oximes are weaker reactivators of BChE (Worek et al., 1999a,b), and IBTC can reactivate both AChE and BChE activities. The reactivation of BChE is very important, since BChE is a co-regulator of acetylcholine in brain (Giacobini, 2000) and replaces AChE in the maintenance of the structure and physiological integrity of the cholinergic system (Mesulam et al., 2002). Darvesh et al. (2004) also showed that BChE is highly active in the synaptic cleft in intrinsic cardiac neurons, helping to reduce high acetylcholine levels (Darvesh et al., 2004). IBTC seems to reactivate cholinesterases via its position at the peripheral anionic site and the acyl binding pocket, which is in agreement with previous results obtained for mono-oxime bisquaternary acetylcholinesterase reactivators (Musilek et al., 2011).

As illustrated in Scheme 1, we observed that the imino hydrogen (A) from IBTC can react with a carboxylate group (RCOO^-) of the Asp74 residue (the distance of the imino hydrogen of the IBTC and the RCOO^- group of the enzyme is about 2.8 Å), which could lead to IBTC deprotonation and formation of an anionic intermediate (B). Then, a nucleophilic attack by the thiolate on the electrophilic center of methamidophos (B) can occur, which is the site of inhibition of the enzyme AChE (OR'). This intermediate has the phosphate group (P) penta coordinated (C), which causes methamidophos to leave the active site of the enzyme (OR'), reactivating the enzyme and releasing the phosphate group, which returns to the tetrahedral geometry bound only to IBTC (D). Based in this mechanism, the SGX, not the SGR, conformation of the MAP-inhibited AChE seems to be the more likely conformation to be reactivated since the sulfur group is positioned closer to the electrophilic attack site (OP moiety in the modified Ser203). This is in agreement with previous work that showed that Sp enantiomers (SGX conformation) of methylphosphonate esters are more reactive in forming the conjugate with the enzyme and the rates of reactivation by oximes also indicate a preference of Sp over Rp (Wong et al., 2000).

5. Conclusion

The thiosemicarbazone derived compound, IBTC, besides acting like an antioxidant and antiatherogenic (Barcelos et al., 2011), has low toxicity and does not alter the antioxidant system. We have demonstrated for the first time that a thiosemicarbazone derivative can protect AChE and BChE from MAP intoxication by preventing MAP binding at the active site of the enzymes and can also reactivate AChE and BChE activities by interacting with MAP and releasing the active site. Future studies are needed to test IBTC against intoxication by other OPs and also evaluate its efficacy after long-term exposure to MAP. However, our work indicates that IBTC may be a useful therapeutic compound for MAP intoxication.

Conflict of interest

The authors declare that there are no conflicts of interest.

Acknowledgements

Work supported by the FINEP research grant "Rede Instituto Brasileiro de Neurociência (IBN-Net)" # 01.06.0842-00. INCT - National Institute of Science and Technology for Excitotoxicity and Neuroprotection/CNPq also supported this work. F.A.A.S. and N.B.V.B. received a fellowship from CNPq. R.P.B., T.H.L. and G.P.A. received a fellowship from CAPES.

References

Abdollahi, M., Ranjbar, A., Shadnia, S., Nikfar, S., Rezaie, A., 2004. Pesticides and oxidative stress: a review. *Med. Sci. Monit.* 10 (6), RA141–RA147.

Aebi, H., 1984. Catalase in vitro. *Methods Enzymol.* 105, 121–126.

- Ashani, Y., Radić, Z., Tsigelny, I., Vellom, D.C., Pickering, N.A., Quinn, D.M., Doctor, B.P., Taylor, P., 1995. Amino acid residues controlling reactivation of organophosphoryl conjugates of acetylcholinesterase by mono- and bisquaternary oximes. *J. Biol. Chem.* 270 (11), 6370–6380.
- Atkinson, A., Gatenby, A.D., Lowe, A.G., 1973. The determination of inorganic orthophosphate in biological systems. *Biochim. Biophys. Acta* 320 (1), 195–204.
- Balk, R.E.S., Bridi, J.C., Portella, R.E.L., Carvalho, N.R., Dobrachinski, F., da Silva, M.H., Amaral, G.P., Dias, G.R., Barbosa, N.E.V., Soares, F.A., 2010. Clomipramine treatment and repeated restraint stress alter parameters of oxidative stress in brain regions of male rats. *Neurochem. Res.* 35 (11), 1761–1770.
- Banerjee, B.D., Seth, V., Bhattacharya, A., Pasha, S.T., Chakraborty, A.K., 1999. Biochemical effects of some pesticides on lipid peroxidation and free-radical scavengers. *Toxicol. Lett.* 107 (1–3), 33–47.
- Barcelos, R.P., de Lima Portella, R., da Rosa, E.J., Fonseca, A.E.S., Bresolin, L., Carratu, V., Soares, F.A., Barbosa, N.V., 2011. Thiosemicarbazone derivative protects from AAPH and Cu(2+)-induced LDL oxidation. *Life Sci.* 89 (1–2), 20–28.
- Bardin, P.G., van Eeden, S.F., Moolman, J.A., Foden, A.P., Joubert, J.R., 1994. Organophosphate and carbamate poisoning. *Arch. Intern. Med.* 154 (13), 1433–1441.
- Bavareco, C.S., Calcagnotto, T., Tagliari, B., Delwing, D., Lamers, M.L., Wannmacher, C.M., Wajner, M., Wyse, A.T., 2003. Brain Na⁺, K⁺-ATPase inhibition induced by arginine administration is prevented by vitamins E and C. *Neurochem. Res.* 28 (6), 825–829.
- Bechara, E., Medeiros, M., Monteiro, H., 1993. A free radical hypothesis of lead poisoning and inborn porphyrias associated with 5-aminolevulinic acid overload. *Quim. Nova* 16, 7.
- Beraldo, H., Gambino, D., 2004. The wide pharmacological versatility of semicarbazones, thiosemicarbazones and their metal complexes. *Mini Rev. Med. Chem.* 4 (1), 31–39.
- Bourne, Y., Taylor, P., Marchot, P., 1995. Acetylcholinesterase inhibition by fasciculins: crystal structure of the complex. *Cell* 83 (3), 503–512.
- Böyum, A., 1968. Isolation of mononuclear cells and granulocytes from human blood. Isolation of mononuclear cells by one centrifugation, and of granulocytes by combining centrifugation and sedimentation at 1 g. *Scand. J. Clin. Lab. Invest. Suppl.* 97, 77–89.
- Carlton, F.B., Simpson, W.M., Haddad, L.M., 1998. The organophosphate and other insecticides. In: *Clinical Management of Poisoning and Drug Overdose*. W.S. Company, Philadelphia, Pennsylvania, USA, pp. 836–850.
- da Silva, A.P., Farina, M., Franco, J.L., Dafre, A.L., Kassa, J., Kuca, K., 2008. Temporal effects of newly developed oximes (K027, K048) on malathion-induced acetylcholinesterase inhibition and lipid peroxidation in mouse prefrontal cortex. *Neurotoxicology* 29 (1), 184–189.
- da Silva, A.P., Meotti, F.C., Santos, A.R., Farina, M., 2006. Lactational exposure to malathion inhibits brain acetylcholinesterase in mice. *Neurotoxicology* 27 (6), 1101–1105.
- Darvesh, S., Arora, R.C., Martin, E., Magee, D., Hopkins, D.A., Armour, J.A., 2004. Cholinesterase inhibitors modify the activity of intrinsic cardiac neurons. *Exp. Neurol.* 188 (2), 461–470.
- Das, U.N., 2007. Acetylcholinesterase and butyrylcholinesterase as possible markers of low-grade systemic inflammation. *Med. Sci. Monit.* 13 (12), RA214–RA221.
- de Assis, D.R., Ribeiro, C.A., Rosa, R.B., Schuck, P.F., Dalcin, K.B., Vargas, C.R., Wannmacher, C.M., Dutra-Filho, C.S., Wyse, A.T., Briones, P., Wajner, M., 2003. Evidence that antioxidants prevent the inhibition of Na⁺, K⁺-ATPase activity induced by octanoic acid in rat cerebral cortex in vitro. *Neurochem. Res.* 28 (8), 1255–1263.
- Ekström, F., Åkfur, C., Tunemalm, A.K., Lundberg, S., 2006. Structural changes of phenylalanine 338 and histidine 447 revealed by the crystal structures of tabun-inhibited murine acetylcholinesterase. *Biochemistry* 45 (1), 74–81.
- Ellman, G.L., 1959. Tissue sulfhydryl groups. *Arch. Biochem. Biophys.* 82 (1), 70–77.
- Ellman, G.L., Courtney, K.D., Andres Jr., V., Feather-Stone, R.M., 1961. A new and rapid colorimetric determination of acetylcholinesterase activity. *Biochem. Pharmacol.* 7, 88–95.
- Farina, M., Folmer, V., Bolzan, R.C., Andrade, L.H., Zeni, G., Braga, A.L., Rocha, J.B., 2001. Selenoxides inhibit delta-aminolevulinic acid dehydratase. *Toxicol. Lett.* 119 (1), 27–37.
- Folmer, V., Soares, J.C., Gabriel, D., Rocha, J.B., 2003. A high fat diet inhibits delta-aminolevulinic acid dehydratase and increases lipid peroxidation in mice (*Mus musculus*). *J. Nutr.* 133 (7), 2165–2170.
- Fonseca, A.D.S., Peres, G.L., Storino, T.G., Bresolin, L., Carratu, V.S., Giglio, V.F., Crespan, E.D.R., Manfredo, H., 2010. Synthesis and structural characterization of the ligand isatin-3-(N⁴-benzylthiosemicarbazone) and its mercury(II) complex. *Quim. Nova* 33, 1453–1456.
- Giacobini, E., 2000. Cholinesterase and Cholinesterase Inhibitors. From Molecular Biology to Therapy, vol. 46. Martin Dunitz Publishers, London, pp. 181–226.
- Grosfeld, H., Barak, D., Ordentlich, A., Velan, B., Shafferman, A., 1996. Interactions of oxime reactivators with diethylphosphoryl adducts of human acetylcholinesterase and its mutant derivatives. *Mol. Pharmacol.* 50(3), 639–649.
- Gultekin, F., Öztürk, M., Akdoğan, M., 2000. The effect of organophosphate insecticide chlorpyrifos-ethyl on lipid peroxidation and antioxidant enzymes (in vitro). *Arch. Toxicol.* 74 (9), 533–538.
- Gupta, R.C., Milatovic, D., Dettbarn, W.D., 2001. Depletion of energy metabolites following acetylcholinesterase inhibitor-induced status epilepticus: protection by antioxidants. *Neurotoxicology* 22 (2), 271–282.
- Hardman, J.G., Gilman, A.G., Limbird, L.E., 1996. Anticholinesterase agents. In: *The Pharmacological Basis of Therapeutics*. Goodman & Gilman's, pp. 161–176.

Please cite this article in press as: Barcelos, R.P., et al. Isatin-3-N⁴-benzylthiosemicarbazone, a non-toxic thiosemicarbazone derivative, protects and reactivates rat and human cholinesterases inhibited by methamidophos in vitro and in silico. *Toxicol. in Vitro* (2012), <http://dx.doi.org/10.1016/j.tiv.2012.04.008>

- Holmstedt, B., 1959. Pharmacology of organophosphorus cholinesterase inhibitors. *Pharmacol. Rev.* 11, 567–688.
- Jaffe, E.K., 1995. Porphobilinogen synthase, the first source of heme's asymmetry. *J. Bioenerg. Biomembr.* 27 (2), 169–179.
- Kovarik, Z., Radić, Z., Berman, H.A., Simeon-Rudolf, V., Reiner, E., Taylor, P., 2004. Mutant cholinesterases possessing enhanced capacity for reactivation of their phosphorylated conjugates. *Biochemistry* 43 (11), 3222–3229.
- Kryger, G., Silman, I., Sussman, J.L., 1998. Three-dimensional structure of a complex of E2020 with acetylcholinesterase from *Torpedo californica*. *J. Physiol. Paris* 92 (3–4), 191–194.
- Kuang, Z.H., Wang, P.F., Zheng, R.L., Liu, Z.L., Liu, Y.C., 1994. Making vitamin C liposoluble enhances its protective effect against radical induced hemolysis of erythrocytes. *Chem. Phys. Lipids* 71 (1), 95–97.
- Lowry, O., Rosebrough, N., Farr, A., Randall, R., 1951. Protein measurement with the Folin phenol reagent. *J. Biol. Chem.* 193 (1), 265–275.
- Maciel, E.N., Bolzan, R.C., Braga, A.L., Rocha, J.B., 2000. Diphenyl diselenide and diphenyl ditelluride differentially affect delta-aminolevulinic acid dehydratase from liver, kidney, and brain of mice. *J. Biochem. Mol. Toxicol.* 14 (6), 310–319.
- Marrs, T.C., 1993. Organophosphate poisoning. *Pharmacol. Ther.* 58 (1), 51–66.
- Mesulam, M.M., Guillozet, A., Shaw, P., Levey, A., Duysen, E.G., Lockridge, O., 2002. Acetylcholinesterase knockouts establish central cholinergic pathways and can use butyrylcholinesterase to hydrolyze acetylcholine. *Neuroscience* 110 (4), 627–639.
- Morris, G.M., Huey, R., Lindstrom, W., Sanner, M.F., Bellew, R.K., Goodsell, D.S., Olson, A.J., 2009. AutoDock4 and AutoDockTools4: automated docking with selective receptor flexibility. *J. Comput. Chem.* 30 (16), 2785–2791.
- Mosmann, T., 1983. Rapid colorimetric assay for cellular growth and survival: application to proliferation and cytotoxicity assays. *J. Immunol. Methods* 65 (1–2), 55–63.
- Mukherjee, P.K., Kumar, V., Mal, M., Houghton, P.J., 2007. Acetylcholinesterase inhibitors from plants. *Phytomedicine* 14 (4), 289–300.
- Musilek, K., Komloova, M., Holas, O., Horova, A., Pohanka, M., Gunn-Moore, F., Dohnal, V., Dolezal, M., Kuca, K., 2011. Mono-oxime bisquaternary acetylcholinesterase reactivators with prop-1,3-diyl linkage-preparation, in vitro screening and molecular docking. *Bioorg. Med. Chem.* 19 (2), 754–762.
- Muszbeck, L., Szabó, T., Fésüs, L., 1977. A high sensitive method for the measurement of ATPase activity. *Anal. Biochem.* 77 (1), 286–288.
- Myhre, O., Andersen, J.M., Aarnes, H., Fonnum, F., 2003. Evaluation of the probes 2',7'-dichlorofluorescein diacetate, luminol, and lucigenin as indicators of reactive species formation. *Biochem. Pharmacol.* 65 (10), 1575–1582.
- Ohkawa, H., Ohishi, N., Yagi, K., 1979. Assay for lipid peroxides in animal tissues by thiobarbituric acid reaction. *Anal. Biochem.* 95 (2), 351–358.
- Paglia, D.E., Valentine, W.N., 1967. Studies on the quantitative and qualitative characterization of erythrocyte glutathione peroxidase. *J. Lab. Clin. Med.* 70 (1), 158–169.
- Pérez-Severiano, F., Rodríguez-Pérez, M., Pedraza-Chaverri, J., Maldonado, P.D., Medina-Campos, O.N., Ortiz-Plata, A., Sánchez-García, A., Villeda-Hernández, J., Galván-Arzate, S., Aguilera, P., Santamaría, A., 2004. S-Allylcysteine, a garlic-derived antioxidant, ameliorates quinolinic acid-induced neurotoxicity and oxidative damage in rats. *Neurochem. Int.* 45 (8), 1175–1183.
- Pettersen, E.F., Goddard, T.D., Huang, C.C., Couch, G.S., Greenblatt, D.M., Meng, E.C., Ferrin, T.E., 2004. UCSF Chimera – a visualization system for exploratory research and analysis. *J. Comput. Chem.* 25 (13), 1605–1612.
- Puntel, G.O., Carvalho, N.R., Amaral, G.P., Lobato, L.D., Silveira, S.O., Daubermann, M.F., Barbosa, N.V., Rocha, J.B., Soares, F.A., 2011. Therapeutic cold: an effective kind to modulate the oxidative damage resulting of a skeletal muscle contusion. *Free Radic. Res.* 45 (2), 125–138.
- Puntel, G.O., de Carvalho, N.R., Gubert, P., Palma, A.S., Dalla Corte, C.L., Avila, D.S., Pereira, M.E., Carratu, V.S., Bresolin, L., da Rocha, J.B., Soares, F.A., 2009. Butane-2,3-dionethiosemicarbazone: an oxime with antioxidant properties. *Chem. Biol. Interact.* 177 (2), 153–160.
- Sassa, S., 1982. Delta-aminolevulinic acid dehydratase assay. *Enzyme* 28 (2–3), 133–145.
- Seeliger, D., de Groot, B.L., 2010. Ligand docking and binding site analysis with PyMOL and Autodock/Vina. *J. Comput. Aided Mol. Des.* 24 (5), 417–422.
- Sussman, J.L., Harel, M., Frolow, F., Oefner, C., Goldman, A., Tokor, L., Silman, I., 1991. Atomic structure of acetylcholinesterase from *Torpedo californica*: a prototypic acetylcholine-binding protein. *Science* 253 (5022), 872–879.
- Taylor, P., Radić, Z., Hosea, N.A., Camp, S., Marchot, P., Berman, H.A., 1995. Structural bases for the specificity of cholinesterase catalysis and inhibition. *Toxicol. Lett.* 82–83, 453–458.
- Tomlin, C., (1994). *The Pesticide Manual, A World Compendium*. Croydon, British Crop Protection Council.
- Trott, O., Olson, A.J., 2010. AutoDock Vina: improving the speed and accuracy of docking with a new scoring function, efficient optimization, and multithreading. *J. Comput. Chem.* 31 (2), 455–461.
- Verma, R.S., Srivastava, N., 2001. Chlorpyrifos induced alterations in levels of thiobarbituric acid reactive substances and glutathione in rat brain. *Indian J. Exp. Biol.* 39 (2), 174–177.
- Wada, K., Fujibayashi, Y., Yokoyama, A., 1994. Copper(II)[2,3-butanedionebis(N4-methylthiosemicarbazone)], a stable superoxide dismutase-like copper complex with high membrane penetrability. *Arch. Biochem. Biophys.* 310 (1), 1–5.
- WHO, 1993. *Methamidophos Health and Safety Guide*. Geneva, World Health Organization.
- Wong, L., Radić, Z., Brüggemann, R.J., Hosea, N., Berman, H.A., Taylor, P., 2000. Mechanism of oxime reactivation of acetylcholinesterase analyzed by chirality and mutagenesis. *Biochemistry* 39 (19), 5750–5757.
- Worek, F., Aurbek, N., Koller, M., Becker, C., Eyer, P., Thiermann, H., 2007. Kinetic analysis of reactivation and aging of human acetylcholinesterase inhibited by different phosphoramidates. *Biochem. Pharmacol.* 73 (11), 1807–1817.
- Worek, F., Diepold, C., Eyer, P., 1999a. Dimethylphosphoryl-inhibited human cholinesterases: inhibition, reactivation, and aging kinetics. *Arch. Toxicol.* 73 (1), 7–14.
- Worek, F., Mast, U., Kiderlen, D., Diepold, C., Eyer, P., 1999b. Improved determination of acetylcholinesterase activity in human whole blood. *Clin. Chim. Acta* 288 (1–2), 73–90.
- Worek, F., Reiter, G., Eyer, P., Szinicz, L., 2002. Reactivation kinetics of acetylcholinesterase from different species inhibited by highly toxic organophosphates. *Arch. Toxicol.* 76 (9), 523–529.
- Worek, F., Thiermann, H., Szinicz, L., Eyer, P., 2004. Kinetic analysis of interactions between human acetylcholinesterase, structurally different organophosphorus compounds and oximes. *Biochem. Pharmacol.* 68 (11), 2237–2248.
- Xiong, Z.Q., Stringer, J.L., 2000. Sodium pump activity, not glial spatial buffering, clears potassium after epileptiform activity induced in the dentate gyrus. *J. Neurophysiol.* 83 (3), 1443–1451.
- Zayed, S.M., Fakhr, I.M., el-Magraby, S., 1984. Some toxicological aspects of methamidophos exposure in mice. *J. Environ. Sci. Health B* 19 (4–5), 467–478.

2.2 Artigo 2: “Efeito de diferentes oximas sobre colinesterases de ratos e humanos inibidas por metamidofós: estudo comparativo *in vitro* e *in silico*.”

Basic and Clinical Pharmacology and Toxicology

Doi: 10.1111/j.1742-7843.2012.00912.x

Effect of different oximes on rat and human cholinesterases inhibited by methamidophos: a comparative *in vitro* and *in silico* study.

Thiago Henrique Lugokenski, Priscila Gubert, Diones Caeran Bueno, Pablo Andrei Nogara, Rogério de Aquino Saraiva, Rômulo Pillon Barcelos, Vanessa Santana Carratu, Leandro Bresolin, Nilda Berenice de Vargas Barbosa, Maria Ester Pereira, João Batista Teixeira da Rocha, Félix Alexandre Antunes Soares.

Effect of Different Oximes on Rat and Human Cholinesterases Inhibited by Methamidophos: A Comparative *In Vitro* and *In Silico* Study

Thiago Henrique Lugokenski¹, Priscila Gubert¹, Diones Caeran Bueno¹, Pablo Andrei Nogara¹, Rogério de Aquino Saraiva¹, Rômulo Pillon Barcelos¹, Vanessa Santana Carratu², Leandro Bresolin², Nilda Berenice de Vargas Barbosa¹, Maria Ester Pereira¹, João Batista Teixeira da Rocha¹ and Félix Alexandre Antunes Soares¹

¹Department of Chemistry, Federal University of Santa Maria, Santa Maria, Rio Grande do Sul, Brazil and ²Department of Chemistry, Federal University of Rio Grande, Rio Grande, Rio Grande do Sul, Brazil

(Received 11 December 2011; Accepted 25 May 2012)

Abstract: Methamidophos is one of the most toxic organophosphorus (OP) compounds. It acts via phosphorylation of a serine residue in the active site of acetylcholinesterase (AChE) and butyrylcholinesterase (BChE), leading to enzyme inactivation. Different oximes have been developed to reverse this inhibition. Thus, our work aimed to test the protective or reactivation capability of pralidoxime and obidoxime, as well as two new oximes synthesised in our laboratory, on human and rat cholinesterases inhibited by methamidophos. In addition, we performed molecular docking studies in non-aged methamidophos-inhibited AChE to understand the mechanisms involved. Our results suggested that pralidoxime protected and reactivated methamidophos-inhibited rat brain AChE. Regarding human erythrocyte AChE, all oximes tested protected and reactivated the enzyme, with the best reactivation index observed at the concentration of 50 μM . Concerning BChE, butane-2,3-dionethiosemicarbazone oxime (oxime 1) was able to protect and reactivate the methamidophos-inhibited BChE by 45% at 50 μM , whereas 2(3-(phenylhydrazono)butan-2-one oxime (oxime 2) reactivated 28% of BChE activity at 100 μM . The two classical oximes failed to reactivate BChE. The molecular docking study demonstrated that pralidoxime appears to be better positioned in the active site to attack the O-P moiety of the inhibited enzyme, being near the oxyanion hole, whereas our new oximes were stably positioned in the active site in a manner similar to that of obidoxime. In conclusion, our work demonstrated that the newly synthesised oximes were able to reactivate not only human erythrocyte AChE but also human plasma BChE, which could represent an advantage in the treatment of OP compounds poisoning.

Acetylcholinesterase (EC 3.1.1.7, AChE) is an enzyme that catalyses the hydrolysis of acetylcholine to choline and acetate. The biological function of this enzyme is to terminate acetylcholine activity in the terminal nervous junction with its effector organs or post-synaptic sites [1]. The mechanism of action of organophosphorus (OP) compounds with anticholinesterase activity involves the phosphorylation of the serine hydroxyl group in the active site of AChE, leading to an inactive enzyme (AChE-OP) [2]. The inactivation of AChE results in the accumulation of acetylcholine at cholinergic receptor sites, causing a cholinergic crisis that can lead to death [3].

Methamidophos is a potent AChE inhibitor used to control plague of insects on a variety of crops [4] and may present anticholinesterase activity against human cholinesterases [5,6]. In Brazil in particular, methamidophos is commonly used on many crops, including cotton, soybeans and wheat, resulting in food [7] and occupational exposure [8]. A recent study demonstrated that over 90% of small farmers use methamidophos and nearly 60% of them exhibit typical OP intoxication symptoms [9]. Mechanistically, methamidophos may inhibit AChE by covalently binding a serine residue (Ser203) in the

active site, and this moiety could form two different enantiomers, S_p and R_p . The S_p enantiomer is more likely to occur and is more easily reactivated by oximes [10].

Currently, treatment for OP poisoning consists of patient stabilisation, reduction of OP absorption, the use of an antimuscarinic agent, an oxime reactivator (e.g. pralidoxime and obidoxime) and an anti-convulsant. The mechanism of oxime action is based on displacing the phosphoryl group of the AChE-OP complex, owing to the fact that oxime having a higher affinity for the enzyme than OP does, and the high nucleophilic power of the oxime [2]. Furthermore, no oxime can restore AChE activity in structurally different OP moieties. Thus, the structure of the oxime determines its capacity to restore the function of AChE [11].

Despite various positive experimental evidence, the clinical trials with oximes have been controversial [12–14]. As pralidoxime and obidoxime are the most common reactivators available for clinical use, and considering the scarcity of literature data concerning the use of oximes in cases of methamidophos poisoning in physiological conditions, further studies are required to clarify the efficacy of oximes against methamidophos for different cholinesterases and develop new oximes capable of acting as cholinesterase reactivators against different OPs with better results. Furthermore, several *in silico* studies exemplified the capacity of simulation models to

Author for correspondence: Félix Alexandre Antunes Soares, Department of Chemistry, Federal University of Santa Maria, Santa Maria, RS CEP 97105-900, Brazil (fax + 55 55 3220 8978, e-mail felix@ufsm.br)

predict the molecular interactions with relative reliability. Therefore, the aim of our work was to study the effectiveness of the newly synthesised oximes in reactivating methamidophos-inhibited AChE in comparison with the effectiveness of the classical oximes (pralidoxime and obidoxime) and perform a molecular docking study to clarify the possible interaction between the oximes and the active site of AChE.

Materials and Methods

Chemicals. 2, 2-dinitro-5, 5-ditiobenzoic acid (DTNB) and acetylthiocholine iodide were purchased from Merck; pralidoxime chloride (2-hydroxyiminomethyl-1-methyl-pyridinium), obidoxime dichloride (1,1'-(Oxydimethylene)bis(pyridinium-4-carbaldoxime) dichloride) and methamidophos (O,S-Dimethyl phosphoramidothioate) were purchased from Sigma-Aldrich. The newly synthesised oximes were designated as oxime 1 (butane-2,3-dionethiosemicarbazone oxime) and oxime 2 (3-phenylhydrazono)butan-2-one oxime (fig. 1). All other chemicals were of the highest grade available commercially.

Animals. Adult male Wistar rats (200–250 g) were obtained from University of Santa Maria and maintained in an air-conditioned room (20–25°C) under natural lighting conditions (cycle 12:12 hr) with water and food (Guabi-RS, Brazil) *ad libitum*. All experimental procedures were performed according to the guidelines of the Committee on Care and Use of Experimental Animal Resources of the Federal University of Santa Maria, Brazil.

Preparation of erythrocyte ghosts. Haemoglobin-free erythrocyte ghosts were prepared according to previously described method [15] with minor modifications. Briefly, blood of non-fasted healthy voluntary donors was collected. Heparinised human blood was centrifuged (3000 × g, 10 min.) and the plasma removed and kept to test butyrylcholinesterase (BChE) activity. Erythrocytes were washed three times with two volumes of sodium/potassium phosphate buffer (0.1 M, pH 7.4). Then, the packed erythrocytes were diluted in 20 volumes (w/v) of hypotonic sodium/potassium phosphate buffer (6.7 mM, pH 7.4) to facilitate the haemolysis, followed by centrifugation at 30,000 × g (30 min., 4°C). The supernatant was removed and the pellet resuspended in hypotonic phosphate buffer.

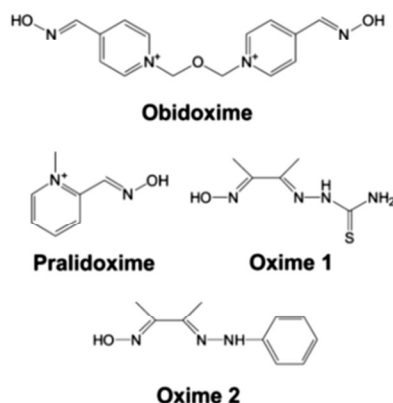


Fig. 1. Chemical structures of obidoxime, pralidoxime, butane-2,3-dionethiosemicarbazone oxime (oxime 1) and 3-(phenylhydrazono)butan-2-one oxime (oxime 2).

After two additional washing cycles, the pellet was resuspended in sodium/potassium phosphate buffer (0.1 M, pH 7.4), passed through one more centrifugation at 30,000 × g (30 min., 4°C) and were gently removed. Next, the AChE activity was adjusted to the original activity by appropriate dilution with phosphate buffer (0.1 M, pH 7.4). Aliquots of the erythrocyte ghosts were stored at –20°C until use.

Haemoglobin content present in ghost membranes was measured at 540 nm as the cyano-met-Hb form, but no haemoglobin was detected.

Cerebral tissue preparation. Animals were anaesthetised and killed by decapitation. Brain was quickly removed, placed on ice and homogenised in 10 volumes of 0.1 M sodium/potassium phosphate buffer (pH 7.4) and Triton X100. The homogenate was centrifuged at 400 × g at 4°C for 10 min. to yield a low-speed supernatant fraction (S1) that was used in the experiments. Aliquots were stored at –20°C until use.

Cholinesterases activity. Brain and ghost erythrocyte AChE and human plasma butyrylcholinesterase activities were estimated by the method of Ellman [16], using acetylthiocholine and butyrylthiocholine iodide as substrate, respectively. The rate of hydrolysis of substrate was measured at 412 nm through the release of the thiol compound that, when reacted with DTNB, produces the colour-forming compound TNB [17].

Reactivation/protection of OP-inhibited cholinesterase. Brain and ghost erythrocyte AChE and human plasma butyrylcholinesterase were exposed to oximes in two different assay conditions to identify a possible protective or a reactivation capacity of oximes:

1 Protection: the enzyme was exposed to methamidophos and oximes at the same time making up a total incubation period of 60 min.

2 Reactivation: the enzyme was firstly exposed to methamidophos for 10 min. After this, the oxime tested was added into the medium and the incubation followed for 50 min. (to perform an equal total incubation time period of 60 min.). Enzyme activities were referred to control activity.

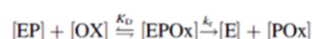
The values of the reactivation index (*R*) were calculated according to the following equation:

$$R = \left[\frac{\Delta A_r - \Delta A_i}{\Delta A_0 - \Delta A_i} \right] \times 100 (\%)$$

The symbol ΔA_0 is absorbance provided by mixture with intact AChE (in the final mixture, there was no organophosphate as well as no reactivator); ΔA_i is the absorbance of mixture with inhibited AChE (inhibition by organophosphate, no reactivator). Absorbance provided by mixture where AChE activity was influenced by organophosphate and consequently by reactivator was presented by the last symbol ΔA_r [18].

For the determination of reactivation rate constants, the method described by Worek *et al.* [19] was used, with some modifications. Briefly, an aliquot of ghosts inhibited by methamidophos (25 μM) for 10 min. was incubated with different oxime concentrations. For the AChE activity measurement, mixture aliquots (40 μL) were transferred to cuvettes containing sodium/phosphate buffer (0.1 M) at pH 7.4, DTNB (0.35 mM) and acetylthiocholine (0.9 mM), at various time intervals within 2-hr incubation.

According to Aldridge and Reiner [20], the reactivation consists of two consecutive steps, represented by the following scheme:



where [EP] is the phosphorylated enzyme, [Ox] the reactivator, [EPOx] the phosphonylenzyme-oxime complex, [E] the reactivated enzyme and [POx] the phosphorylated oxime; K_D ($[\text{EP}] \times [\text{Ox}]/[\text{EPOx}]$) is the dissociation constant which describes the affinity of the oxime to [EP] and k_r the rate constant for the displacement of the phosphoryl residue from [EPOx] by the oxime. In case of complete reactivation and with $[\text{Ox}] \gg [\text{EP}]_0$, a pseudo first-order rate equation can be derived for the reactivation process [21]:

$$k_{\text{obs}} = \frac{k_r \times [\text{Ox}]}{K_D + [\text{Ox}]}$$

k_{obs} is determined at various oxime concentrations. The amount of k_{obs} is not proportional to the oxime concentration but underlies saturation kinetics [22]. Under pseudo first-order conditions, the observed rate constant for the reactivation of the phosphorylated enzyme can be expressed by the following equation [23]:

$$\ln \frac{v_0 - v_t}{v_0 - v_i} = -k_{\text{obs}} \times t$$

representing the activities of the control enzyme (v_0), the inhibited enzyme (v_i) and the reactivated enzyme at time t (v_t). If $[\text{Ox}] \ll K_D$, the second-order reactivation rate constant k_{r2} (mM/min.), describing the specific reactivity, can be derived from the equation:

$$k_{r2} = \frac{k_r}{K_D}$$

Molecular docking. Docking simulations of the oximes with *Mus musculus* AChE were carried out using AutoDock Vina 1.1.1 [24], followed by redocking with Autodock 4.0.1. The non-aged methamidophos-inhibited *Mus musculus* AChE obtained from the RCSB Protein Data Bank (<http://www.rcsb.org/pdb/>) was used as macromolecule (PDB code 2jge). The oximes 1 (butane-2,3-dionethiosemicarbazone oxime) and 2 (3-(phenylhydrazono)butan-2-one oxime), as well as the two classical oximes, were constructed using the programme Avogadro 0.9 and their geometry were optimised with the MMFF 94 force field. Both ligands and macromolecule are previously prepared using AutoDock Tools [25] and Chimera 1.5 [26]. All rotatable bonds within the ligands were allowed to rotate freely, and the receptor was considered rigid. The grid was centred on the active site of AChE and the dimensions of the grid box consisted of $30 \times 22 \times 30$ Å points, with spacing of 1 Å. The exhaustiveness was set to 50. All other parameters were used as defaults. For each ligand docked, the conformation from the lowest binding free energy with inferred inhibitory reactivity was accepted as the best affinity model. The redocking calculation was carried out using Autodock 4.0.1, following the method of Musilek *et al.* [27]. Briefly, a Lamarckian genetic algorithm (Amber force field) was used, and a population of 150 individuals and 2,500,000 function evaluations were applied. The structure optimisation was performed for 27,000 generations. Docking calculations were set to 100 runs. At the end of calculation, Autodock performed cluster analysis. The 3D

affinity grid box was designed to include the full active and peripheral site of AChE. The number of grid points in the x -, y - and z -axes was 60, 60 and 60 with grid points separated by 0.253 Å. The conformations and interactions were analysed using the programmes Accelrys Discovery Studio Visualizer 2.5 and PyMOL [28].

Statistical analysis. Differences between groups were evaluated by one-way ANOVA, followed by Duncan's multiple range tests when appropriate. All values were presented as mean \pm S.E.M. and the differences were considered significant when $p < 0.05$. Data analysis and calculation of kinetic constants by linear and nonlinear regression analysis were performed with GraphPad Prism 5.0 (GraphPad, San Diego, CA, USA).

Results

Erythrocyte ghosts were exposed to methamidophos at various concentrations (ranging from 1 to 250 μM) and an aliquot was removed at different time intervals to test the AChE activity (fig. 2). The concentration of 25 μM of methamidophos was chosen to the next experiments, to have an inhibition of approximately 50% of AChE activity for approximately all the incubation period and thus, avoiding a possible re-inhibition process by the excess of methamidophos in the oxime-induced reactivation protocols. A spontaneous reactivation of AChE was not observed in the time interval used at this concentration. The same protocol was used to rat brain AChE and human plasma BChE, with similar results (data not shown). None of the tested oximes had significant effects *per se* on the activities of AChE and BChE at the tested concentrations. In addition, no direct hydrolytic effect on acetylthiocholine or butyrylthiocholine was observed (data not shown) in the protocols used.

Effects of oximes on methamidophos-inhibited rat brain AChE. Fig. 3 shows the effects of exposure to 25 μM methamidophos and the protective effect of oximes on AChE from the rat brain. Obidoxime (fig. 3A) had a slight, but significant, protective effect on methamidophos-induced AChE inactiva-

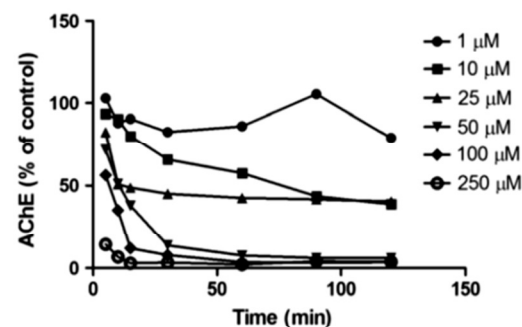


Fig. 2. Kinetics of methamidophos inhibition on AChE activity. The activities are expressed as percentage of control. Enzyme preparations were treated as described in the Materials and Methods section.

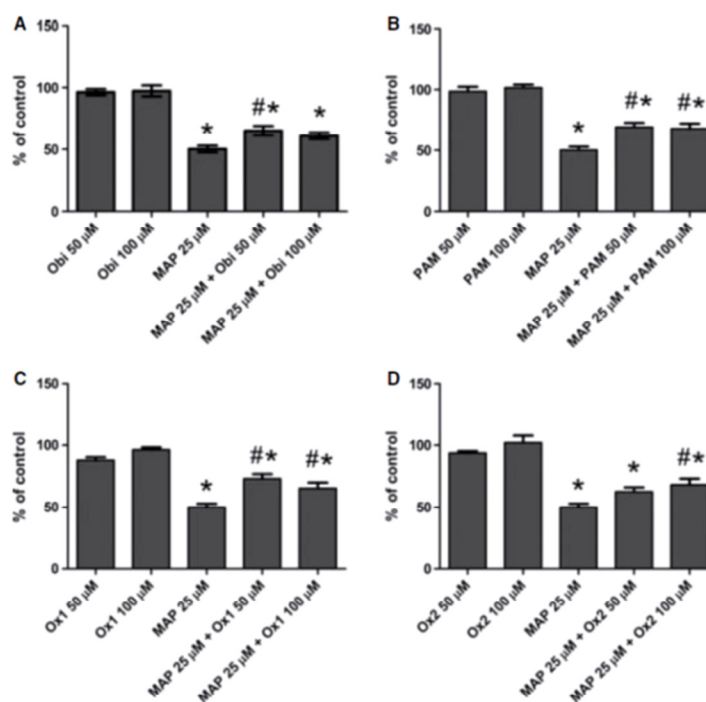


Fig. 3. Protective effect of obidoxime (A), pralidoxime (B), oxime 1 (C) and oxime 2 (D) on methamidophos (MAP)-inhibited AChE activity from rat brain homogenate. Oximes were added to the reaction medium at the same time of methamidophos. The data are expressed as percentage from control group (100%). *Statistically different from control group ($p < 0.05$); #statistically different from methamidophos 25 μM group ($p < 0.05$). Results are presented as the mean \pm S.E. of at least three independent experiments performed in duplicate.

tion. Pralidoxime (fig. 3B) significantly protected AChE from methamidophos-induced inhibition at all tested concentrations ($p < 0.05$). Similarly, oxime 1 (fig. 3C) at concentrations of 50 μM and 100 μM significantly ($p < 0.05$) protected against methamidophos-induced AChE inhibition, whereas oxime 2 was able to significantly protect the enzyme activity only at higher concentrations (fig. 3D).

Effect of oximes on methamidophos-inhibited human erythrocyte ghost AChE.

Fig. 4 shows the protective effects of oximes on methamidophos-inhibited AChE from human erythrocyte ghosts. Obidoxime at 50 μM (fig. 4A) plus methamidophos significantly increased cholinesterase activity in comparison with that observed for methamidophos alone ($p < 0.05$); however, it did not restore the enzyme activity to control levels. Pralidoxime (fig. 4B) exhibited significant protection of AChE activity at both concentrations tested compared with the findings for the methamidophos group ($p < 0.05$); however, this protective effect did not allow the enzyme to reach control activity levels. Oxime 1 (fig. 4C) exhibited protective activity for AChE ($p < 0.05$), as AChE activity was maintained at control levels at both concentrations of oxime 1 in the presence of methamidophos. Oxime 2 (fig. 4D) exerted a significant ($p < 0.05$) protective effect on methamidophos-induced AChE

inactivation at 100 μM , with control levels of enzyme activity being observed at this concentration.

Effect of oximes on methamidophos-inhibited plasma BChE.

Fig. 5 shows the protective effects of oximes on methamidophos-inhibited BChE from human plasma. Obidoxime (fig. 5A), pralidoxime (fig. 5B) and oxime 2 (fig. 5D) exerted no protective effects on methamidophos-induced BChE inhibition. Oxime 1 (fig. 5C) was the only oxime that significantly ($p < 0.05$) protected against methamidophos-induced BChE inhibition relative to the activity of BChE observed in the methamidophos group.

Reactivation of methamidophos-inhibited cholinesterases by oximes.

The results from the reactivation protocol were calculated as the percentage of reactivation, as summarised in table 1. For AChE from erythrocyte ghosts, obidoxime and pralidoxime had reactivation rates of 67.1% and 57.77%, respectively, at 50 μM , but this tendency was not statistically significant compared with the protective effects of the newly synthesised oximes 1 and 2 at the same concentration. For all tested oximes, better results were achieved at 50 μM than at 100 μM . For rat brain AChE, pralidoxime provided the best results regarding reactivation

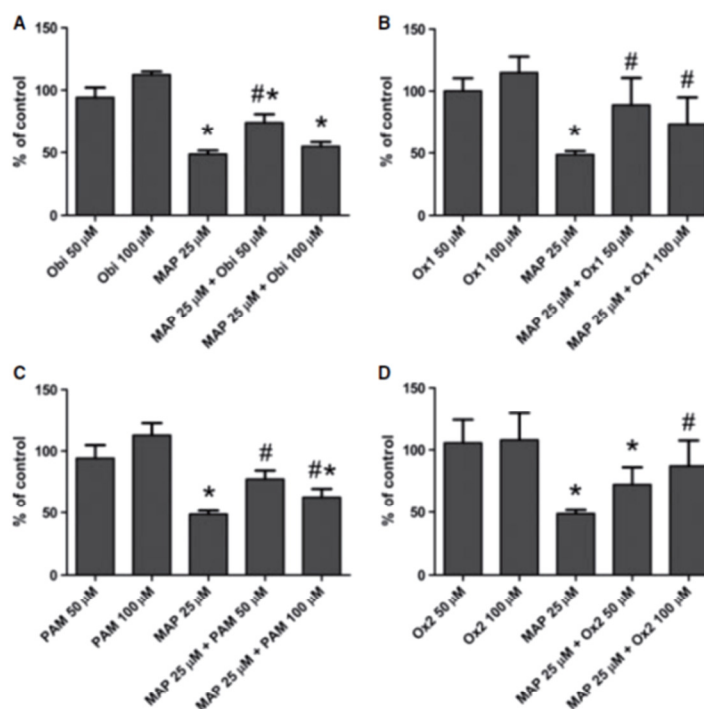


Fig. 4. Protective effect of obidoxime (A), pralidoxime (B), oxime 1 (C) and oxime 2 (D) on methamidophos (MAP)-inhibited AChE activity from human erythrocyte ghost. Oximes were added to the reaction medium at the same time that methamidophos. The data are expressed as % from control group (100%). *Statistically different from control group ($p < 0.05$); #statistically different from methamidophos 25 μM group ($p < 0.05$). Results are presented as the mean \pm S.E. of at least three independent experiments performed in duplicate.

capacity, whereas obidoxime and the two new oximes exhibited low reactivation capacities compared with that of pralidoxime.

Concerning BChE, the two currently available oximes, pralidoxime and obidoxime, had no reactivation effect on methamidophos-inhibited BChE, whereas oximes 1 (44.98%) and 2 (28.27%) exhibited significant reactivation activity at 50 and 100 μM , respectively.

The reactivation potencies, characterised by $1/K_D$ (affinity) and k_t (reactivity), were calculated for reactivation of methamidophos-inhibited AChE and BChE. In human erythrocyte AChE, the order of reactivity (k_t) and affinity (K_D) was pralidoxime > obidoxime > oxime 2 > oxime 1. The comparison of the second-order rate constants, k_{t2} , demonstrated a superior potency of pralidoxime.

In human plasma BChE, no rate constants could be calculated for the classical oxime (obidoxime and pralidoxime), owing to the absence of reactivation of the inhibited enzyme. For the new oximes 1 and 2, the rate constant analysis shows a higher reactivation and affinity constants for oxime 1, which is reflected in the second-order rate constant (k_{t2}).

Molecular docking results.

Molecular docking studies were performed on all tested oximes to rationalise their possible interactions with the oximes.

Pralidoxime which had the best reactivation capacity (table 1) presented binding energies of -5.83 and -5.3 kcal/mol for the S_p and R_p conformations of methamidophos, respectively. In the R_p conformation, the oxime group of pralidoxime is stabilised by hydrogen bonds with residues Arg296 and Phe295 in the acyl-binding pocket region (Trp236, Phe295, Phe297 and Phe338), and the aromatic ring is sandwiched among the peripheral anionic site (PAS) residues. For the S_p conformation, the oxime group of pralidoxime is stabilised by hydrogen bonds with residues Tyr133, Ala127, and Gly120, stabilising in the region between the oxyanion hole and the anionic subsite. The pyridine ring is sandwiched among the residues Trp86 (anionic subsite), Gly121 (oxyanion hole) and Ser203 (catalytic triad).

In the R_p conformation of methamidophos, obidoxime (fig. 6B) has a binding energy of -9.61 kcal/mol, and it is stabilised by hydrogen bonds with residues Tyr72, Asn87, and Arg296, being positioned between the acyl-binding pocket and the PAS. The linker between the pyridine rings is sandwiched among the residues Tyr124, Tyr337 and Tyr341 (PAS), forming a hydrogen bond with Tyr124. In the S_p conformation, the binding energy is -9.59 kcal/mol, and obidoxime exhibits a similar conformation to that of the R_p form of methamidophos, with the molecule being positioned in the PAS region among residues Asp74 and Ser125 and with hydrogen bonds

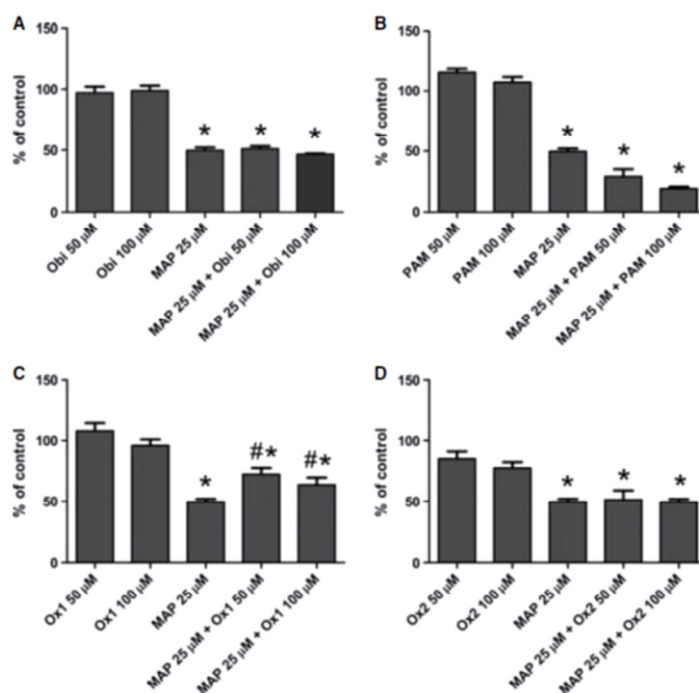


Fig. 5. Protective effect of obidoxime (A), pralidoxime (B), oxime 1 (C) and oxime 2 (D) on methamidophos (MAP)-inhibited BChE activity from human plasma. Oximes were added to the reaction medium at the same time as methamidophos. The data are expressed as percentage from control group (100%). *Statistically different from control group ($p < 0.05$); #statistically different from methamidophos 25 μM group ($p < 0.05$). The results are presented as the mean \pm S.E. of at least three independent experiments performed in duplicate.

Table 1.

Per cent reactivation of methamidophos-inhibited AChE by oximes in human erythrocyte ghost and rat brain AChE, and BChE from human plasma.

	Obidoxime		Pralidoxime		Oxime 1		Oxime 2	
	50 μM	100 μM	50 μM	100 μM	50 μM	100 μM	50 μM	100 μM
AChEery	67.1 \pm 6.53 ^{a,1}	22.23 \pm 9.69 ^{a,1}	58.77 \pm 30.77 ^{a,1}	30.57 \pm 11.65 ^{a,1}	41.50 \pm 18.13 ^{a,1}	3.97 \pm 3.3 ^{b,1}	47.98 \pm 8.59 ^{a,1}	7.96 \pm 3.03 ^{a,1}
AChEbra	3.55 \pm 1.89 ^{a,2}	0.95 \pm 1.2 ^{a,2}	52.74 \pm 5.89 ^{b,1}	66.05 \pm 4.70 ^{b,2}	15.71 \pm 6.3 ^{a,2}	5.31 \pm 5.1 ^{a,1}	6.36 \pm 2.67 ^{a,2}	5.89 \pm 4.37 ^{a,1}
BChE	<0	<0	<0	<0	44.98 \pm 8.18 ^{a,1}	<0	5.71 \pm 1.96 ^{b,2}	28.27 \pm 16.11 ^{a,1}

Superscript letters indicate statistical difference between oximes at the same concentrations.

Superscript numbers indicate statistical difference between the different enzymes.

AChE, acetylcholinesterase; BChE, butyrylcholinesterase.

formed with Tyr72, Asp74 and Asn87. The linker between the pyridine rings is stabilised among residues Tyr124, Tyr337 and Tyr341 (PAS).

The oxime moiety of the newly synthesised oxime 1 (fig. 6C) is stabilised by hydrogen bonds with residues Phe295, Arg296 and Phe338, being positioned between the PAS residues (Trp286 and Tyr341) and the acyl-binding pocket residues (Phe295, Phe297 and Phe338). The binding energy was -6.01 kcal/mol for both R_p and S_p enantiomers, and the conformation within the active site was similar. Oxime 2 (fig. 6D) exhibited a binding energy of -7.68 kcal/mol for both R_p and S_p enantiomers as well, and the oxime conformation was

practically the same for both enantiomers. Overall, the molecule was stabilised by hydrogen bonds with residues Tyr72, Asp74, Asn87 and Tyr124, with the aromatic ring sandwiched among the PAS residues (Tyr337 and Tyr341), acyl-binding pocket (Phe295, Phe297 and Phe338), and the catalytic residue Ser203, and the oxime group is close to the PAS residue Asp74.

Discussion

The main objective of our study was to investigate methamidophos-induced toxicity and oxime-mediated protection/reactivation of methamidophos-inhibited cholinesterases. We

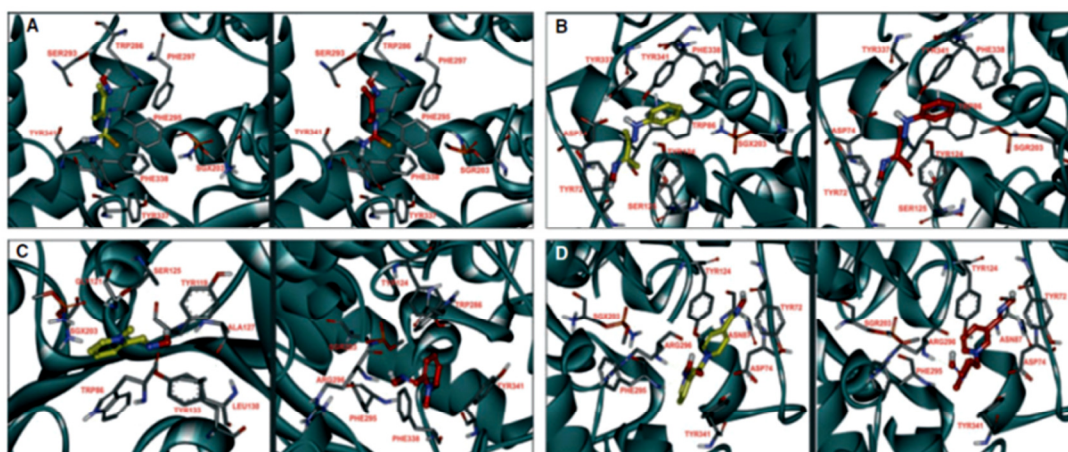


Fig. 6. Docking of the conformation corresponding to the oximes: oxime 1 (A), oxime 2 (B), pralidoxime (C) and obidoxime (D) inside MmAChE active site. The left panel refers to the SGX conformation of the modified Ser203 by methamidophos, whereas the right panel refers to the SGR conformation.

compared the effects of two classical oximes (pralidoxime and obidoxime) and two newly synthesised oximes in protecting or reactivating methamidophos-inhibited cholinesterases. The two newly synthesised oximes had previously been found to be related with a protective effect on LDL oxidation [29] and have shown no signs of toxicity during *in vivo* or *ex vivo* use [30,31]. In addition, these new oximes have been found to have LD₅₀ values similar to other oximes, including pralidoxime and obidoxime [32]. It has also been previously demonstrated that the oximes 1 and 2 reactivate AChE inhibited by chlorpyrifos, diazinon and malathion with a potency similar to that of pralidoxime, but to a lesser extent than obidoxime [33]. The results found in this study showed that both new oximes could reactivate AChE, although less than the classical oximes, and, unlike the classical oximes, reactivate BChE.

Methamidophos has become an important public health issue, particularly in Brazil, largely because of its frequent use on crops, resulting in high rates of occupational [8] and food [7] exposure. In regard to oxime reactivation of methamidophos-inhibited AChE, Pohanka *et al.* [34] showed an *in vitro* reactivation of human AChE by obidoxime and pralidoxime; however, the experimental protocol used focused on the qualitative analysis of contaminated water, with no physiological conditions included in the analysis. Furthermore, Wan *et al.* [35] showed a positive effect of pralidoxime in individuals poisoned with methamidophos, and Satar *et al.* [36] demonstrated a hepatoprotective effect of pralidoxime against methamidophos-induced (30 mg/kg) toxicity in rats. Necrosis of the diaphragm induced by methamidophos was also found to be protected against by pralidoxime under *in vivo* conditions [37]. In our work, we also observed a protection/reactivation effect of oximes on methamidophos-inhibited AChE, using obidoxime and pralidoxime as positive controls for comparison with the new oximes.

There are numerous studies in the literature relating oximes and the reactivation of organophosphate-inhibited AChE, with a published review by Jokanovic and Stojiljkovic [2]. However, the understanding of the structure–activity relationships for oxime reactivation of cholinesterases remains limited [11]. The mechanism of action of oxime reactivation is based on the displacement of the phosphoryl group of the AChE-OP complex [2]. The reactivation potency of the oximes depends on the nucleophilicity and orientation of the oxime [38], making molecular studies vital for the comprehension of this phenomenon. Here, the two new oximes tested have only one aldoxime group, similar to pralidoxime, while obidoxime has two aldoxime groups. Kassa *et al.* [39] previously demonstrated that the number of aldoxime groups is not that critical to enzyme reactivation. However, Cabal *et al.* [40] showed that other characteristics of the oxime could interfere with its reactivation power, such as the number of pyridinium rings and the position of the oxime group within the pyridinium ring. In our case, none of the new oximes tested contained pyridinium rings and, to some extent, could reactivate both AChE and BChE inhibited by methamidophos (tables 2 and 3). Additionally, the compounds showed reactivation of AChE inhibited by chlorpyrifos, diazinon and malathion to a similar level as pralidoxime [33], indicating that oximes not based on pyridinium rings could be promising for further studies with modifications to their molecular structure.

Wong *et al.* [10] previously demonstrated that the oxyanion hole could be the subsite through which pralidoxime attacks the OP bound on the tabun-modified Ser203, while Musilek *et al.* [27] demonstrated that mono-bisquaternary AChE reactivators appear to be positioned between the PAS and the acyl-binding pocket. Our docking results strongly agree with these previous works, with pralidoxime being positioned in the oxyanion hole and obidoxime between the PAS and the acyl-binding pocket. In this way, pralidoxime seems to be better

Table 2.

Oxime	Reactivation constant		
	k_r (/min)	K_D (μ M)	K_{r2} (mM/min.)
Obidoxime	0.013	712.9	0.018
Pralidoxime	0.014	475.3	0.029
Oxime 1	0.004	1008.2	0.004
Oxime 2	0.008	873.3	0.009

Human erythrocyte ghosts were incubated with methamidophos at 25 μ M for 10 min. at 37°C. Inhibited acetylcholinesterase was reactivated by oximes (in six different concentrations, ranging from 0.01 to 1 mM) by adding oximes to inhibited ghosts. Small aliquots were transferred after various intervals to a cuvette for measurement of AChE activity.

Table 3.

Oxime	Reactivation constant		
	k_r (min^{-1})	K_D (μ M)	K_{r2} (mM/min.)
Obidoxime	–	–	–
Pralidoxime	–	–	–
Oxime 1	0.007	763.9	0.009
Oxime 2	0.004	968.3	0.004

Human plasma was incubated with methamidophos at 25 μ M for 10 min. at 37°C. Inhibited acetylcholinesterase was reactivated by oximes (in six different concentrations, ranging from 0.01 to 1 mM) by adding oximes to inhibited ghosts. Small aliquots were transferred after various intervals to a cuvette for measurement of butyrylcholinesterase activity.

positioned into the active site for the reactivation process in the case of methamidophos-inhibited AChE. Surprisingly, the new oximes were not positioned as deeply into the active site as pralidoxime, but near the mouth of the gorge similar to obidoxime. This could explain the lesser reactivation potency of these oximes compared with pralidoxime and the fact that the new oximes protected AChE from inhibition to the same degree as the classical oximes, but with less potency for the reactivation of AChE. Furthermore, Wong *et al.* [10] also demonstrated that S_p enantiomers of cycloheptyl methylphosphonate-conjugated AChE are more likely to occur and are easily reactivated by oximes. Our molecular docking suggests the same behaviour for methamidophos-inhibited AChE, while pralidoxime had the best 'pose' in the S_p enantiomer (SGX in fig. 6).

Butyrylcholinesterase is able to catalyse the hydrolysis of acetylcholine to a lesser extent than AChE, thus regulating cholinergic neurotransmission. It has been suggested that BChE could act as a co-regulator for the action of acetylcholine (see Darvesh *et al.* [41]), and its inhibition can lead to a dose-dependent increase in the levels of acetylcholine in the brain [42]. Neuro-anatomical data demonstrated that BChE is expressed by specific populations of central [43,44] and peripheral [45] neurons, consistent with a co-regulatory role of BChE in cholinergic neurotransmission. In AChE-null mice, BChE was suggested to have a prominent role in the hydrolysis of acetylcholine, once

inhibition of BChE shown to be lethal [46]. This situation is analogous to AChE inhibition by OP compounds and, as BChE is present at 10 times higher levels in the human body than AChE (about 680 nmol of BChE and 62 nmol of AChE) [47], the hydrolysis of acetylcholine by the BChE may represent a way to deal with the high levels of acetylcholine caused by AChE inhibition. In this way, our results show that the new oximes reactivated BChE, while the classical oximes failed. This fact could represent an advantage in the treatment of a cholinergic crisis, with a minor reactivation effect on AChE. Modifications to the oximes' molecular structure may increase AChE reactivation, without loss of the effect on BChE.

Conclusions

Our work demonstrates that the newly synthesised oximes are able to protect and reactivate human erythrocyte AChE, however, less efficiently than pralidoxime and obidoxime, and reactivate human plasma BChE, where the classical oximes failed. In addition, our work demonstrates that the attack through the oxyanion hole of the active site of AChE appears to be the best subsite for the nucleophilic attack of oximes on methamidophos-inhibited AChE, which could guide the development of new oximes.

Acknowledgements

This work was supported by the FINEP research grant 'Rede Instituto Brasileiro de Neurociências (IBN-Net)' # 01.06.0842-00. P.G. receives a fellowship from PIBIC/CNPq/UFMS. T.H.L. receives a fellowship from CAPES. J.B.T.R., F.A.A.S., M.E.P., R.A.S. and N.B.V.B receive a fellowship by CNPq. Additional support was given by CAPES, CNPq, FAPERGS and INCT – National Institute of Science and Technology for Excitotoxicity and Neuroprotection/CNPq; and to Scripps Research Institute and Accelrys Inc. for providing free academic licence of programmes used in this study.

Conflict of Interest

The authors declare that there are no conflicts of interest.

References

- Silver A. The Biology of Cholinesterases. Elsevier, Amsterdam, 1974.
- Jokanovic M, Stojilkovic MP. Current understanding of the application of pyridinium oximes as cholinesterase reactivators in treatment of organophosphate poisoning. *Eur J Pharmacol* 2006; 553:10–7.
- Marrs TC. Organophosphate poisoning. *Pharmacol Ther* 1993;58: 51–66.
- WHO. Methamidophos Health and Safety Guide. World Health Organization, Geneva, 1993.
- Worek F, Thiermann H, Szinicz L, Eyer P. Kinetic analysis of interactions between human acetylcholinesterase, structurally different organophosphorus compounds and oximes. *Biochem Pharmacol* 2004;68:2237–48.
- Worek F, Aurbek N, Koller M, Becker C, Eyer P, Thiermann H. Kinetic analysis of reactivation and aging of human acetylcholinesterase inhibited by different phosphoramidates. *Biochem Pharmacol* 2007;73:1807–17.

- 7 Caldas ED, Boon PE, Tressou J. Probabilistic assessment of the cumulative acute exposure to organophosphorus and carbamate insecticides in the Brazilian diet. *Toxicology* 2006;222:132–42.
- 8 Recena MC, Pires DX, Caldas ED. Acute poisoning with pesticides in the state of Mato Grosso do Sul, Brazil. *Sci Total Environ* 2006;357:88–95.
- 9 Recena MC, Caldas ED, Pires DX, Pontes ER. Pesticides exposure in Culturama, Brazil—knowledge, attitudes, and practices. *Environ Res* 2006;102:230–6.
- 10 Wong L, Radic Z, Brüggemann RJM, Hosea N, Berman HA, Taylor P. Mechanism of oxime reactivation of acetylcholinesterase analyzed by chirality and mutagenesis. *Biochemistry* 2000;39:5750–7.
- 11 Kuca K, Jun D, Musilek K. Structural requirements of acetylcholinesterase reactivators. *Mini Rev Med Chem* 2006;6:269–77.
- 12 Eddleston M, Szinicz L, Eyer P, Buckley N. Oximes in acute organophosphorus pesticide poisoning: a systematic review of clinical trials. *QJM* 2002;95:275–83.
- 13 Eyer P. The role of oximes in the management of organophosphorus pesticide poisoning. *Toxicol Rev* 2003;22:165–90.
- 14 Helden HP, Busker RW, Melchers BP, Buijzeel PL. Pharmacological effects of oximes: how relevant are they? *Arch Toxicol* 1996;70:779–86.
- 15 Worek F, Eyer P, Kiderlen D, Thiermann H, Szinicz L. Effect of human plasma on the reactivation of sarin-inhibited human erythrocyte acetylcholinesterase. *Arch Toxicol* 2000;74:21–6.
- 16 Ellman GL, Courtney KD, Andres V Jr, Feather-Stone RM. A new and rapid colorimetric determination of acetylcholinesterase activity. *Biochem Pharmacol* 1961;7:88–95.
- 17 Worek F, Mast U, Kiderlen D, Diepold C, Eyer P. Improved determination of acetylcholinesterase activity in human whole blood. *Clin Chim Acta* 1999;288:73–90.
- 18 dos Santos AA, dos Santos DB, Dafre AL, de Bem AF, Souza DO, da Rocha JBT *et al.* In vitro reactivating effects of standard and newly developed oximes on malaoxon-inhibited mouse brain acetylcholinesterase. *Basic Clin Pharmacol Toxicol* 2010;107:768–73.
- 19 Worek F, Thiermann EH, Szinicz EL. Reactivation and aging kinetics of human acetylcholinesterase inhibited by organophosphorylcholines. *Arch Toxicol* 2004;78:212–7.
- 20 Aldridge WN, Reiner E. *Enzyme Inhibitors as Substrates—Interactions of Esterases With Esters of Organophosphorus and Carbamic Acids.* North-Holland Publishing, Amsterdam, 1972.
- 21 Su CT, Wang PH, Liu RF, Shih JH, Ma C, Lin CH *et al.* Kinetic studies and structure–activity relationships of bispyridinium oximes as reactivators of acetylcholinesterase inhibited by organophosphorus compounds. *Fundam Appl Toxicol* 1986;6:506–14.
- 22 Green AL, Smith HJ. The reactivation of cholinesterase inhibited with organophosphorus compounds. 2. Reactivation by pyridinealdoxime methiodides. *Biochem J* 1958;68:32–5.
- 23 Wang EIC, Braid PE. Oxime reactivation of diethylphosphoryl human serum cholinesterase. *J Biol Chem* 1967;242:2683–7.
- 24 Trott O, Olson AJ. AutoDock Vina: improving the speed and accuracy of docking with a new scoring function, efficient optimization and multithreading. *J Comput Chem* 2010;31:455–61.
- 25 Morris GM, Huey R, Lindstrom W, Sanner MF, Belew RK, Goodsell DS *et al.* AutoDock4 and AutoDockTools4: automated docking with selective receptor flexibility. *J Comput Chem* 2009;30:2785–91.
- 26 Pettersen EF, Goddard TD, Huang CC, Couch GS, Greenblatt DM, Meng EC *et al.* UCSF Chimera—a visualization system for exploratory research and analysis. *J Comput Chem* 2004;25:1605–12.
- 27 Musilek K, Komloova M, Holas O, Horova A, Pohanka M, Gunn-Moore F *et al.* Mono-oxime bisquaternary acetylcholinesterase reactivators with prop-1,3-diyl linkage—preparation, in vitro screening and molecular docking. *Bioorg Med Chem* 2011;19:754–62.
- 28 Seeliger D, De Groot BL. Ligand docking and binding site analysis with PyMOL and Autodock/Vina. *J Comput Aided Mol Des* 2010;24:417–22.
- 29 de Lima Portella R, Barcelos RP, de Bem AF, Carratu VS, Bresolin L, da Rocha JB *et al.* Oximes as inhibitors of low density lipoprotein oxidation. *Life Sci* 2008;83:878–85.
- 30 Puntel GO, Gubert P, Peres GL, Bresolin L, Rocha JB, Pereira ME *et al.* Antioxidant properties of oxime 3-(phenylhydrazono) butan-2-one. *Arch Toxicol* 2008;82:755–62.
- 31 Puntel GO, de Carvalho NR, Gubert P, Palma AS, Dalla Corte CL, Avila DS *et al.* Butane-2,3-dionethiosemicarbazone: an oxime with antioxidant properties. *Chem Biol Interact* 2009;177:153–60.
- 32 Arena JM. *Poisoning, Toxicology, Symptoms, Treatments*, 4th edn. Charles C. Thomas, Springfield, IL, 1979:133.
- 33 Costa MD, Freitas ML, Soares FAA, Carratu VS, Brandão R. Potential of two new oximes in reactivate human acetylcholinesterase and butyrylcholinesterase inhibited by organophosphate compounds: an in vitro study. *Toxicol In Vitro* 2011;25:2120–3.
- 34 Pohanka M, Jun D, Kuca K. Improvement of acetylcholinesterase-based assay for organophosphates in way of identification by reactivators. *Talanta* 2008;77:451–4.
- 35 Wan WG, Zheng SC, Zou HJ, Ma SD, Tao GZ, Xu ZF *et al.* Different therapeutic efficacy of pralidoxime chloride PAM-Cl on AChE against acute toxicity of methamidophos, dichlorovos and omethoate. *Chin J Ind Hyg Occup Dis* 2007;25:586–9.
- 36 Satar S, Satar D, Tap O, Koseoglu Z, Kaya M. Ultrastructural changes in rat liver treated with pralidoxime following acute organophosphate poisoning. *Mt Sinai J Med* 2004;71:405–10.
- 37 Santos RP, Cavaliere MJ, Puga FR, Narciso ES, Pelegrino JR, Calore EE. Protective effect of early and late administration of pralidoxime against organophosphate muscle necrosis. *Ecotoxicol Environ Saf* 2002;53:48–51.
- 38 Ashani Y, Radic Z, Tsigelny I, Vellom DC, Pickering NA, Quinn DM *et al.* Amino acid residues controlling reactivation of organophosphoryl conjugates of acetylcholinesterase by mono- and bisquaternary oximes. *J Biol Chem* 1995;270:6370–80.
- 39 Kassa J, Jun D, Karasova J, Bajgar J, Kuca K. A comparison of reactivating efficacy of newly developed oximes (K074, K075) and currently available oximes (obidoxime, HI-6) in soman, cyclosarin and tabun-poisoned rats. *Chem Biol Interact* 2008;175:425–7.
- 40 Cabal J, Kuca K, Kassa J. Specification of the structure of oximes able to reactivate tabun inhibited acetylcholinesterase. *Basic Clin Pharmacol Toxicol* 2004;95:81–6.
- 41 Darvesh S, Hopkins DA, Geula C. Neurobiology of butyrylcholinesterase. *Nat Rev* 2003;4:131–8.
- 42 Giacobini E. Cholinesterase inhibitors: from the Calabar bean to Alzheimer therapy. In: Giacobini E (ed.). *Cholinesterases and Cholinesterase Inhibitors*. Martin Dunitz, London, UK, 2000; 181–226.
- 43 Darvesh S, Hopkins DA. Differential distribution of butyrylcholinesterase and acetylcholinesterase in the human thalamus. *J Comp Neurol* 2003;463:25–43.
- 44 Tago H, Maeda T, McGeer PL, Kimura H. Butyrylcholinesterase-rich neurons in rat brain demonstrated by a sensitive histochemical method. *J Comp Neurol* 1992;325:301–12.
- 45 Darvesh S, MacDonald SE, Losier AM, Martin E, Hopkins DA, Armour JA. Cholinesterases in cardiac ganglia and modulation of canine intrinsic cardiac neuronal activity. *J Auton Nerv Syst* 1998;71:75–84.
- 46 Mesulam MM, Guillozer A, Shaw P, Levey A, Duysen EG, Lockridge O. Acetylcholinesterase knockouts establish central cholinergic pathways and can use butyrylcholinesterase to hydrolyze acetylcholine. *Neuroscience* 2002;110:627–39.
- 47 Manoharan I, Boopathy R, Darvesh S, Lockridge O. A medical health report on individuals with silent butyrylcholinesterase in the Vysya community of India. *Clin Chim Acta* 2007;378:128–35.

2.3 *Manuscrito 1:* “Explicando a eficácia da reativação de oximas na AChE inibida pelo metamidofós por bioquímica quântica computacional”

Explaining Oximes Reactivation Effectiveness on Methamidophos-Inhibited
AChE by Quantum Biochemistry Computations

Thiago Henrique Lugokenski, Rogério de Aquino Saraiva, Roner Ferreira da
Costa, Eveline Matias Bezerra, João Batista Teixeira da Rocha, Ewerton
Wagner Santos Caetano, Valder Nogueira Freire, Felix Alexandre Antunes
Soares.

Explaining Oximes Reactivation Effectiveness on Methamidophos-Inhibited AChE by
Quantum Biochemistry Computations

Thiago Henrique Lugokenski, Rogério de Aquino Saraiva, Roner Ferreira da Costa,
Eveline Matias Bezerra, João Batista Teixeira da Rocha, Ewerton Wagner Santos
Caetano, Valder Nogueira Freire, Felix Alexandre Antunes Soares.

T.H. Lugokenski, R.A. Saraiva, J.B.T. Rocha, F.A.A. Soares (Correspondent Author)
Departamento de Química,
Universidade Federal de Santa Maria,
Santa Maria – Brazil
e-mail: felix@ufsm.br
R.F. Costa, E.M. Bezerra, V.N. Freire, E.W.S. Caetano,
Departamento de Física,
Universidade Federal do Ceará
Fortaleza – Brazil

ABSTRACT

Organophosphorus compounds (OPC), as methamidophos, are neurotoxic agents that act by inhibiting the enzyme acetylcholinesterase (AChE), which is fundamental for the control of transmission of nervous impulses. The main way of counteract OPC poisoning is the administration of oximes, however none of them are efficient against all the known OPC. By taking advantage of the crystallographic data of AChE complexed with methamidophos, a quantum biochemistry study based on the density functional theory were performed to estimate the interaction energy of four oximes with individual amino acids residues of the binding pocket of the AChE. For this purpose, we applied a density matrix (DM) scheme based on Molecular Fractionation with Conjugated Caps (MFCC). The classical oximes, obidoxime and pralidoxime, are shown to be the most strongly oximes bound to the AChE. A binding site, interaction energy between residues and oximes atoms, and residues domain (BIRD) panel were constructed, and indicating clear quantum biochemistry-based routes for the development of new oximes. Besides, novelties about the role of distant amino acids residues, that were neglected until far, and the mechanism of enzyme reactivation are also demonstrated.

INTRODUCTION

The principal biological function of acetylcholinesterase (AChE, acetylcholine hydrolase, E.C. 3.1.1.7) is to terminate the excitatory effect of the neurotransmitter acetylcholine (ACh) in the terminal nervous junction with its effector organs or post-synaptic sites. This occurs by the rapid hydrolysis of ACh to choline and acetate catalysed by AChE [1]. This reaction is particularly important since ACh participates in a number of essential processes in a variety of peripheral organs such as heart, urinary bladder, gastrointestinal tract and ciliary muscle. Particularly important, ACh is responsible for muscle endplates stimulation that results in a partial depolarization followed by Ca^{2+} release, leading to the muscle contraction. The muscle tone is maintained by spontaneous and intermittent release of ACh in the neuromuscular junction [2].

The catalytic site of AChE is located close to the base of a narrow active site gorge that extends 20 Å into the enzyme [1], being the enzyme diameter of approximately 40 Å. The catalytic triad (Glu334-His447-Ser203) is found at the bottom of the active site gorge, surrounded by four structural features important for catalytic activity: the acyl binding pocket (residues Trp236, Phe295, Phe297, and Phe338), the oxyanion hole (main chain nitrogen from residues Gly121, Gly122, and Ala204), the anionic subsite (residues Trp86, Tyr133, Glu202, Gly448, and Ile451) and the peripheral anionic site (residues Asp74, Tyr124, Ser125, Trp286, Tyr337, and Tyr341) [1,3].

AChE is a known target for a variety of drugs, being used for treatment of Alzheimer disease, and also for plague control in agriculture. For this purpose, several organophosphate compounds with anti-AChE effects were developed and largely used

in a variety of cultivations such as brassica, cotton, tobacco, sugar beet, lettuce, potatoes, and tree fruits [4]. Besides the importance of the use of organophosphates in agriculture, the toxic exposure to humans is a great issue, being classified by the World Health Organization as a major problem with unknown and high dread risks [5].

Organophosphorus compounds (OPC) acts, mainly, by inhibiting AChE through covalently binding to the catalytic residue Ser203, forming an inactive enzyme (AChE-OP). In humans, this inhibition lead to several problems related with a cholinergic crisis, mainly muscle paralysis and fasciculation, as the result of the increased ACh in the synapse of the neuromuscular junction, which leads to a persistent depolarization of the motor endplate. This paralysis affects the muscles responsible by the respiration, mainly diaphragm and intercostal muscles, leading to respiratory failure and, eventually, to death [2,6]. Among the organophosphate compounds, methamidophos is one of the most common pesticides used in developing countries, with more than 90% of Brazilian small farmers reporting its use, with nearly 60% of them exhibiting typical organophosphate intoxication symptoms [7], being an important issue regarding food and occupational exposure [8,9].

Currently, treatment for OP poisoning consists of patient stabilization, reduction of OP absorption, the use of an antimuscarinic agent, an oxime reactivator (e.g. pralidoxime and obidoxime), and an anticonvulsant. The oxime mechanism of action is based on displacing the phosphoryl group of the AChE-OP complex, which is based on the higher oxime affinity for the enzyme in comparison with OP, as well as the high nucleophilic power of the oxime [4]. Furthermore, no oxime can restore AChE activity in structurally different OP moieties. Thus, the structure of the oxime determines its capacity to restore the function of AChE [7].

In order to molecularly explain the interactions between ligands and proteins and for scoring functions, several docking programs have been some success in obtain the correct binding mode [10]. However, the calculation of the binding free energy has proven challenging [11], once that there is a complex interplay of interactions between the ligand and the protein that interferes in the free energy of binding. So, besides a good prediction of the “pose” of the ligand into the protein, docking scoring functions are compromised, been simplistic empirical or statistical potentials that relate observables to the free energy of binding by using statistical methods. In this way, QM/MM (quantum mechanics/molecular mechanics) methods are beginning to be used to compute protein-ligand binding affinities. Khandelwal et al. [12] used an approach that involves docking, QM/MM optimization, molecular dynamics and QM/MM interaction energy calculation. On other hand, higher levels of theory, such as the Density Functional Theory (DFT), have been used to calculate wavefunctions of macromolecules. Gao et al. [13] have described the application of a density matrix (DM) scheme based on Molecular Fractionation with Conjugated Caps (MFCC), where the DM is calculated for capped fragments at high levels of theory and the total energy is the sum of the fragment DMs. Recently, da Costa et al. [14] successfully applied a MFCC-based scheme to calculated the individual contribution of each residue and the binding free energy of statins bond to the active site of HMG-CoA reductase, using DFT-based methods.

The molecular mechanisms by which oximes reactivate organophosphate-inhibited AChE has been the target of a number of docking studies. In a general way, these studies point out to an important participation of the aromatic residues Tyr124, Trp286, Tyr337 and Tyr341 in the stabilization of mono-oxime bisquaternary compounds in the active site of AChE, by forming π - π and cation- π interactions [15].

Furthermore, Ekström et al. [16] employed molecular dynamics simulation in sarin-inhibited AChE together with the oxime HI6, finding that one of the HI6 rings (the carboxyamino-pyridinium ring) is sandwiched by the residues Tyr124 and Trp286. On the other hand, the oxime-pyridinium ring is disordered and could reach the sarin-modified Ser203 through a hydrogen-bond network. Delfino and Figueroa-Villar [17] used density functional theory (DFT) to model the sarin-inhibited AChE adduct, obtaining the reactivation potency of other nucleophiles rather than oximes. Finally, Castro and Figueroa-Villar [18] used DFT calculations to investigate the molecular structure, conformational analysis and charge distribution of pralidoxime.

Although these findings been very interesting, all of the employed techniques are very limited on quantify the effectiveness of each residue to the oxime-AChE-OP bonding. The knowledge of the individual contribution of each residue is essential to the understanding of the ligand pathway actions leading to its bond to the AChE-OP and the subsequent reactivation process, and should be very useful to the design of new oximes. Quantum mechanical (QM) methods are becoming popular in computational drug design and development mainly because high accuracy is required to estimate (relative) binding affinities [19]. Kee et al. [20] demonstrated, using the enzyme HMG-CoA reductase, that local density functional theory (DFT) match quantum chemistry MP2 energy values for aromatic binding better than hybrid or gradient- corrected DFT methods, what could be applied for the studies of oximes (that frequently presents aromatic rings) and AChE (active site rich in aromatic residues).

The purpose of this work is to present a description of the binding of four different oximes on methamidophos-inhibited AChE, through a docking study followed by quantum chemistry investigation of the oximes interactions with residues inside a 14 Å radius region encircling the oxime binding region. We take full advantage of the

already published 2.6 Å resolution X-ray structure of the *Mus musculus* AChE crystalized with methamidophos [21]. We simulated the position of the oximes into the AChE active site using docking methods, followed by the calculation of the interaction energy between AChE and the oximes, by the Molecular Fractionation with Conjugate Cap (MFCC) scheme, as described in the Methods section.

MATERIALS AND METHODS

The X-ray diffraction data of reference [21] provides the structures of *Mus musculus* AChE complexed with methamidophos with a resolution of 2.6 Å at neutral pH (PDB code 2jge) [21]. Methamidophos is covalently attached in the AChE binding site, at the catalytic residue Ser203, in a non-aged form (not occur the dealkylation process). This data were taken as an input for the subsequent steps. This crystallographic data is very useful; however, no crystallographic data with methamidophos plus oximes were available. For contour this limitation, we used docking simulations to predict the best “pose” of the oximes into the AChE active site.

The docking procedure was done accordingly with Musilek et al. [15]. Briefly, both ligands and macromolecule are prepared using AutoDock Tools [22] e Chimera 1.5 [23]. All rotatable bonds within the ligands were allowed to rotate freely, and the receptor was considered rigid. The oximes were previously constructed using the program Avogadro 0.9 and their geometry were optimized with the MMFF 94 force field. In the AutoDock program, a Lamarckian genetic algorithm (Amber force field) was used, and a population of 150 individuals and 2500000 function evaluations were applied. The structure optimization was performed for 27000 generations. Docking calculations were set to 100 runs. At the end of calculation, Autodock performed cluster

analysis. The 3D affinity grid box was designed to include the full active and peripheral site of AChE. The number of grid points in the x-, y- and z-axes was 60, 60 and 60 with grid points separated by 0.253 Å. The conformations and interactions were analyzed using the programs Accelrys Discovery Studio Visualizer 2.5 and PyMOL [24].

The quantum mechanics methods, *ab initio*, were becoming popular in the study of biological systems, for example enzymatic reactions and the structure of proteins and their ligand binding site. Particularly, the development of improved quantum methods, as DFT and Hartree-Fock, is allowing the application of quantum mechanics to explain ligand-protein bound [14]. Here, we used the DFT approach to estimate the interaction energy between the oximes and specific residues of AChE. Initially, the atomic positions of the non-hydrogen atoms at the binding pocket (including those belonging to the oximes molecules) were kept fixed, while the hydrogen atomic positions were initially optimized by using the Universal force field. Afterwards, simulations within the Density Functional Theory formalism using the Local Density Approximation for the exchange-correlation functional (DFT/LDA) were carried out using the DMOL3 code [25, 26]. A double numerical plus polarization (DNP) basis set was chosen to expand the electronic Kohn-Sham orbitals taking into account all electrons. The DNP basis set is very accurate with neglectful basis set superposition error (BSSE) [25-27]. The orbital cutoff was global and the self consistent field convergence threshold was adjusted to 10^{-6} Ha. Interaction energies between each oxime molecule and neighbour amino acid residues at the binding pocket of AChE were calculated by using the MFCC (molecular fractionation with conjugate caps) strategy [14]. The interaction (binding) energy between the oximes molecule O and the amino acid residue Ri , is given by

$$E(O - R^i) = E(O - C^{i-1}R^iC^{i+1}) - E(C^{i-1}R^iC^{i+1}) + \\ - E(O - C^{i-1}C^{i+1}) + E(C^{i-1}C^{i+1})$$

where the C_i cap is obtained by attaching a carboxyl or amine group to the dangling bond of the residue R_i . At the right side of Eq. (1), $E(O - C^{i-1}R^iC^{i+1})$ is the total energy of the system formed by the statin and the capped residue; the $E(C^{i-1}R^iC^{i+1})$ term is the total energy of the capped residue alone; $E(O - C^{i-1}C^{i+1})$ is the total energy of the system formed by the statin molecule and the caps alone. Finally, $E(C^{i-1}C^{i+1})$ is the total energy of the system formed only by the molecular caps. The total binding energy of each statin is obtained by adding the binding energies with each one of the amino acid residues taken into account within the chosen interaction radius.

RESULTS AND DISCUSSION

The oxime-based reactivators of AChE acts in a specific way, being that no oxime with broad spectrum is available to counteract the inhibition caused by different organophosphorus compounds. Thus, the molecular structure of the oximes and the interacting residues determines the efficacy of each oxime to reactivate the AChE. The knowledge of which residues of the binding pocket are contributing to the oxime binding is very useful for the development of new drugs, and is not trivial specify which using only crystallographic data or structural docking information. For example, there is not a simple relationship between interaction energy and statin-amino acid residue distance on HMG-CoA reductase. However, docking studies has obtained success in predict the exact “pose” of ligands in the binding pocket, but the free energy of binding and the participation of each residue to the stabilization of the ligand are not accurate. Here, we use a two-step approach to reach the information of how the oximes bind in the active site of AChE and which are the principal residues involved in the stabilization of the oxime; firstly we perform a docking study to predict the more stable

conformation of oxime into the active site; next, we used the molecular fractionation with conjugate caps (MFCC, see Materials and Methods section) scheme, that allows one to calculate the interaction energy between a given residue and its close oxime atom at higher levels of quantum theory [28].

Figure 2 shows the dimer of AChE (fig. 2A) and the main residues involved in the oxime bond at the AChE active site (fig. 2B). In figure 3, we may see the lowest energy “pose” of obidoxime and pralidoxime given by the docking procedure, while in figure 4 is possible observe the lowest energy conformation of the new oximes 1 and 2. Here, we define the binding pocket sphere (BPS) with radius r as an imaginary sphere centered at the ligand centroid and a binding pocket of radius r , $BP(r)$, is defined as the set of amino acid residues with at least one atom into the corresponding BPS. The interactions of a oxime molecule complexed with AChE is defined as a function of r , $E(r)$, and is obtained by adding up the energies of all the interacting elements inside the $BP(r)$. So, is expected that at small r only the contributions of the neighbor residues; at intermediate BPS sizes, the interaction energy will probably change slowly, reaching to a convergence point at larger r values.

In figure 5, we show the interaction energy as a function of r for obidoxime (long dashed), pralidoxime (dashed), oxime 1 (dashed – dotted) and oxime 2 (solid). Here, is possible observe that at r larger than 12 Å the total interaction energy stabilizes (varies by less than 10%) for all oximes. Besides, there are clearly distinct patterns for all four oximes, exhibiting a sharp decrease starting at $r \sim 4$ and 6.5 Å, for obidoxime and pralidoxime, respectively, and a slight decrease for oximes 1 and 2, starting at $r \sim 3.5$ and 4 Å, respectively. A total energy minimum for $E(r)$ occur at $r \sim 12$ Å for obidoxime and pralidoxime, $r \sim 11.5$ and 10 Å for oximes 1 and 2, respectively. After

this energy range, $E(r)$ present only small oscillations, mainly due to presence of charged amino acid residues which weakly repel or attract the ligands.

To a better comparison of the four oximes complexed with methamidophos-inhibited AChE, figure 6 shows the interaction energies $E(r)$ in different radius from 4 to 14 Å, varying at each 2 Å. Its observable that obidoxime has the higher interaction energy for all r showed in the figure and, presumably, the best reactivator potency on methamidophos-inhibited AChE. Pralidoxime shows an increased affinity to the binding pocket beyond ~ 8 Å, where oximes 1 and 2 shows an increased affinity at the smallest binding pocket (similar to pralidoxime). These data indicates that the classical oximes (obidoxime and pralidoxime) are more stabilized into the active site than the oximes 1 and 2, and could be better reactivators than the new ones. Agreeing with that, a previous work of our group that shows reactivity constants (k_r) of 0.013 and 0.014 min^{-1} for obidoxime and pralidoxime, respectively, and 0.04 and 0.08 min^{-1} for oximes 1 and 2, respectively. Besides the better interaction energy for obidoxime, pralidoxime shows practically the same k_r value than obidoxime. This is explained by the reason of that reactivation is dynamic process, where the not just the stabilization of the ligand is relevant, but also its position into the site. Wong et al. [29] shows that the oxyanion hole (G120, G121 and A204), could be the subsite through which pralidoxime attacks the OP bound on the modified S203, when Musilek et al [14] demonstrated that mono-bisquaternary AChE reactivators (similar to obidoxime) appear to be positioned between the peripheral anionic site and the acyl-binding pocket. In this way, pralidoxime seems to be better positioned into the site for the reactivation process, once it's much more proximal of the target residue S203, where obidoxime probably pass for an "activation" process [30] where one of the oxime groups (C=OH) become

deprotonated, exposing a negative charge ($C=O^-$) that is attracted to P atom of the modified S203.

The oximes residues inside 0.5 Å thick spherical shells centered at each oxime centroid are shown in Table 1. The negatively (positively) charged residues are shown in red (blue) color. The important positively charged arginine residue R296 occurs in the 4.5 Å (for oxime 1), 8 Å (obidoxime), 10.5 Å (oxime 2) and 13 Å shells (pralidoxime). The negatively charged aspartic acid residue, D74, belongs to the 4 Å shells for the oxime 2, 5 Å for obidoxime, 7.5 Å for pralidoxime and 8.5 Å for oxime 1. The others charged residues that are beyond the 9.0 Å binding pocket sphere do not contribute to the interaction energy by a significant amount, except for the residue E202 in the case of obidoxime, that markedly contribute to the oxime bonding, and occurs at 12 Å BPS.

Figures 7 and 8 are an aid to understand the results obtained for the specific interaction between each oxime molecule and neighbor amino acid residues at the binding pocket of AChE. These figures show the most relevant amino acid residues in the binding of the oximes in the active site. Figure 1 also is an aid to the understand of the results presented in Figures 9-12, it depicts the structure and relevant functional groups of the oximes, which are the main focus of the present study. The number of the atoms and regions presented in the figure are also shown in the Figures 9-12 to present the possible atoms that are interaction strongly with the respective amino acid residue.

Figures 9 to 12 show graphic panels with the interaction energies between the four oximes and the most important amino acid residues at the binding region of AChE. These graphic panels are called BIRD, following description of da Costa et al. [14]. BIRD is an acronym of the keywords: binding site, interaction energy and residues domain, and have the advantage of shows in just one graphic the interaction energy (in

kcal/mol) of the residue with the drug and the region and atoms of the drug which are interacting to each residue at the binding site. The different patterns of interaction energy are reflex of two main characteristics: the molecular structure of each oxime and the position at the binding pocket. First of all, these two features should be analyzed together, once the interaction between the ligands and specific residues depends not only of the ligand, but also of the characteristics of the residue and the relative distance of this to the ligand.

We can see from figure 9 that the electrostatic interactions are the main forces contributing to the stabilization of obidoxime. The residues D74 and E202 present the main attractive forces, when the residue R296 is the main repulsive charge. This is an expected result, once obidoxime has two positively charged nitrogen atoms; however, the strong repulsive power of the distant residue R296 is quite surprising, and could limit the access of the oxime group of the second pyridinium ring to the target residue S203. This residue is neglected as a contributing force to the binding of oximes into the AChE binding site, and is an important find of our work. The second most important residues to the stabilization of obidoxime into the binding site are the hydrophobic ones, the residues F338, Y72 and Y337 presumably made π - π interactions with the pyridinium rings of obidoxime, when the residues Y124 and Y341 are most likely to interact with the quaternary nitrogen of the pyridinium rings, by cation- π interactions.

Pralidoxime follows the same pattern of interactions than obidoxime, with the electrostatic interaction with D74, E202 and R296 being the most contributing forces, followed by the π - π and cation- π interactions with the residues Y72, W86 and Y133. Furthermore, hydrogen interaction with the residues G120, G121 and ALA204 are also important, stabilizing the pralidoxime in the oxyanion hole region, which was shown to be the best position for this oxime attack the O-P bond of the modified S203 [29]. For

the new oximes 1 and 2, which do not have any formal charge, the electrostatic interactions have a secondary importance, being the hydrogen and π interactions more evident. This lack of quaternary nitrogen is probably a limiting factor to the AChE reactivator potency of the new oximes, as evidenced for the minor total interaction energy show in Figures 5 and 6.

Interestingly, all oximes (except oxime 2) show repulsive energies with the target of the reactivation process, the modified S203. This is in agreement with the possibility of an activation process of the oximes prior of the reactivation process, where the oximes could be un-protonated (to the oximate form) and expose a negative charge that would be attracted by the partial positive charge of the phosphorus atom of the organophosphate bond to the S203 [30]. However, there are indications pointing to the possibility that the reaction occurs with the neutral oxime, instead of the oximate form [18], raising the needed of additional studies to elucidate this question.

CONCLUSIONS

This work showed for the first time the contributions of each amino acid residue of the AChE in the binding of oximes, using quantum chemistry methods. From our data is possible confirm the importance of, at least, one quaternary nitrogen atom to the stabilization of oximes into the active site and, supposedly, a better reactivation potency, with evidences that the active form of the oximes is the un-protonated one, instead the neutral form. Particularly important, we demonstrated the main contributions of distant (longer than 8 Å) amino acids to stabilization of oximes into the active site of AChE, detaching the importance of the residue R296 for the geometric conformational adopted by obidoxime.

REFERENCES

[1] Sussman JL, Harel M, Frolow F, Oefner C, Goldman A, Toker L, Silman I (1991) Atomic Structure of Acetylcholinesterase from *Torpedo californica*: A Prototypic Acetylcholine-Binding Protein. *Science* 253:872-879.

[2] Taylor P, Brown JH (2006) In: Siegel GJ (ed.) *Basic Neurochemistry*, 7th edn. Elsevier Academic Press, Burlington.

[3] Giacobini E (2000) *Cholinesterases and Cholinesterase Inhibitors*. Martin Dunitz, London.

[4] Jokanovic M, Stojiljkovic MP (2006) Current understanding of the application of pyridinium oximes as cholinesterase reactivators in treatment of organophosphate poisoning. *Eur J Pharmacol* 553:10-17.

[5] WHO. World Health Report 2002. Reducing risks, promoting healthy life. Geneva: World Health Organization.

[6] WHO. Methamidophos Health and Safety Guide. World Health Organization, Geneva.

[7] Kuca K, Jun D, Musilek K (2006). Structural requirements of acetylcholinesterase reactivators. *Mini Rev Med Chem* 6:269-277.

[8] Recena MC, Caldas ED, Pires DX, Pontes ER (2006) Pesticides exposure in Culturama, Brazil--knowledge, attitudes, and practices. *Environ Res* 102:230-236.

[9] Wong L, Radic Z, Brüggemann RJM, Hosea N, Berman HA, Taylor P (2000) Mechanism of oxime reactivation of acetylcholinesterase analyzed by chirality and mutagenesis. *Biochemistry* 39:5750-5757.

[10] Taylor R, Jewsbury PJ, Essex JW (2002) A review of protein–small molecule docking methods. *J Comput Aided Mol Des* 16:151-166.

[11] Warren GL, Andrews CW, Capelli AM, Clarke B, LaLonde J, Lambert MH, Lindvall M, Nevins N, Semus SF, Senger S, Tedesco G, Wall ID, Woolven JM, Peishoff CE, Head MS (2006) A critical assessment of docking programs and scoring functions. *J Med Chem* 49:5912-5931.

[12] Khandelwal A, Lukacova V, Comez D, Kroll DM, Raha S, Balaz S (2005) A combination of docking, QM/MM methods, and MD simulation for binding affinity estimation of metalloprotein ligands. *J Med Chem* 48:5437-5447.

[13] Gao AM, Zhang DW, Zhang JZH, Zhang Y (2004) An efficient linear scaling method for ab initio calculation of electron density of proteins. *Chem Phys Lett* 394:293-297.

[14] da Costa RF, Freire VN, Bezerra EM, Cavada BS, Caetano EW, de Lima Filho JL, Albuquerque EL (2012) Explaining statin inhibition effectiveness of HMG-CoA reductase by quantum biochemistry computations. *Phys Chem Chem Phys* 14:1389-1398.

[15] Musilek K, Komloova M, Holas O, Horova A, Pohanka M, Gunn-Moore F, Dohnal V, Dolezal M, Kuca K (2011) Mono-oxime bisquaternary acetylcholinesterase reactivators with prop-1,3-diyl linkage — Preparation, in vitro screening and molecular docking. *Bioorg & Med Chem* 19:754-762.

[16] Ekström F, Hörnberg A, Artursson E, Hammarström L-G, Schneider G, Pang Y-P (2009) Structure of HI-6NSarin-Acetylcholinesterase Determined by X-Ray Crystallography and Molecular Dynamics Simulation: Reactivator Mechanism and Design. *PLoS ONE* 4:1-19.

[17] Delfino RT, Figueroa-Villar JD (2009) Nucleophilic Reactivation of Sarin-Inhibited Acetylcholinesterase: A Molecular Modeling Study. *J Phys Chem B* 113:8402–8411.

[18] Castro AT, Figueroa-Villar JD (2002) Molecular Structure, Conformational Analysis and Charge Distribution of Pralidoxime: Ab Initio and DFT Studies. *Int J Quant Chem* 89:135-146.

[19] Zhou T, Huang D, Caflich A (2010) Quantum mechanical methods for drug design. *Curr Top Med Chem* 10:33-45.

[20] Kee EA, Livengood MC, Carter EE, McKenna M, Cafiero M (2009) Aromatic Interactions in the Binding of Ligands to HMGCoA Reductase. *J Phys Chem B* 113:14810–14815.

[21] Hörnberg A, Tunemalm A, Ekström F (2007) Crystal Structures of Acetylcholinesterase in Complex with Organophosphorus Compounds Suggest that the Acyl Pocket Modulates the Aging Reaction by Precluding the Formation of the Trigonal Bipyramidal Transition State. *Biochemistry* 46:4815-4825.

[22] Morris GM, Huey R, Lindstrom W, Sanner M F, Belew R K, Goodsell DS (2009) AutoDock4 and AutoDockTools4: Automated Docking with Selective Receptor Flexibility. *J. Comput. Chem.* 58:2785–91.

[23] Pettersen EF, Goddard TD, Huang CC, Couch GS, Greenblatt DM, Meng EC (2004) UCSF Chimera--a visualization system for exploratory research and analysis. *J. Comput Chem.* 25:1605-12.

[24] Seeliger D and De Groot B L (2010) Ligand docking and binding site analysis with PyMOL and Autodock/Vina. *J. Comput. Aided Mol. Des.* 24:417–422.

[25] Delley B (1990) An all-electron numerical method for solving the local density functional for polyatomic molecules. *J. Chem. Phys.* 92:508–517.

[26] Delley B (2000) From molecules to solids with the DMol3 approach *J. Chem. Phys.* 113:7756–7764.

[27] Inada Y and Orita H (2008) Efficiency of numerical basis sets for predicting the binding energies of hydrogen bonded complexes: Evidence of small basis set superposition error compared to Gaussian basis sets. *J. Comp. Chem.* 29:225–232.

[28] Zhang DW and Zhang JZH (2003) Molecular fractionation with conjugate caps for full quantum mechanical calculation of protein–molecule interaction energy. *J. Chem. Phys.* 119:3599–3605.

[29] Wong L, Radic Z, Brüggemann RJM, Hosea N, Berman HA, Taylor P (2000) Mechanism of oxime reactivation of acetylcholinesterase analyzed by chirality and mutagenesis. *Biochemistry* 39:5750-5757.

[30] Ashani Y, Radic Z, Tsigelny I, Vellom DC, Pickering NA, Quinn DM, Doctor BP, Taylor P (1995) Amino Acid Residues Controlling Reactivation of Organophosphonyl Conjugates of Acetylcholinesterase by Mono- and Bisquaternary Oximes. *J. Biol. Chem.* 270:6370-6380.

FIGURES

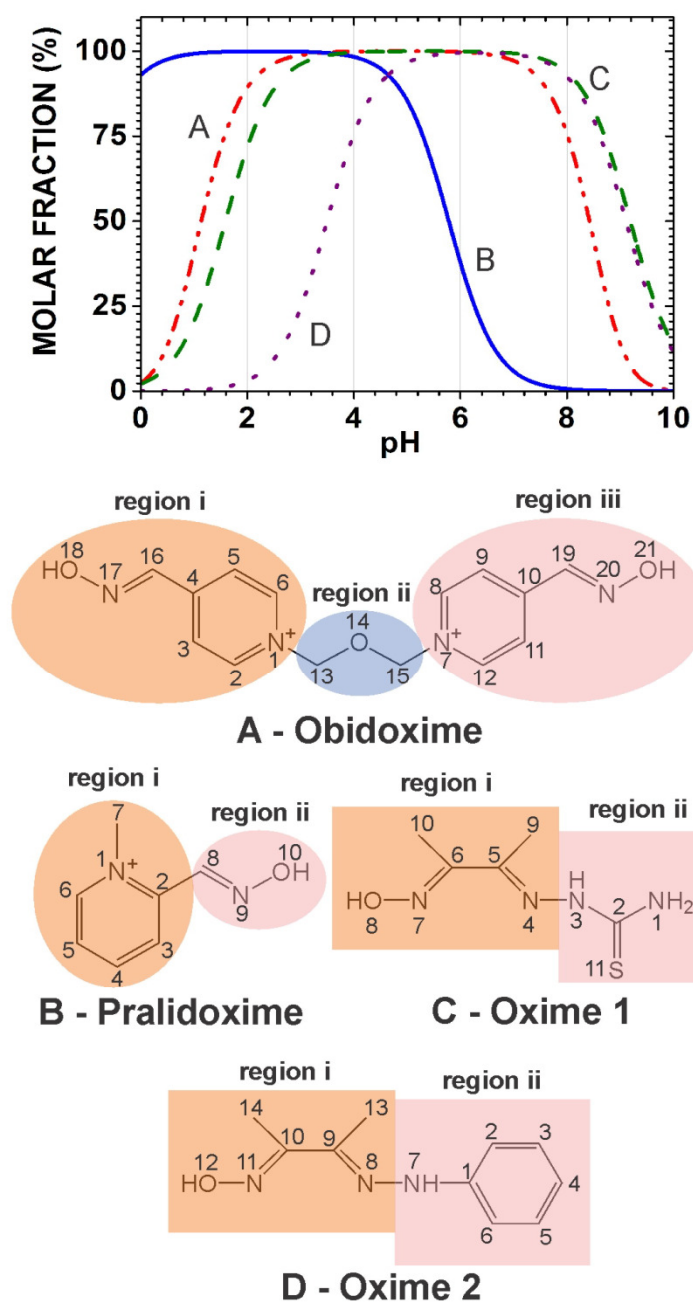


Figure 1 – Obidoxime, pralidoxime, oxime 1 and oxime 2 chemical structure with the main functional groups and the protonation state as a function of the pH.

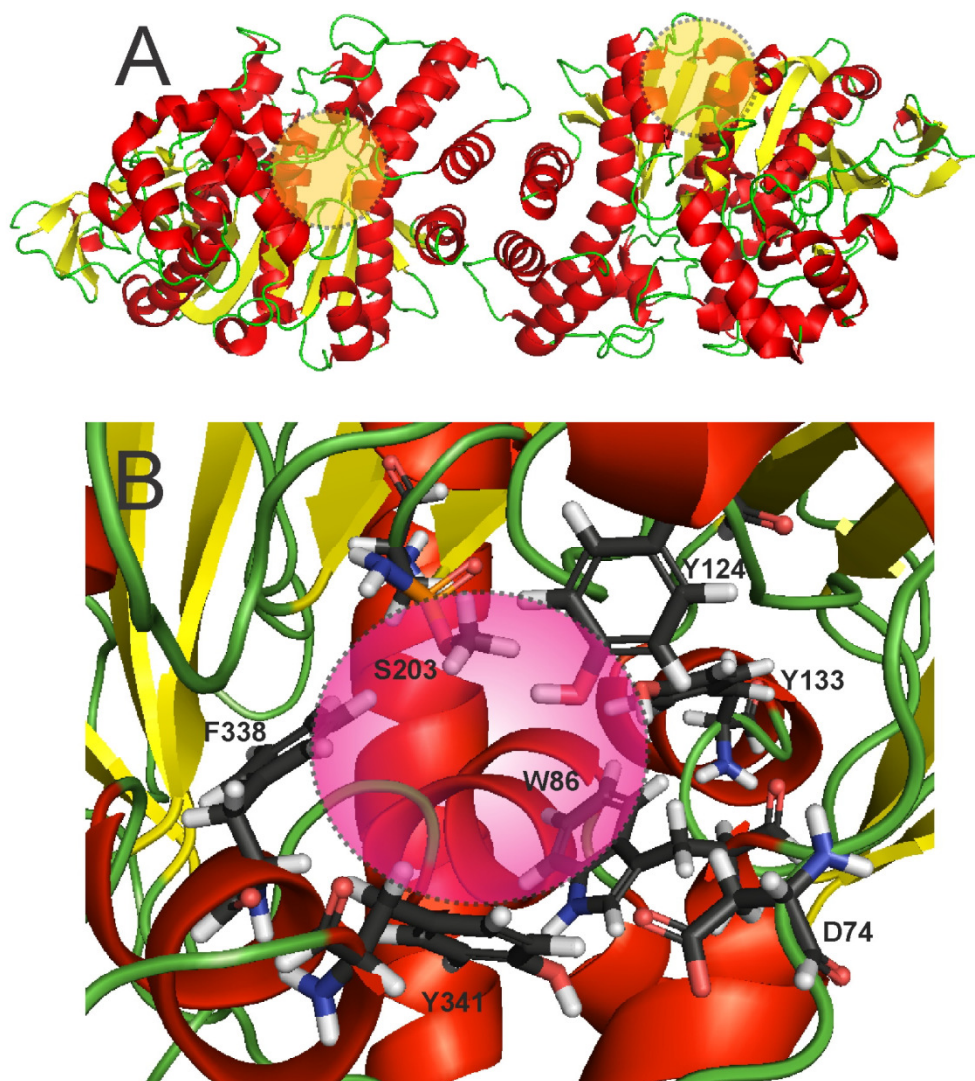


Figure 2 – The AChE dimer (A) and binding pocket of AChE (B) detaching the most important residues to the oxime binding.

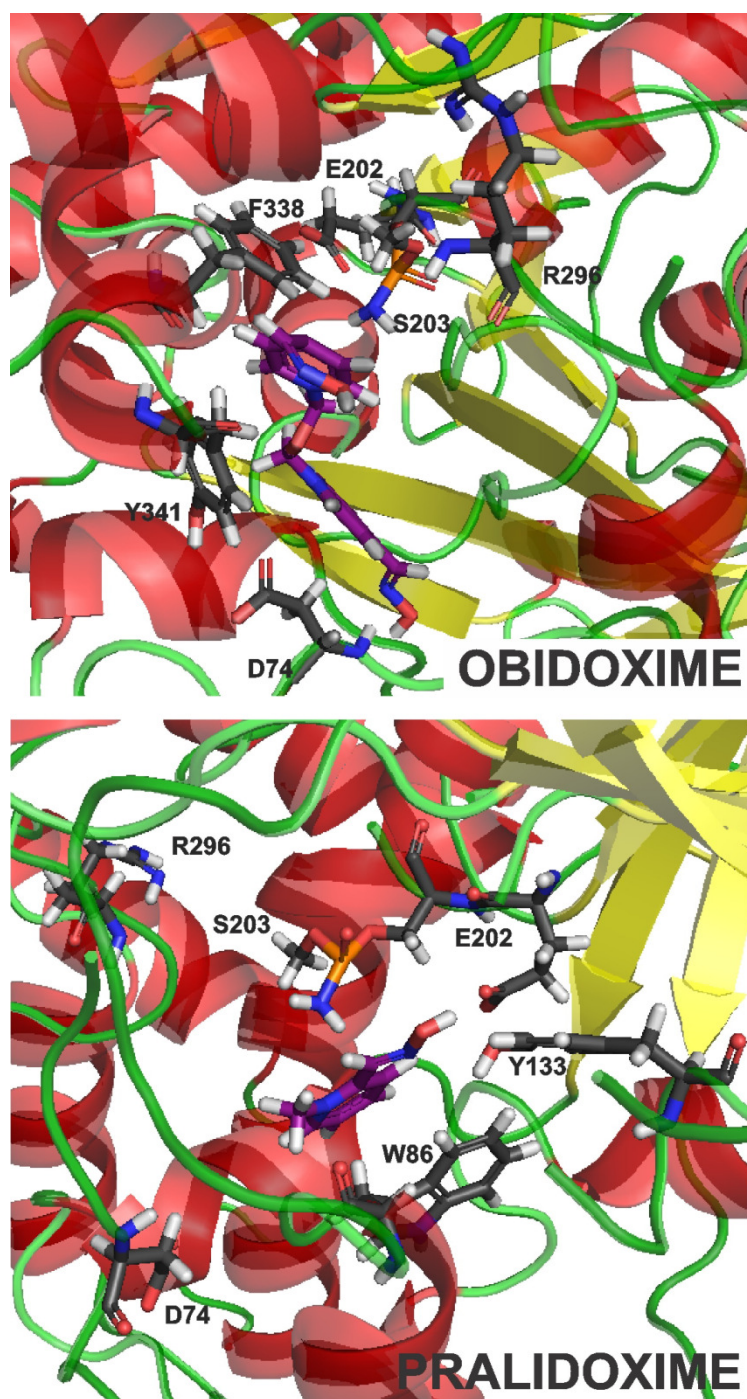


Figure 3 – Binding sites of obidoxime and pralidoxime.

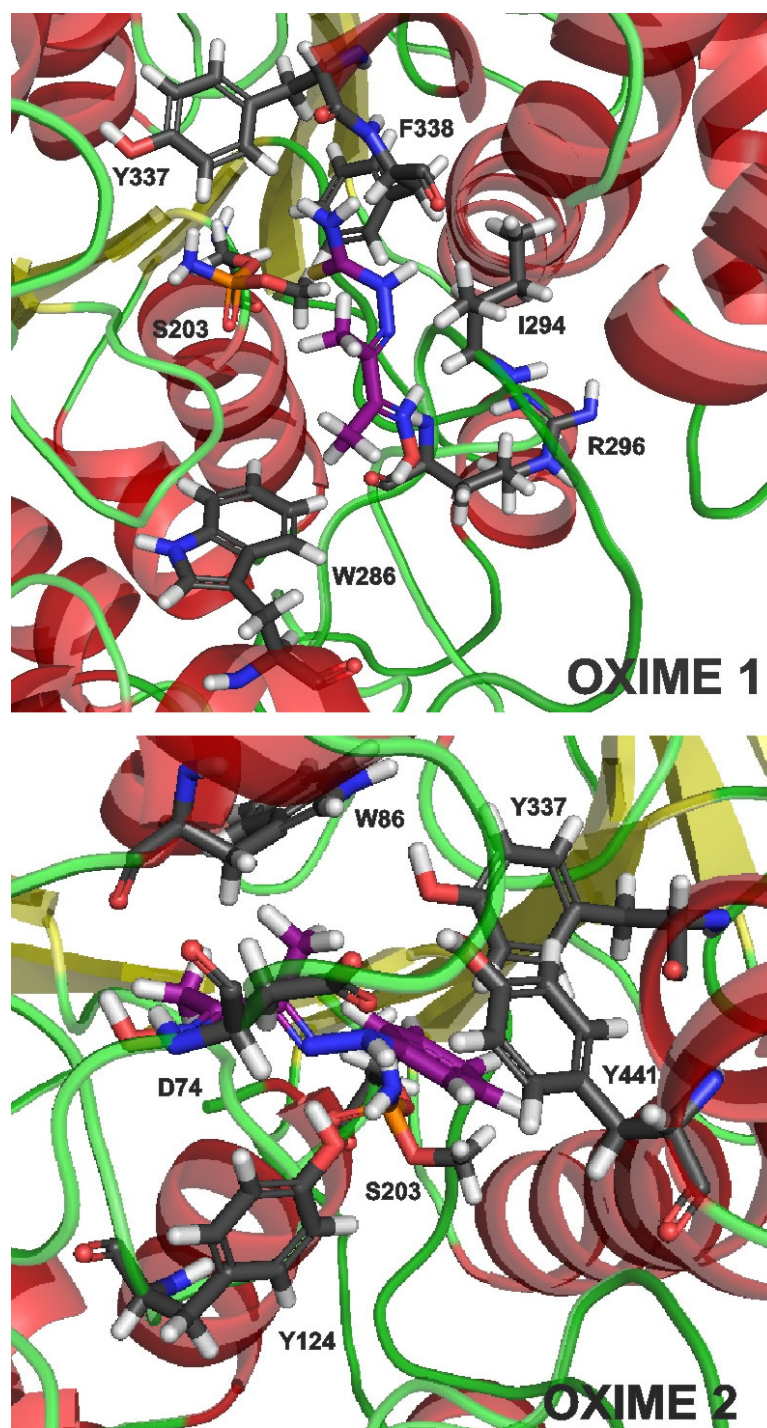


Figure 4 – Binding sites of oxime 1 and oxime 2.

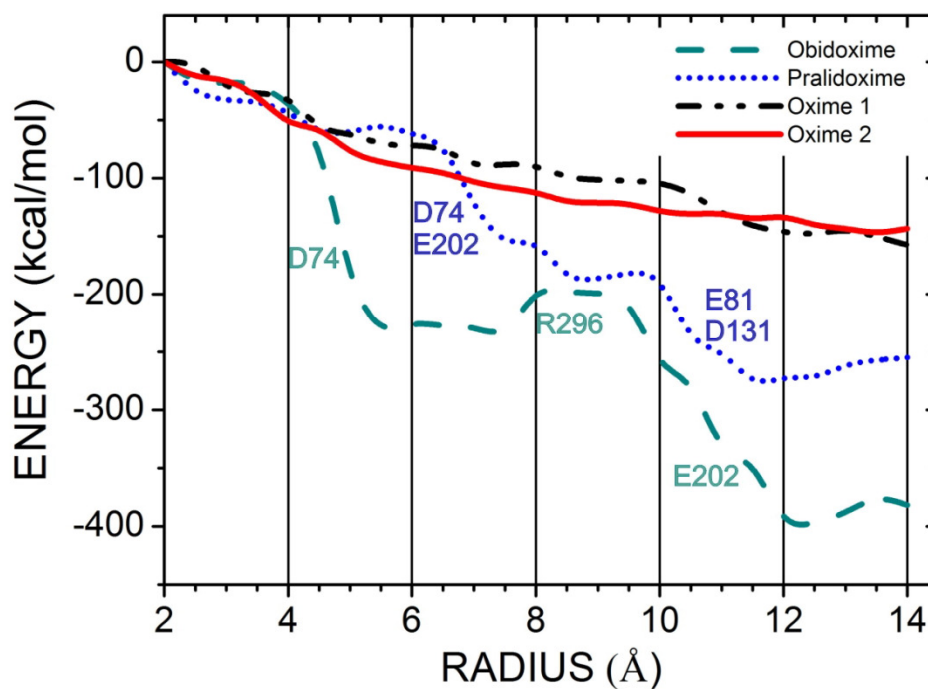


Figure 5 – Variation of the interaction energy as a function of the interaction radius for: obidoxima (dashed), pralidoxima (dotted), oxime 1 (dash-dotted-dash) and oxime 2 (solid). The binding pocket radii are given by the distance between each statin centroid and the most distant AChE residue binding the ligand.

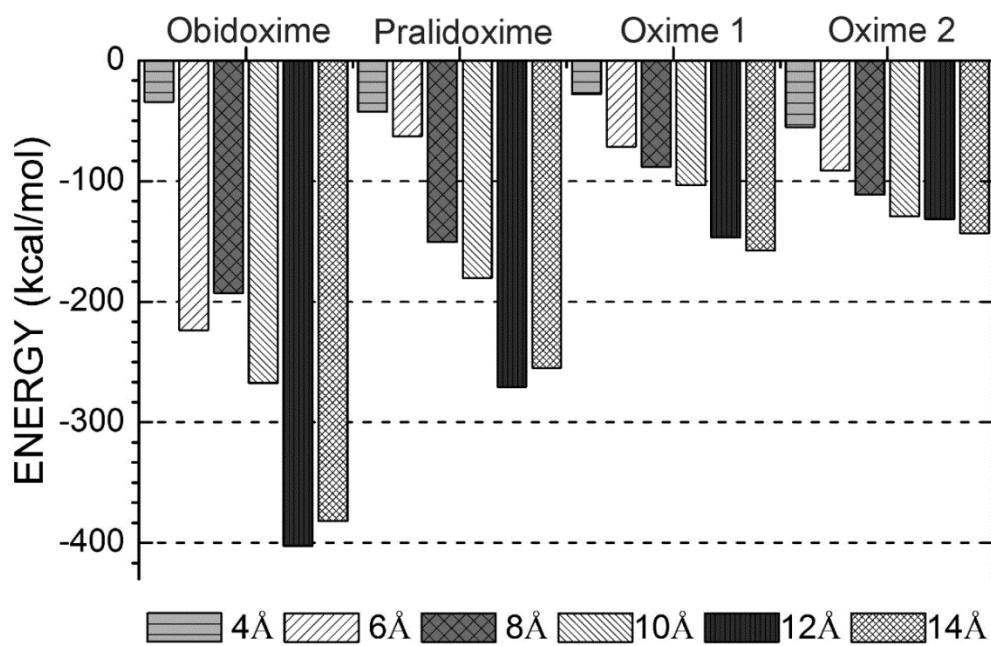


Figure 6 – Total AChE interaction energy of oximes for interaction radii of 4 Å, 6 Å, 8 Å, 10 Å, 12 Å and 14 Å.

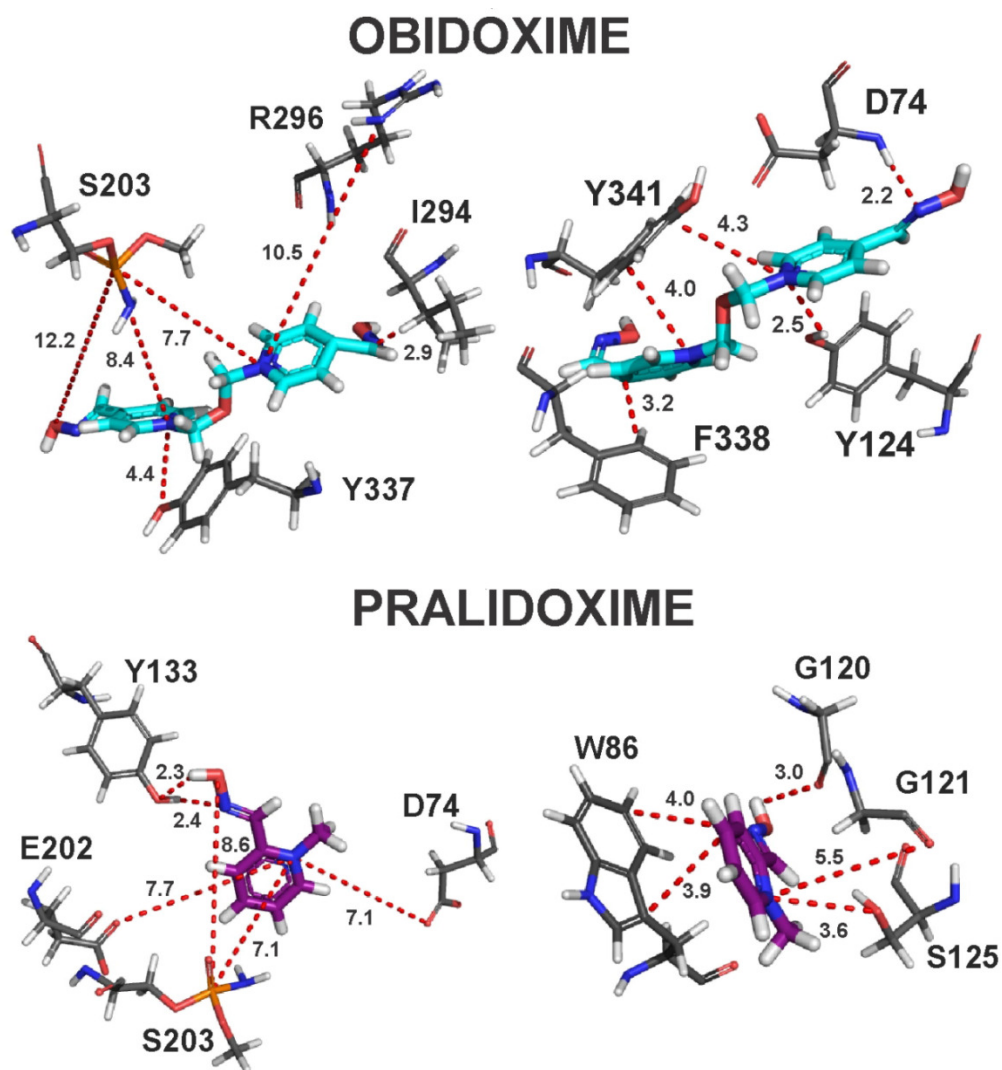


Figure 7 – Distances between AChE residues and obidoxime and pralidoxime. Their interaction energies are the most important contributions to the total binding energy of the AChE-oxime complex.

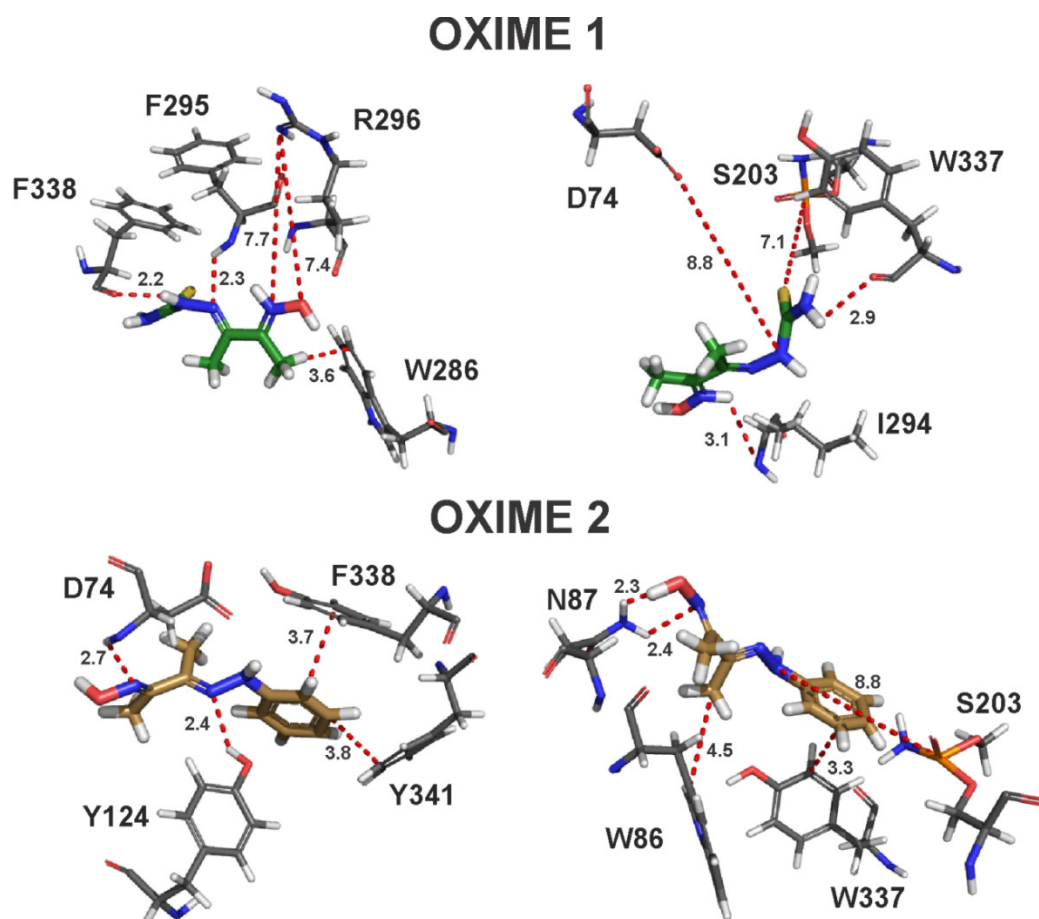


Figure 8 – Distances between AChE residues and oxime 1 and oxime 2. Their interaction energies are the most important contributions to the total binding energy of the AChE-oxime complex.

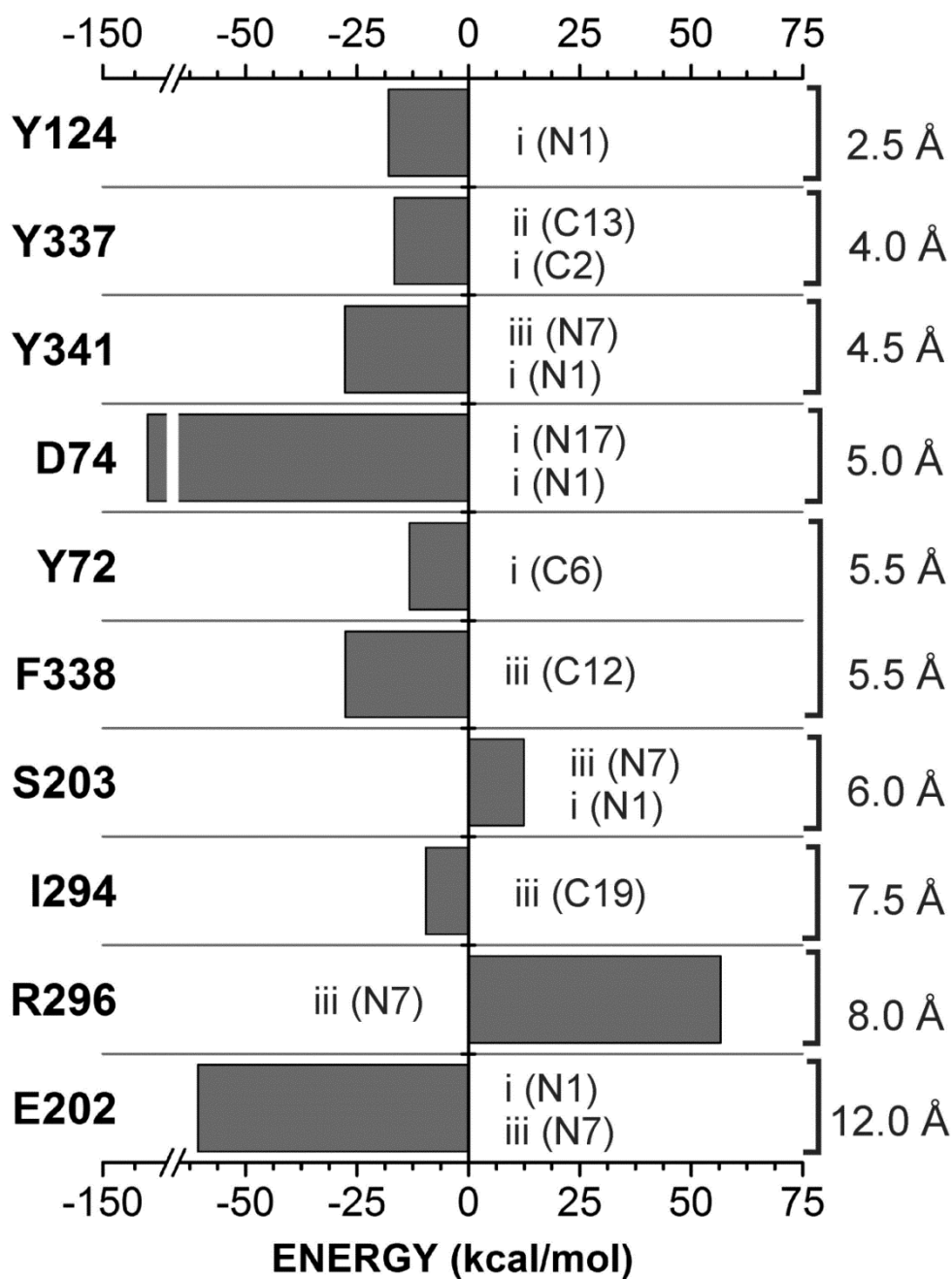


Figure 9 – Binding site, interaction energy and residues domain (BIRD) graphic panel showing the most relevant residues of AChE which contribute to the obidoxime binding.

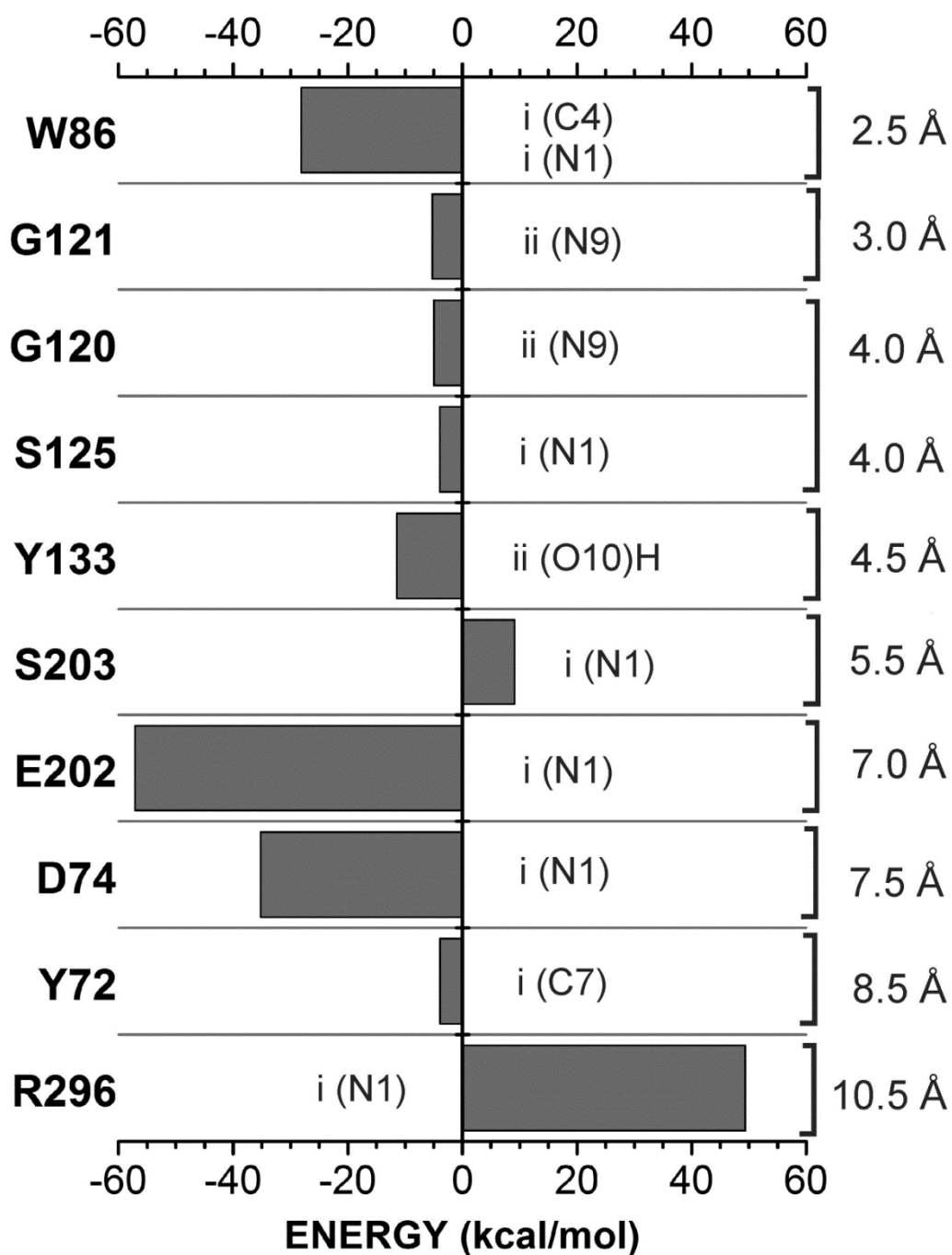


Figure 10 – Binding site, interaction energy and residues domain (BIRD) graphic panel showing the most relevant residues of AChE which contribute to the pralidoxime binding.

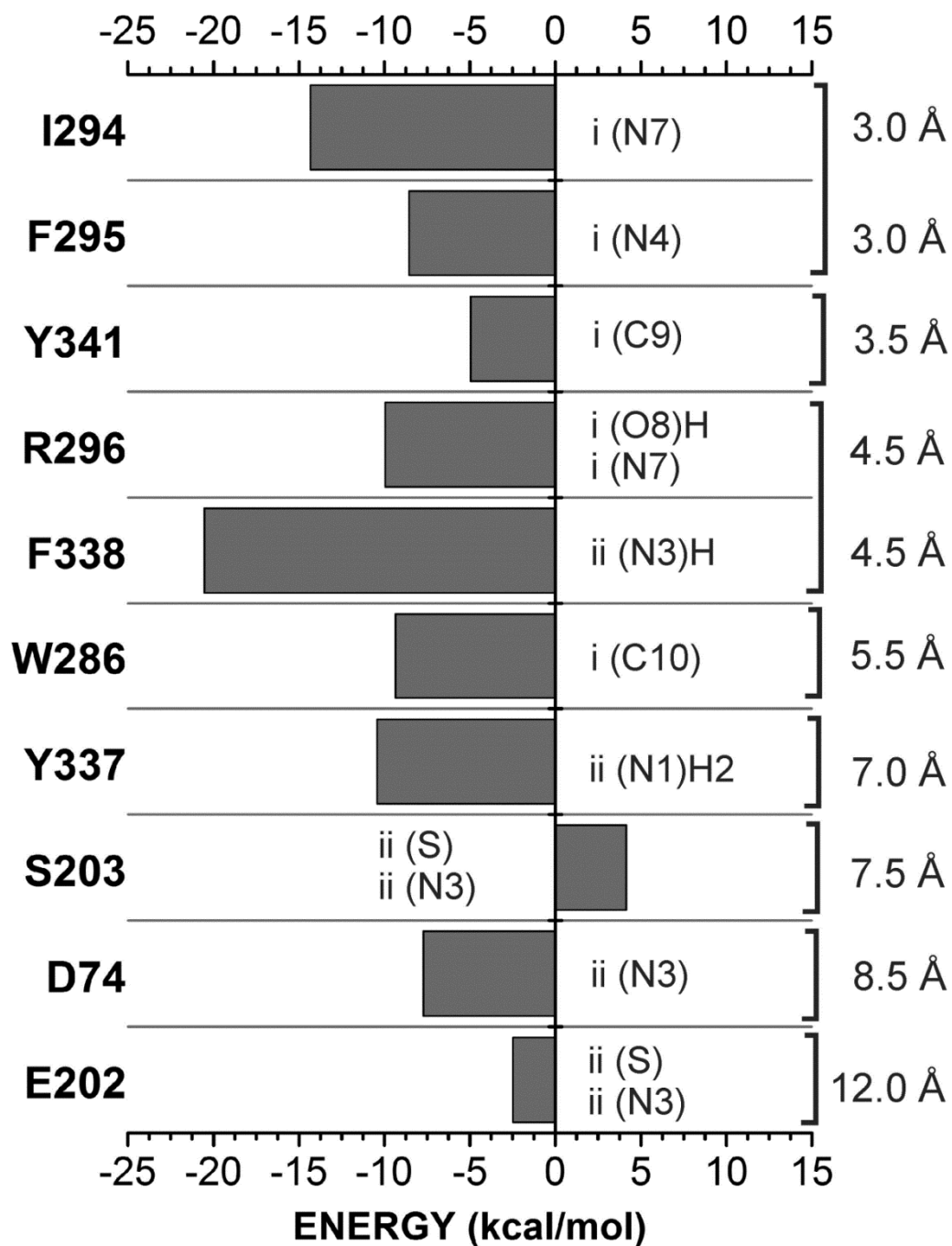


Figure 11 – Binding site, interaction energy and residues domain (BIRD) graphic panel showing the most relevant residues of AChE which contribute to the oxime 1 binding.

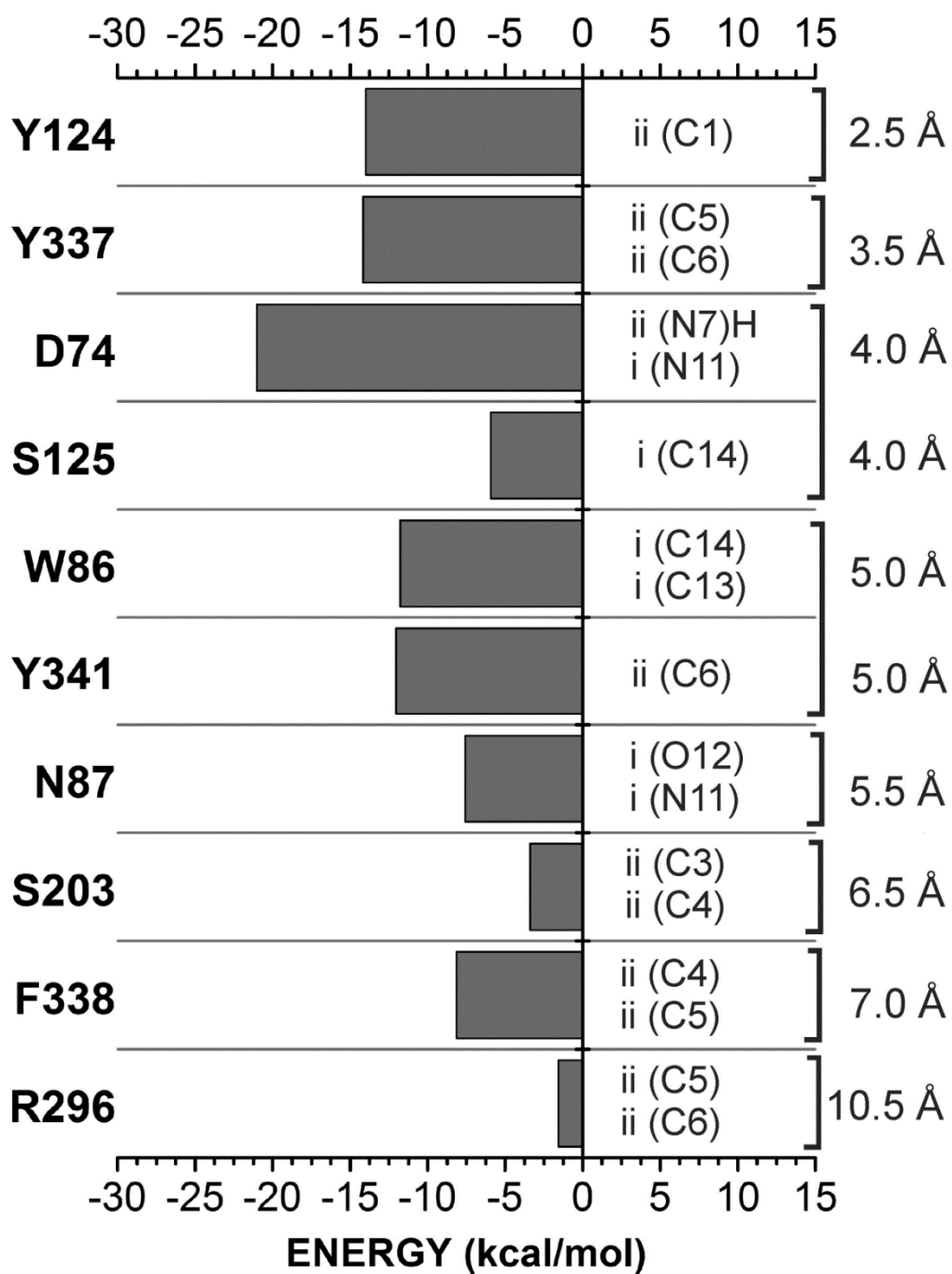


Figure 12 – Binding site, interaction energy and residues domain (BIRD) graphic panel showing the most relevant residues of AChE which contribute to the oxime 2 binding.

3 DISCUSSÃO

Muitos estudos têm relacionado as oximas com a reativação da AChE inibida por OPs (para uma revisão veja, Jokanovic e Sojiljkovic, 2006). Contudo, o entendimento da relação estrutura-atividade das oximas no processo de reativação de colinesterases ainda é muito limitado (Kuca e cols., 2006). O mecanismo molecular envolvido no processo de reativação da AChE por oximas é baseado na retirada de um grupo fosforil do complexo AChE-OP (Jokanovic e Sojiljkovic, 2006), sendo que o potencial de uma oxima como reativador enzimático depende, principalmente, de seu poder nucleofílico e orientação geométrica adotada no sítio ativo da AChE (Ashani e cols., 1995). Tais pressupostos tornam vital o uso de ferramentas de modelagem molecular para a compreensão dos mecanismos envolvidos no processo de reativação da AChE, e no desenvolvimento de novas oximas. As duas novas oximas testadas neste trabalho tem somente um grupo aldoxima, similarmente a pralidoxima, enquanto a obidoxima apresenta dois grupos aldoxima. Kassa e cols. (2008) demonstraram que o número de grupos aldoxima não é decisivo para o processo de reativação, enquanto Cabal e cols. (2004) mostram que outras características moleculares das oximas podem interferir com seu poder reativador, tais como: o número de anéis piridina e a posição do grupo oxima na molécula. Entre as novas moléculas testadas neste trabalho, nenhuma delas apresenta anéis piridina, porém são capazes de reativar a AChE e a BChE inibidas por metamidofós (Artigos 1 e 2), e já se mostraram bons reativadores da AChE inibida por outros OPs, como clorpirifós, diazinon e malation (Costa e cols., 2011), demonstrando que tais compostos não baseados em anéis piridina podem ser promissores para estudos futuros, sendo que tais compostos foram pouco testados até o

momento, e uma grande quantidade de modificações na estrutura molecular destas novas oximas são possíveis.

Wong e cols. (2000) demonstraram que a região conhecida como “oxyanion hole” (constituída pelos resíduos Gly121, Gly122 e Ala204) é o sítio através do qual a pralidoxima ataca a ligação O-P da Ser203 modificada por tabun, e o mesmo comportamento ocorre quando o inibidor é o metamidofós (Figura 6, Artigo 2). Musilek e cols. (2011) mostraram que oximas com dois anéis piridina são posicionados em uma região mais externa do sítio ativo, estando posicionado entre o sítio aniônico periférico (PAS) e os resíduos do “acyl pocket”, em um posicionamento similar ao encontrado em nossos estudos com a obidoxima (que também apresenta dois anéis piridina). Apesar de as principais interações moleculares entre os ligantes (oximas) e a enzima envolvam os resíduos de aminoácidos que circundam o sítio ativo, outros resíduos que se encontram em camadas mais internas da enzima podem contribuir para a conformação adotada pelo ligante e, dessa forma, no seu potencial como reativador da AChE, porém tais resíduos foram completamente negligenciados até o momento. Neste sentido, nossos dados demonstram, pela primeira vez, que o resíduo Arg296 fortemente repele as oximas carregadas positivamente, obidoxima e pralidoxima (Manuscrito 1). No caso da obidoxima, tal repulsão parece impedir a aproximação de um dos anéis piridina à ligação O-P da Ser203 (alvo no processo de reativação), sendo provável que a presença de um átomo de nitrogênio quaternário (com carga formal +1) neste anel piridina seja desvantajosa em comparação a um nitrogênio terciário (carga formal 0). De forma geral, no caso da AChE inibida por metamidofós, a pralidoxima parece estar melhor posicionada para o processo de reativação que a obidoxima, que apresentou maior energia de interação com o sítio (Manuscrito 1, Figura 5), porém com constantes de reativação similares aos encontrados com a pralidoxima (Artigo 2, Tabela 1).

Foi previamente demonstrado que a AChE possui um forte momento dipolo que se orienta ao longo do sítio e que atrai o substrato ACh para dentro do sítio (Stojan e cols., 2004). Além disso, os resíduos Asp72, Glu199 e Glu443 (carregados negativamente) formam um gradiente potencial no sítio ativo, e que afeta não só o substrato como outros compostos positivamente carregados, como a obidoxima e a pralidoxima (Delfino e cols., 2009). Tal efeito parece ser essencial para que as oximas possam reativar a AChE com sucesso, sendo que em nosso trabalho as oximas clássicas (positivamente carregadas) foram superiores as novas oximas testadas (neutras). Apesar de o potencial gerado dentro do sítio ativo afetar também ligantes não carregados, nossos dados sugerem fortemente que este efeito é limitado no caso de oximas neutras, uma vez que as novas oximas testadas apresentaram menor energia de ligação ao sítio da AChE (Manuscrito 1, Figura 5) e menores constantes de reativação (Artigo 2, Tabela 1).

Apesar de serem os únicos reativadores da AChE disponíveis clinicamente, as oximas apresentam efeitos tóxicos significantes (Bardin e cols., 1994; Carlton e cols., 1998; Hardman e cols., 1996), tornado importante a procura por novos compostos capazes de contornar os efeitos tóxicos de OPs com menos efeitos colaterais. Nesse sentido, nosso grupo de pesquisa tem relatado alguns efeitos farmacologicamente úteis de tiosemicarbazonas, em especial a isatina-3-N⁴-benziltiosemicarbazona (IBTC), que demonstrou efeitos antioxidantes e antiaterogênicos em estudo anterior (Barcelos e cols., 2011), e apresentou efeito tanto protetor como reativador da AChE (Artigo 1, Figuras 5 e 6) e não demonstrou significativo efeito tóxico *in vivo* em nenhum dos indicadores bioquímicas usualmente envolvidos com o envenenamento por OPs, e com valores de LD₅₀ superiores a 500 mg/kg.

O mecanismo molecular da reativação da AChE pelo IBTC (Artigo 1, Esquema 1), envolve a reação do grupo carboxilato (RCOO^-) do resíduo Asp74 com o átomo de hidrogênio ligado ao nitrogênio do grupo imino da IBTC, o que leva a desprotonação do enxofre e formação de um tiolato. Então, o tiolato (com alta nucleofilicidade) pode atacar o centro eletrofílico do metamidofós. Há a formação de um intermediário com o fosfato penta coordenado, fazendo com que o OP deixe o sítio ativo e retorne ao seu estado tetraédrico ligado ao IBTC e, desta forma, reative a enzima. Wong e cols. (2000) demonstraram que a formação de dois enantiômeros, S_p e R_p , são possíveis na inibição da AChE por metilfosfnados, sendo que os S_p enantiômeros são mais reativados em formar conjugados com a enzima e apresenta maiores taxas de reativação por oximas que o R_p . Baseado no mecanismo de reativação da AChE pelo IBTC aqui proposto, o mesmo padrão de reativação com oximas no estudo de Wong e cols. (2000) é válido também para as tiosemicarbazonas, como o IBTC, onde a conformação que melhor se adequa ao processo de reativação é a conformação S_p do complexo AChE-OP, devido ao posicionamento apical do tiolato em relação a Ser203 modifica pelo metamidofós.

A enzima butirilcolinesterase (BChE) é considerada uma enzima acessória ao sistema colinérgico, porém, tal enzima é dez vezes mais presente em humanos que a própria AChE (cerca 680 nmol de BChE e 62 nmol de AChE) (Manoharan e cols., 2007), o que sugere que a BChE possa ter um importante papel fisiológico. A BChE consegue catalisar a hidrólise da ACh, apesar de fazê-lo com menos eficiência que a AChE, e, desta forma, regular a neurotransmissão colinérgica. Outras evidências apontam que a BChE pode agir como um corregulador da ação da ACh (Darvesh e cols., 2003), e sua inibição leva a um aumento dose dependente nos níveis de ACh no cérebro (Giacobini, 2000). Dados neuroanatômicos demonstraram que a BChE é expressa por populações específicas de neurônios nos sistemas nervoso central (Tago e

cols., 1992; Darvesh e Hopkins, 2003) e periféricos (Darvesh e cols., 1998), consistente com uma função corregulatória da BChE na neurotransmissão colinérgica. Em estudo com camundongos que não expressam a enzima AChE, a BChE demonstrou ter importante função na hidrólise da ACh, uma vez que a inibição da BChE, neste caso, se mostrou letal (Mesulam e cols., 2002). Tal situação pode ser considerada análoga a inibição da AChE por compostos OPs onde, devido a maior presença da BChE que a AChE em humanos, a hidrólise da ACh pela BChE pode representar um modo de lidar com os altos níveis de ACh causada pela inibição da AChE. Deste modo, os resultados desta tese mostram que as novas oximas e a IBTC foram superiores em reativar a BChE quando comparado com os fármacos utilizados atualmente na clínica (obidoxima e pralidoxima), e este fato pode representar uma vantagem em conter a crise colinérgica. Modificações futuras na estrutura molecular das novas oximas testadas, que levem a uma melhor taxa de reativação da AChE, sem perda do efeito sobre a BChE, seria de grande significado para o desenvolvimento de novos fármacos capazes de conter os efeitos do envenenamento por OPs.

4 CONCLUSÕES

Baseando-se nos resultados aqui apresentados, pode-se concluir que:

- Análises *in vitro*:

- As duas novas oximas e a IBTC apresentaram capacidade de reativar a AChE inibida pelo metamidofós, porém de maneira menos eficiente que as oximas clássicas, obidoxima e pralidoxima.
- Em relação à reativação da BChE, todas as novas drogas testadas foram capazes de reativar esta enzima inibida pelo metamidofós, enquanto que as oximas clássicas falharam em reativar a BChE em todos os testes feitos.

- Análises *in silico*

- Pela metodologia de atracamento molecular (“docking”) observamos que os novos compostos encontram-se em posição similar a obidoxima, em uma região mais externa do sítio ativo da AChE, entre as regiões do sítio aniônico periférico e o sítio catalítico aniônico. Já a pralidoxima teve a sua conformação mais estável na região do “oxyanion hole”, próximo à tríade catalítica, em uma região supostamente mais vantajosa ao processo de reativação.
- As principais forças que estabilizam as oximas no sítio ativo da AChE são: forças eletrostáticas, principalmente envolvendo os resíduos Asp74, Glu202 e Arg296; e as interações do tipo π - π e π -cátion, envolvendo os resíduos aromáticos do sítio ativo, destacando-se os resíduos Tyr72, Trp86, Tyr124, Trp286, Phe295, Tyr337 e Phe338.

- Demonstramos também que, o resíduo Arg296 contribui significativamente para a estabilização dos ligantes no sítio ativo da AChE, sendo que tal resíduo se encontra distante do centro dos ligantes e foi ignorado até o momento como uma força contributiva a ligação de oximas.

- Análises *ex vivo*

- O composto isatina-3-N⁴-benziltiosemicarbazona apresentou baixa toxicidade em camundongos, não alterando os principais indicadores de estresse oxidativo ou a atividade das enzimas delta aminolevulinato desidratase e Na⁺/K⁺ ATPase.

5 REFERÊNCIAS

- Aldunate R, Casar JC, Brandan E, Inestrosa NC, (2004) Structural and functional organization of synaptic acetylcholinesterase. *Brain Res Brain Res Rev* 47:96–104.
- Araújo AJ, Lima JS, Moreira JC, Jacob SC, Soares MO, Monteiro MCM, (2007) Exposição múltipla a agrotóxicos e efeitos à saúde: estudo transversal em amostra de 102 trabalhadores rurais, Nova Friburgo, RJ. *Ciência Saúde Coletiva* 12:115–130.
- Arena JM, (1979) *Poisoning, Toxicology, Symptoms, Treatments* (4th ed.), Springfield Ill, Charles C. Thomas p. 133.
- Ashani Y, Radic Z, Tsigelny I, Vellom DC, Pickering NA, (1995) Amino acid residues controlling reactivation of organophosphonyl conjugates of acetylcholinesterase by mono- and bisquaternary oximes. *J Biol Chem* 270:6370–6380.
- Barak D, Kronman C, Ordentlich A, Ariel N, Bromberg A, Marcus D, Lazar A, Velan B, Shafferman A, (1994) Acetylcholinesterase peripheral anionic site degeneracy conferred by amino acid arrays sharing a common core. *J Biol Chem* 269:6296–6305.
- Barak D, Kaplan D, Ordentlich A, Ariel N, Velan B, Shafferman A, (2002) The aromatic "trapping" of the catalytic histidine is essential for efficient catalysis in acetylcholinesterase. *Biochemistry* 41:8245–8252.
- Barcelos RP, de Lima Portella R, da Rosa EJ, Fonseca AS, Bresolin L, Carratu V, Soares FA, Barbosa NV, (2011) Thiosemicarbazone derivate protects from AAPH and Cu(2+)-induced LDL oxidation. *Life Sci* 89:20–28.
- Bardin PG, van Eeden SF, Moolman JA, Foden AP, Joubert JR, (1994) Organophosphate and carbamate poisoning. *Arch Intern Med* 154:1433–1441.
- Bazelyansky M, Robey E, Kirsch JF, (1986) Fractional diffusion-limited component of reactions catalyzed by acetylcholinesterase. *Biochemistry* 25:125–130.
- Beraldo H, Gambino D, (2004) The wide pharmacological versatility of semicarbazones, thiosemicarbazones and their metal complexes. *Mini Rev Med Chem* 4:31–39.
- Bon S, Vigny M, Massoulie J, (1979) Asymmetric and globular forms of acetylcholinesterase in mammals and birds. *Proc Natl Acad Sci USA* 76:2546–2550.
- Bošković B, Jokanović M, Maksimović M, (1984) Effects of sarin, soman and tabun on plasma and brain aliesterase activity in the rat. In: Brzin M. (Ed.), *Cholinesterases*

— fundamental and applied aspects. Walter de Gruyter and Co., Berlin–New York, pp.365–374.

- Bošković B, Tadić V, Kušić R, (1980) Reactivating and protective effects of pro-2-PAM in mice poisoned with paraoxon. *Toxicol Appl Pharmacol* 55:32–36.
- Cabal J, Kuca K, Kassa J, (2004) Specification of the structure of oximes able to reactivate tabun inhibited acetylcholinesterase. *Bas Clin Pharm Tox* 95:81–86.
- Caldas ED, Boon PE, Tressou J, (2006) Probabilistic assessment of the cumulative acute exposure to organophosphorus and carbamate insecticides in the Brazilian diet. *Toxicology* 222:132-142.
- Carlton FB, Simpson WM, Haddad LM, (1998) In: *Clinical Management of Poisoning and Drug Overdose*. Haddad LM, Shannon MW, Winchester JF, eds., 3rd ed., WB Saunders Company: Philadelphia, pp.836-850.
- Casida JE, Quistad GB, (2005) Serine hydrolase targets of organophosphorus toxicants. *Chem-Biol Interact* 157-158:277-283.
- Castro AT, Figueroa-Villar JD (2002) Molecular Structure, Conformational Analysis and Charge Distribution of Pralidoxime: Ab Initio and DFT Studies. *Int J Quant Chem* 89:135-146.
- Chan TYK, Cristchley AJH, Chan AYW, (1996) An estimate of the incidence of pesticide poisoning in Hong Kong. *Vet Human Toxicol* 38:362-364.
- Clement J, (1979) Pharmacological actions of HS-6, an oxime, on the neuromuscular junction. *Eur. J. Pharmacol.* 53:135–141.
- Costa MD, Freitas ML, Soares FAA, Carratu VS, Brandão R, (2011) Potential of two new oximes in reactivate human acetylcholinesterase and butyrylcholinesterase inhibited by organophosphate compounds: An in vitro study. *Toxic. in vitro* 25:2120-23.
- da Costa RF, Freire VN, Bezerra EM, Cavada BS, Caetano EW, de Lima Filho JL, Albuquerque EL, (2012) Explaining statin inhibition effectiveness of HMG-CoA reductase by quantum biochemistry computations. *Phys Chem Chem Phys* 14:1389-1398.
- Darvesh S, MacDonald SE, Losier AM, Martin E, Hopkins DA, (1998) Cholinesterases in cardiac ganglia and modulation of canine intrinsic cardiac neuronal activity. *J Auton Nerv Syst* 71:75– 84.
- Darvesh S, Hopkins DA, Geula C, (2003) Neurobiology of butyrylcholinesterase. *Nat Rev* 4:131-138.
- Darvesh S, Hopkins DA, (2003) Differential distribution of butyrylcholinesterase and acetylcholinesterase in the human thalamus. *J Comp Neurol* 463:25– 43.

- Darvesh S, Arora RC, Martin E, Magee D, Hopkins DA, Armour JA, (2004) Cholinesterase inhibitors modify the activity of intrinsic cardiac neurons. *Exp. Neurol.* 188:461-470.
- Delfino RT, Ribeiro TS, Figueroa-Villar JD, (2009) Organophosphorus compounds as chemical warfare agents: a review. *J Braz Chem Soc* 20:407-428.
- Delgado IF, Paumgarten FJR, (2004) Intoxicações e uso de pesticidas por agricultores do Município de Paty do Alferes, Rio de Janeiro, Brasil. *Cadernos de Saúde Pública* 20:180-186.
- Ecobichon DJ, (1996) Toxic Effects of Pesticides. In: Klassen, Casarett & Doull's Toxicology: The Basic Science of Poisons, 5th ed. Pergamon Press Inc., New York.
- Ekström F, Hörnberg A, Artursson E, Hammarström L-G, Schneider G, Pang Y-P, (2009) Structure of HI-6NSarin-Acetylcholinesterase Determined by X-Ray Crystallography and Molecular Dynamics Simulation: Reactivator Mechanism and Design. *PLoS ONE* 4:1-19.
- Felder CE, Botti SA, Lifson S, Silman I, Sussman JL, (1997) External and internal electrostatic potentials of cholinesterase models. *J Mol Graph Model* 15:318-327.
- Ferrer A, Cabral R, (1995) Recants Epidemics of Poisoning by Pesticides. *Toxicol Lett* 82-83:55-63.
- Frobert Y, Creminon C, Cousin X, Remy MH, Chatel JM, Bon S, Bon C, Grassi J, (1997) Acetylcholinesterases from Elapidae snake venoms: biochemical, immunological and enzymatic characterization. *Biochim Biophys Acta* 1339:253-267.
- Fuxreiter M, Warshel A, (1998) Origin of the catalytic power of acetylcholinesterase: computer simulation studies. *J Am Chem Soc* 120:183-194.
- Gao AM, Zhang DW, Zhang JZH, Zhang Y, (2004) An efficient linear scaling method for ab initio calculation of electron density of proteins. *Chem Phys Lett* 394:293-297.
- Gary NE, Lorenzen K, (1989) Effect of methamidophos on honey bees (Hymenoptera: Apidae) during alfalfa pollination. *J Econ Entomol* 82:1067-1072.
- Giacobini E, (2000) Cholinesterase inhibitors: from the Calabar bean to Alzheimer therapy. In: E Giacobini (Ed), *Cholinesterases and Cholinesterase Inhibitors*, Martin Dunitz, London, UK, 181-226.
- Greig NH, De Micheli E, Holloway HW, Yu QS, Utsuki T, Perry TA, Brossi A, van Hamilton MG, Lundy PM, (1989) HI-6 therapy of soman and tabun poisoning in primates and rodents. *Arch. Toxicol.* 63:144-149.
- Gupta RC, (2006) In: *Toxicology of Organophosphate & Carbamate Compounds*; Gupta RC, ed., 1st ed., Elsevier Academic Press: London, pp. 5-24.

- Hamilton G, Lundy PM, (1989) HI-6 therapy of soman and tabun poisoning in primates and rodents. *Arch Toxicol* 63:144–149.
- Hardman JG, Gilman AG, Limbird LE, (1996) Anticholinesterase agents. In: *The Pharmacological Basis of Therapeutics*. Goodman & Gilman's, pp.161–176.
- Harel M, Quinn DM, Nair HK, Silman I, Sussman JL, (1996) The Xray structure of a transition state analog complex reveals the molecular origins of the catalytic power and substrate specificity of acetylcholinesterase. *J Am Chem Soc* 118:2340–2346.
- Harris LW, Stitcher DL, (1983) Reactivation of VX-inhibited cholinesterase by 2-PAM and HS-6 in rats. *Drug Chem Toxicol* 6:235–240.
- Harvey B, Scott RP, Sellers DJ, Watts P, (1986) In vitro studies on the reactivation by oximes of phosphorylated acetylcholinesterase—I. On the reactions of P2S with various organophosphates and the properties of the resultant phosphorylated oximes. *Biochem Pharmacol* 35:737–744.
- Hassal AK, (1990) *The biochemistry and uses of pesticides: structure, metabolism, mode of action and uses in crop protection*. 2nd ed. Weiheim: VCH.
- Heilbronn E, Tolagen B, (1965) Toxogonin in sarin, soman and tabun poisoning. *Biochem Pharmacol* 14:73–77.
- Hosea, N. A.; Berman, H. A.; Taylor, P, (1995) Specificity and orientation of trigonal carboxyl esters and tetrahedral alkylphosphonyl esters in cholinesterases. *Biochemistry* 34:11528-11536.
- Howland MA, Aaron C, (1999) Pralidoxime. In: Goldfrank, L., Flomenbaum, N., Lewin, N., Weisman, R., Howland, M.A., Hofman, R. (Eds.), *Emergencies Toxicology*. Appleton & Lange, USA, pp. 1445–1449.
- ILSE. International Life Science Institute of Brazil. (1995) *Relação de substâncias para uso fitossanitário e domissanitário: portarias do Ministério da Agricultura*. São Paulo.
- Inns RH, Leadbeater L, (1983) The efficacy of bispyridinium derivatives in the treatment of organophosphate poisoning in the guinea-pig. *J Pharm Pharmacol* 35:427–432.
- Johnson JL, Thomas JL, Emani S, Cusack B, Rosenberry TL, (2005) Measuring carbamoylation and decarbamoylation rate constants by continuous assay of AChE. *Chem-Biol Interact* 157:384–385.
- Jokanovic M, Stojiljkovic MP, (2006) Current understanding of the application of pyridinium oximes as cholinesterase reactivators in treatment of organophosphate poisoning. *Eur J Pharmacol* 553:10-17.
- Kaplan D, Barak D, Ordentlich A, Kronman C, Velan B, Shafferman A, (2004) Is aromaticity essential for trapping the catalytic histidine 447 in human acetylcholinesterase? *Biochemistry* 43:3129-3136.

- Karasova JZ, Kassa J, Jung Y-S, Musilek K, Pohanka M, Kuca K, (2008) Effect of several new and currently available oxime cholinesterase reactivators on tabun-intoxicated rats. *Int J Mol Sci* 9:2243-2252.
- Kassa J, (2005) The role of oximes in the antidotal treatment of chemical casualties exposed to nerve agents. In: Monov A, Dishovsky C, (Eds.), *Medical aspects of chemical and biological terrorism: Chemical terrorism and traumatism*. Publishing House of the Union of Scientists in Bulgaria, Sofia, Bulgaria, pp. 193–208. available at <http://www.jmedchemdef.org/archives.html>.
- Kassa J, Jun D, Karasova J, Bajgar J, Kuca K, (2008) A comparison of reactivating efficacy of newly developed oximes (K074, K075) and currently available oximes (obidoxime, HI-6) in soman, cyclosarin and tabun-poisoned rats. *Chem-Biol Inter* 175:425–427.
- Khandelwal A, Lukacova V, Comez D, Kroll DM, Raha S, Balaz S, (2005) A combination of docking, QM/MM methods, and MD simulation for binding affinity estimation of metalloprotein ligands. *J Med Chem* 48:5437-5447.
- Kuca K, Jun D, Musilek K, (2006) Structural requirements of acetylcholinesterase reactivators. *Mini Rev Med Chem* 6:269-277.
- Luo C, Saxena A, Smith M, Garcia G, Radic Z, Taylor P, (1999) Phosphoryl oxime inhibition of acetylcholinesterase during oxime reactivation is prevented by edrophonium. *Biochemistry* 38:9937–9947.
- Lüttringhaus A, Hagedorn I, (1964) Quärtare Hydroxyimino-methylpyridinium Salze. *Arzneimittelforschung* 14:1–5.
- Ma JC, Dougherty DA, (1997) The cation- π interaction. *Chem Rev* 97:1303-1324.
- Majumdar D, Roszak S, Leszczynski J, (2006) Probing the Acetylcholinesterase Inhibition of Sarin: A Comparative Interaction Study of the Inhibitor and Acetylcholine with a Model Enzyme Cavity *J Phys Chem B* 110:13597-13607.
- Maksimović M, Bošković B, Radović LJ, Tadić V, Deljac V, Binenfeld Z, (1980) Antidotal effects of bispyridinium-2-monooxime carbonyl derivatives in intoxications with highly toxic organophosphorus compounds. *Acta Pharm Jugosl* 30:151–160.
- Maksimović M, Kovačević V, Binenfeld Z, (1989) Protective and reactivating effects of HI-6-Toxogonin mixture in rats and guinea-pigs poisoned by nerve agents. *Acta Pharm Jugosl* 39:27–33.
- Manoharan I, Boopathy R, Darvesh S, Lockridge O, (2007) A medical health report on individuals with silent butyrylcholinesterase in the Vysya community of India. *Clin Chim Acta* 378:128-135.
- Marrs TC, (1991) Toxicology of oximes used in treatment of organophosphate poisoning. *Adverse Drug React Toxicol Rev* 10:61–72.
- Marrs TC, (1993) Organophosphate poisoning. *Pharm Therap* 58:51-66.

- Marrs TC, (2007) In: Chemical Warfare Agents- Toxicology and Treatment; Marrs TC, Maynard RL, Sidell FR, eds., 2nd ed., John Wiley & Sons Ltd: West Sussex, pp.191-221.
- Masuda N, Takatsu M, Morinari H, Ozawa T, (1995) Sarin poisoning on the Tokyo subway. *Lancet* 345:1446.
- Mesić M, Deljac A, Deljac V, Binenfeld Z, Kilibarda V, Maksimović M, Kovačević V, (1991) Reactivations of acetylcholinesterase inhibited by organophosphorus compounds. Imidazole derivatives. II. *Acta Pharm Jugosl* 41:203–210.
- Mesulam MM, Guillozer A, Shaw P, Levey A, Duysen EG, (2002) Acetylcholinesterase knockouts establish central cholinergic pathways and can use butyrylcholinesterase to hydrolyze acetylcholine. *Neuroscience* 110:627-39.
- Millard CB, Koellner G, Ordentlich A, Shafferman A, Silman I, Sussman JL, (1999a) Reaction products of acetylcholinesterase and VX reveal a mobile histidine in the catalytic triad. *J Am Chem Soc* 121:9883-9884.
- Millard CB, Kryger G, Ordentlich A, Greenblat HM, Harel M, Raves ML, Segall Y, Barak D, Shafferman A, Silman I, Sussman JL, (1999b) Crystal structures of aged phosphonylated acetylcholinesterase: nerve agent reaction products at the atomic level. *Biochemistry* 38:7032-7039.
- Moreira LF, (1995) Diagnóstico dos problemas ecotoxicológicos causados pelo uso de inseticida (metamidofós) na região agrícola de Viçosa - MG. Viçosa, 95 f. Dissertação (Mestrado em Agroquímica) - Universidade Federal de Viçosa.
- Musilek K, Komloova M, Holas O, Horova A, Pohanka M, Gunn-Moore F, Dohnal V, Dolezal M, Kuca K (2011) Mono-oxime bisquaternary acetylcholinesterase reactivators with prop-1,3-diyl linkage — Preparation, in vitro screening and molecular docking. *Bioorg Med Chem* 19:754-762.
- Nemukhin AV, Lushchekina SV, Bochenkova AV, Golubeva A,A, Varfolomeev SD, (2008) Characterization of a complete cycle of acetylcholinesterase catalysis by ab initio QM/MM modeling. *J Mol Model* 14:409-416.
- Nozaki H, Aikawa N, (1995) Sarin poisoning on the Tokyo subway. *Lancet* 345:1446.
- Ordentlich A, Barak D, Sod-Moriah G, Kaplan D, Mizhari D, Segall Y, Kronman C, Karton Y, Lazar A, Marcus D, Velan B, Shafferman A, (2004) Stereoselectivity toward VX is Determined by Interactions with Residues of Acyl Pocket as well as of the Peripheral Anionic Site of AChE. *Biochemistry* 43:11255-11265.
- Paris E, Rios JC, (2001) Intoxicaciones Epidemiologia, clinica y tratamiento. Ediciones Universidad Catolica de Chile, Santiago, p. 302.
- Petroianu GA, Missler A, Zuleger K, Thyges C, Ewald V, Maleck WH, (2004) Enzyme reactivator treatment in organophosphate exposure: clinical relevance of thiocholinesteratic activity of pralidoxime. *J Appl Toxicol* 24:429-435.

- Pohanka M, Jun D, Kuca K, (2008) Improvement of acetylcholinesterase-based assay for organophosphates in way of identification by reactivators. *Talanta* 77:451–454.
- Puntel GO, Gubert P, Peres GL, Bresolin L, Rocha JB, Pereira ME, Carratu VS, Soares FAA, (2008) Antioxidant properties of oxime 3-(phenylhydrazono) butan-2-one. *Arch Toxicol* 82:755-762.
- Puntel GO, de Carvalho NR, Gubert P, Palma AS, Dalla Corte CL, Avila DS, Pereira ME, Carratu VS, Bresolin L, da Rocha JB, Soares FAA, (2009) Butane-2,3-dionethiosemicarbazone: an oxime with antioxidant properties. *Chem-Biol Interact* 177:153-160.
- Quinn DM, (1987) Acetylcholinesterase: Enzyme Structure, Reaction Dynamics and Virtual Transition States. *Chem Rev* 87:955-79.
- Recena MC, Pires DX, Caldas ED, (2006a) Acute poisoning with pesticides in the state of Mato Grosso do Sul, *Brazil*. *Sci Total Environ* 357:88-95.
- Recena MC, Caldas ED, Pires DX, Pontes ER, (2006b) Pesticides exposure in Culturama, Brazil--knowledge, attitudes, and practices. *Environ Res* 102: 230-236.
- Ripoll DR, Faerman CH, Axelsen PH, Silman I, Sussman JL, (1993) Anelectrostatic mechanism for substrate guidance down the aromatic gorge of acetylcholinesterase. *Proc Natl Acad Sci USA* 90:5128–5132.
- Rothenberg MA, Nachmansohn D (1947) Studies on cholinesterase; purification of the enzyme from electric tissue by fractional ammonium sulfate precipitation. *J Biol Chem* 168:223–231.
- Sant'anna CMR, Viana AS, Junior NMN, (2006) A semiempirical study of acetylcholine hydrolysis catalyzed by *Drosophila melanogaster* acetylcholinesterase. *Bioorg Chem* 34:77-89.
- Santos RP, Cavaliere MJ, Puga FR, Narciso ES, Pelegrino JR, Calore EE, (2002) Protective Effect of Early and Late Administration of Pralidoxime against Organophosphate Muscle Necrosis. *Ecotoxicol Environ Saf* 53:48-51.
- Santos VMR, Donnici CL, DaCosta JBN, Caixeiro JMR, (2007) Compostos organofosforados pentavalentes: histórico, métodos sintéticos de preparação e aplicações como inseticidas e agentes antitumorais. *Quím Nova* 30:159-170.
- Satar S, Satar D, Tap O, Koseoglu Z, Kaya M, (2004) Ultrastructural changes in rat liver treated with pralidoxime following acute organophosphate poisoning. *Mt Sinai J Med* 71:405-10.
- Shafferman A, Ordentlich A, Barak D, Stein D, Ariel N, Velan B, (1996) Aging of phosphorylated human acetylcholinesterase: catalytic processes mediated by aromatic and polar residues of the active centre. *Biochem J* 318:833-840.

- Shen ZX, (2008) Rationale for diagnosing deficiency of ChEs and for applying exogenous HuChEs to the treatment of diseases. *Med Hypotheses* 70:43-51.
- Shrot S, Markel G, Dushnitsky T, Krivoy A, (2009) The possible use of oximes as antidotal therapy in organophosphate-induced brain damage. *NeuroToxicology* 30:167-173.
- Siman I, Joel L, (2008) Acetylcholinesterase: how is structure related to function?. *Chem-Biol Interac* 175:3-10
- Soares W, Almeida RMVR, Moro S, (2003) Trabalho rural e fatores de risco associados ao regime de uso de agrotóxicos em Minas Gerais, Brasil. *Cadernos de Saúde Pública* 19:1117-1127.
- Stojan J, Brochier L, Alies C, Colletier JP, Fournier D, (2004) Inhibition of *Drosophila melanogaster* acetylcholinesterase by high concentrations of substrate. *Eur J Biochem* 271:1364–1371.
- Stojiljković MP, Pantelić D, Maksimović M, (2001) Tabun, sarin, soman and VX poisoning in rats: kinetics of inhibition of central and peripheral acetylcholinesterase, ageing, spontaneous and oxime-facilitated reactivation. VII International Symposium on Protection against Chemical and Biological Agents. Stockholm, Sweden, pp.1–12.
- Stojiljković MP, Jokanović M, (2005) AUM Shinrikyo and terrorist use of nerve agents in Japan. In: Monov A, Dishovsky C, (Eds.) Medical aspects of chemical and biological terrorism: Chemical terrorism and traumatism. Publishing House of the Union of Scientists in Bulgaria, Sofia, Bulgaria, pp. 101–115. available at <http://www.jmedchemdef.org/archives.html>.
- Tago H, Maeda T, McGeer PL, Kimura H, (1992) Butyrylcholinesterase-rich neurons in rat brain demonstrated by a sensitive histochemical method. *J Comp Neurol* 325:301-312.
- Taylor R, Jewsbury PJ, Essex JW (2002) A review of protein–small molecule docking methods. *J Comput Aided Mol Des* 16:151-166.
- Tomlin C, (1994) *The Pesticide Manual, a World Compendium*, British Crop Protection Council, Croydon.
- Van Helden HPM, Busker RW, Melchers BPC, Bruijnzeel PLB, (1996) Pharmacological effects of oximes: how relevant are they? *Arch Toxicol* 70:779–786.
- Vellom DC, Radic Z, Li Y, Pickering N.A, Camp S, Taylor P, (1993) Amino acid residues controlling acetylcholinesterase and butyrylcholinesterase specificity. *Biochemistry* 32:12-17.
- Wada K, Fujibayashi Y, Yokoyama A, (1994) Copper(II)[2,3-butanedionebis(N4-methylthiosemicarbazone)], a stable superoxide dismutase-like copper complex with high membrane penetrability. *Arch Biochem Biophys* 310:1-5.

- Wan WG, Zheng SC, Zou HJ, Ma SD, Tao GZ, Xu ZF, Zhang B, Chen JJ, Fang LY, Zhu ZJ, (2007) Different therapeutic efficacy of pralidoxime chloride PAM-Cl on AChE against acute toxicity of methamidophos, dichlorvos and omethoate. *Chin J Ind Hyg Occup Dis* 25:586-589.
- Wang EIC, Braid PE, (1967) Oxime reactivation of diethylphosphoryl human serum cholinesterase. *J Biol Chem* 242:2683-2687.
- Warren GL, Andrews CW, Capelli AM, Clarke B, LaLonde J, Lambert MH, Lindvall M, Nevins N, Semus SF, Senger S, Tedesco G, Wall ID, Woolven JM, Peishoff CE, Head MS, (2006) A critical assessment of docking programs and scoring functions. *J Med Chem* 49:5912-5931.
- WHO (1993) Methamidophos Health and Safety Guide No. 79. World Health Organization, Geneva.
- Wilson IB, Ginsburg S, (1955) A powerful reactivator of alkylphosphateinhibited acetylcholinesterase. *Biochim Biophys Acta* 18:168-170.
- Wilson IB, Harrison MA, (1961) Turnover number of acetyl-cholinesterase. *J Biol Chem* 236:2292-2295.
- Wilson BW, (1992) Organophosphates—chemistry, fate and effects. Academic Press, Inc.; p. 108-37.
- Wong L, Radic Z, Brüggemann RJM, Hosea N, Berman HA, Taylor P, (2000) Mechanism of oxime reactivation of acetylcholinesterase analyzed by chirality and mutagenesis. *Biochemistry* 39:5750-5757.
- Worek F, Thiermann H, Szinicz L, Eyer P, (2004) Kinetic analysis of interactions between human acetylcholinesterase, structurally different organophosphorus compounds and oximes. *Biochemical Pharmacology* 68:2237-2248.
- Worek F, Koller M, Thiermann H, Szinicz L, (2005) Diagnostic aspects of organophosphate poisoning. *Toxicology* 214:182-189.
- Worek F, Aurbek N, Koller M, Becker C, Eyer P, Thiermann H, (2007) Kinetic analysis of reactivation and aging of human acetylcholinesterase inhibited by different phosphoramidates. *Biochem Pharmacol* 73:1807-1817.
- Zayed SMAD, Fakhr IMI, El-Magraby S, (1984) Some toxicological aspects of methamidophos exposure in mice. *J Environ Sci Health B* 19:467-478.
- Zhang YH, Miyata T, Wu ZJ, Wu G, Xie LH, (2007) Hydrolysis of acetylthiocholine iodide and reactivation of phoxim-inhibited acetylcholinesterase by pralidoxime chloride, obidoxime chloride and trimedoxime. *Arch Toxicol* 81:785-792.